

2 mit

NASA TECHNICAL TRANSLATION

NASA TTF-14, 772

THE BERING EXPERIMENT

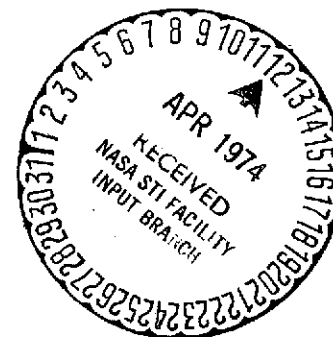
(NASA-TT-F-14772) THE BERING EXPERIMENT
(Scripta Technica, Inc.) 162 p HC
\$11.25 CSCL 04A

N74-19960

Unclass

G3/13 29049

Translation of "Eksperiment 'Bering'" USSR Hydrometeorological Service
A.I. Voevodov Main Geophysical Observatory
Leningrad, 1973, 186 pages



NATIONAL AERONAUTICS AND SPACE ADMINISTRATION
WASHINGTON, D.C. 20546 NOVEMBER 1973

STANDARD TITLE PAGE

1. Report No. NASA TT F-14, 772	2. Government Accession No.	3. Recipient's Catalog No.	
4. Title and Subtitle THE BERING EXPERIMENT		5. Report Date	
		6. Performing Organization Code	
7. Author(s)		8. Performing Organization Report No.	
		10. Work Unit No.	
9. Performing Organization Name and Address Scripta Technica, Inc. 1511 K Street, N.W. Washington, D.C. 20005		11. Contract or Grant No. NASw-2484	
		13. Type of Report and Period Covered Translation	
12. Sponsoring Agency Name and Address National Aeronautics and Space Administration Washington, D.C. 20546		14. Sponsoring Agency Code	
15. Supplementary Notes Translation of Eksperiment "Bering" USSR Hydrometeorological Service A.I. Voyevkov Main Geophysical Observatory Leningrad, 1973, 186 pages			
16. Abstract Presents data collected by the Soviet party to the Soviet-American project on microwave measurement of ice cover, sea state and precipitation in Bering Sea, February 15 to March 7, 1973.			
17. Key Words (Selected by Author(s))		18. Distribution Statement Unclassified-Unlimited	
19. Security Classif. (of this report) Unclassified	20. Security Classif. (of this page) Unclassified	21. No. of Pages 158	22. Price

CONTENTS

	Page
Chap. I. INTRODUCTION	1
Chap. II. OBSERVATIONS ON BOARD THE WEATHER-RESEARCH SHIP "PRIBOI"	3
2.1. Aero-synoptic characteristics of atmospheric processes over the northern Pacific Ocean (Feb.-Apr. 1973)	3
2.2. Aero-synoptic processes during the experiment.	4
2.3. General features of the formation of ice cover in the Bering Sea	7
2.4. Distribution and properties of sea ice in the microwave measurement test areas	8
Chap. III. INFRARED MEASUREMENTS OF THE RADIATION TEM- PERATURE OF WATER AND ICE AND WAVE MEASURE- MENTS	13
3.1. Instrumentation and measuring techniques	13
3.2. Results of water surface temperature measurements ..	14
3.3. Radiation temperature measurements of the ice surface ..	14
3.4. Wave characteristics from weather ship "Priboi" data ..	16
3.5. Characteristics of the horizontal parameters of sea waves in the "Bering" experiment region (radar survey data) ..	18
3.6. Data on salinity, chlorine content and degree of surface foam coverage	22
Chap. IV. AIRCRAFT MEASUREMENTS	24
4.1. Brief resume of aircraft microwave instrumentation and measurement procedure	24
4.2. Results of aircraft microwave measurements	24
4.3. Results of radar survey with the AN-24 aircraft	25
4.4. Airborne thermo-hygrometer measurements	25
4.5. Measurements of cloud water content	25
4.6. Results of airborne heat-scanner measurements	26
4.7. Infrared radiometer measurements ($8-12 \mu$)	26
4.8. Aerial photo-survey data	28
 ENCLOSURES	
Appendix II. 1. Radio sounding data tables	29
Appendix II. 2. Tables of standard meteorological observations at 15-minute intervals	45
Appendix III. 1. Tables of water- and ice- surface radiation temper- atures	52
Appendix IV. 1. Flight plans, time- and coordinate- tables	63

	Page
Appendix IV. 3. Data tables from airborne sounding of the atmosphere	81
Appendix IV. 2. Plots of radio-brightness temperatures	114

CHAPTER 1

/1*

INTRODUCTION

The joint Soviet-American Bering Sea microwave-measurement experiment was conducted during the three weeks from 15 February to 7 March, 1973, in accordance with the agreed-upon technical plan. Nine joint flights were made during this period, covering all program options. The flight plans and time charts have been issued by the Americans in a preliminary report. The Option A flight measurements in precipitation zones were made on 26 February and 2 March. Option B measurements of sea surface state were conducted on 16 and 23 February and 7 March. Option C ice-structure measurements were made in flights on 15, 20 and 28 February and 5 March. The data, including the time of operation of the apparatus in each flight, are shown in Table 1 of the preliminary report.

In addition to the instrumentation specified in the Soviet portion of the technical plan, ice-survey radar gear installed aboard on AN-24 aircraft was used in the experiment. The task of the ice-survey radar was to obtain the ice-field radar picture needed for interpretation of the microwave measurements, to select the boundaries of the ice test area and to establish the starting reference points for the position of the Soviet weather-research ship "Pribor". A radar survey of the sea surface wave state was made on the B program days (sea state measurements). The AN-24 aircraft operation was conducted immediately after the IL-18 and CV-990 aircraft had departed from the operational zone.

The Soviet weather-research ship "Priboi" carried out pre-planned meteorological, and hydrological observations at the time of the joint flights. In addition the following measurements were made:

- wave parameters, using a wave-gage and radar methods.
- water surface radiation temperature measurements using an IR-radiometer (8-12 μ).
- electrophysical properties of the ice.

The following days of joint flight were reduced by the Soviet side: Option A, 26 February and 2 March; Option B, 16, 23 February and 7 March; Option C, 20 February and 5 March.

Meteorological, aerological and hydrological measurements were made on all flight days specified in the program.

The combined flight plans, time- and coordinate-tables are given in the Appendices to the report.

/2

*Numbers in the margin indicate pagination in the foreign text.

Personnel of the USSR Hydrometeorological Service Research Institute participated in compiling the report:

- A. I. Voyeykov Main Geophysical Observatory.
- State Oceanographic Institute.
- Hydrometeorological Center, USSR.
- Far Eastern Hydrometeorological Research Institute and the Leningrad State University.

CHAPTER 2

/3

OBSERVATIONS ON BOARD THE WEATHER RESEARCH SHIP "PRIBOI"

2.1. Aero-synoptic characteristics of atmospheric processes above the northern Pacific Ocean (Feb. -Apr. 1973). The nature of the synoptic processes over the Far Eastern territories, adjacent seas and the northern Pacific differed substantially during February 1973 from the many-year average. The distinguishing feature of the synoptic processes above the northern Pacific and Bering Sea during February was the exceptional cyclonic activity in the arctic and polar fronts, an anomalous arrangement and intensity of the main action centers in the atmosphere: Siberian and sub-tropical anti-cyclones, aleutian low.

A comparison between the mean many-year data for ground-level atmospheric pressure and the averages for February 1973 brought out that all atmospheric action centers during this period were located 13° - 20° west of the many year average position; negative pressure anomalies, equal respectively to 8- and 4-mb, were observed in the Siberian anticyclone and aleutian low. In addition to the westward displacement of the main activity centers of the atmosphere, the position of the polar front over the northern Pacific also differed from the many-year average position, namely, from the southern Japanese islands it was directed NE, not toward the Gulf of Alaska, but toward the western portion of the Bering Sea.

The position of the polar front and the blocking action of a ridge of high pressure from a high center over Honolulu toward Alaska established the general direction of movement of the cyclonic systems and the region in which they became stationary (Bering Sea). The stationary nature of the cyclonic systems during the first days of February near the eastern coasts of Kamchatka and the resulting prevailing southerly flows over the Bering Sea brought about an anomalously northern position of the ice edge: during the first 10 days of the month (beginning of the Bering experiment) the ice edge at 176° W was located north of the 62nd parallel.

At the time of maximum development of cyclones and while they were stationary in the Bering Sea, cyclonic circulation with storm winds extended outward over a large radius of 1500 km. A deeper low (center pressure down to 976 mb) developed, primarily in the Arctic front. Deep lows did not develop in the Pacific branch of the polar front, and they appeared as low-pressure formations. They began their movement as frontal waves from the region of China or from the southern Japanese islands, and, moving NE, flowed into the arctic front high over the Bering Sea. The accompanying heat caused regeneration of the central stationary cyclone. In those cases when the merging of the polar front wave cyclone and the arctic front cyclone occurred earlier, over the eastern Pacific, the development of the cyclonic activity was mainly of a storm nature (over 1-2 days the cyclones deepened to 900-956 mb).

/4

The exceptionally deep lows and the rather high pressure in the Siberian and sub-tropical anticyclones caused the development of storm winds of up to 27-30 m/sec.

The outflow of cold air masses from the continent into the rear portion of the lows located in the SW portion of the Bering Sea, with high winds, high wave state and sea water temperatures near 0°C , led to heavy ship icing in the western Pacific and SW portion of the Bering Sea, in a band between 45° - 55°N . In the front portions of the lows, strong winds in combination with a very long fetch (thousands of kilometers) created sea states up to 6.

2.2. Aero-synoptic processes during the experiment. The weather conditions during the experimental period were distinguished by their variety and instability. Clear, sunny weather was followed by dense, low clouds carrying snow, which reduced visibility to 100-200 m; the temperature (about 0°) was followed by heavy frost (-16°); atmospheric transparency was replaced by fogs in which the visibility was less than 200 meters; relatively calm winds (6-8 km/sec) became storm winds (18-20 m/sec) and the calm sea /5 surface developed 5-meter waves.

This diversity was governed by the geographical features of the site of the experiment and by the winter synoptic processes in this region of the globe. The uniqueness of the geographic site of the test area consisted in that it was located at the juncture between the cold ice surface and the warm surface of the open sea, where the water temperature was close to zero, and also in the proximity of two continental regions of differing temperatures (the cold of Chukatka and the warmer Alaska).

The special features of the synoptic processes were as follows. The paths of the southern cyclones, which supplied heat to the Aleutian depression to maintain it, were characterized by two principal directions from the region of cyclogenesis — are toward the western Bering Sea and the other toward its eastern section, the Aleuts and the Gulf of Alaska. A high-pressure ridge usually developed at the back edge of the cyclones, issuing to the east of the sea, directed southward from Chukatka.

Hence the synoptic situation in the Bering Sea during the experiment was characterized by the presence of two centers of cyclonic activity, periodically separated by a high-pressure ridge. As a rule one of the centers was dominant and the other secondary.

The direction of movement of the cyclones and the region in which they became stationary were determined by the high-altitude pressure field. The presence of a high Pacific ridge in the middle troposphere, directed from the sub-tropical high toward Alaska, and the westerly location of the high-altitude depression (south of Kamchatka) favored the escape of the southern cyclones to the SW or W sections of the Bering Sea. The migration of the high-altitude barometric formations to the east and the weakening of the blocking ridge led to an eastward deflection of the cyclone paths; they emerged at the Aleuts, the peninsulas and Gulf of Alaska. Weather conditions of three navel types were observed in the experimental area, depending on the region in which the cyclonic systems moved and on the intensity of the ridge at the rear of the eastern lows:

- Weather in the fore-section of the cyclone (in case of the emergence of southern cyclones in the western Bering Sea);
- Weather at the rear-sections of a cyclone (if it became stationary over the Aleutian islands or Gulf of Alaska);
- Anticyclone ridge weather (with the development of a ridge back of an eastern cyclone).

Each of these types was different in nature, and in specific cases the meteorological conditions in the surface layer were also governed by the distance from the center of the low or ridge axis.

The specific synoptic situation and weather conditions in the experimental area were summed up as follows. At the beginning of the operation (11-20 February) an anticyclone system was located over Kolyma; its eastern periphery extended over the Alaskan coast and the northern Bering Sea. Intermittent wedges, directed southward from Chukatka, penetrated to 50°N. The weather during this period was generally dependent on the ship's position relative to the axis of the ridge. Weak winds 16-10 m/sec and light cloudiness were observed on the ridge axis (11-14 February); at the periphery of the ridge (15-20 February), in a band of sizeable pressure gradients, the windspeed reached 19 m/sec. With NE winds, snow fell in the form of flurries, which were especially intense and prolonged with a more northerly position of the eastern cyclonic center; the visibility was at times less than 1 km (Figs. 2.1, 2.2).

During 17-21 February, with an air temperature of -14° or lower and windspeeds above 10 m/sec (see charts of meteorological elements), intense steaming was observed above the ice-free water surface, lowering the visibility to 50 m or less at times.

The ice mass immediately to the north of the ship limited the wave fetch, and hence, even with a 17-19 m/sec NE-wind, wave height did not exceed 4 meters.

The vertical structure of the temperature field during this period was characterized by the presence of a super-adiabatic gradient in the lower half-kilometer layer (1.18-1.52 deg/100 m), with gradients of -1.26 to -3.20 deg/100 m in the adjacent layer of thickness 400-1000 meters. It should be noted that in the presence of transfer from Chukatka to the SW portion of Alaska (13-14 and 19-20 February), i.e. from areas of anticyclonic circulation, the vertical distribution of humidity had features characteristic of subsidence inversions (compression) — namely, the humidity decreases sharply with height from the lower boundaries of the inversion. During 15-18 February, with air mass transfer from the south of Alaska, when the air over most of the path moved in the curved isobar field of the cyclone, the inversion was weaker, and at times an isothermal- or trapped layer with weak positive gradients was observed instead of an inversion. The vertical trend of the humidity was in this case distinguished by a monotonic decrease with altitude.

The presence of superadiabatic gradients in the lower 500-meter layer of the troposphere, strong winds and a relatively warm sea with high relative humidity in the surface layer, creates favorable conditions for forced convection and strong vertical displacement of an air mass. This may explain the existence of the heavy snow flurries from the thin (< 1 km in thickness) cumulo-nimbus clouds; due to the enhanced vertical mixing, the cloud layer is continuously resupplied by new batches of water vapor.

At the beginning of this period (13-14 February), strong easterly and north-easterly winds (up to 20-25 m/sec) prevailed throughout the troposphere in the periphery of the high anticyclone centered over the northwest Bering Sea. In connection with the inflow of dry cold air masses from Alaska, the temperature dropped significantly at all levels in the troposphere. The minimum value noted at the tropopause (10.1 km) was -64.7°. The relative humidity above 1.5 km did not exceed 40%.

During the period 15-18 February a further temperature decrease was observed. As compared with 14 February, the temperature decreased by 10°-12° over the entire

troposphere. The polar tropopause simultaneously lowered to 6.7-7.1 km. At the same time the highest temperatures recorded during the experimental period were observed in the lower stratosphere and at the tropopause ($\sim -50^{\circ}$, Fig. 2.3).

On 21 February the cyclone which had been over the Aleutian islands shifted somewhat north; the weather in the area of the experiment assumed a backedge character — N and NE winds of 8-12 m/sec, snow flurries, steaming sea, visibility at times less than 1 km (Fig. 2.4). On 22 February, the southern cyclone, with a center pressure of 965 mb, moved toward the northern portion of the Bering Sea, forcing the high-pressure ridge toward Kalyma (Fig. 2.5). Between 22-25 February the weather was first governed by the leading edge of the cyclone, and later by the N and NW sections of this and other cyclones that had emerged into the Bering Sea or had been generated above it.

At the beginning of the period solid stratiform clouds with snowfall were noted, with a SE wind of 12-17 m/sec and abrupt warming (from -14° to 0°). Subsequently the air temperature fluctuated between -0.2° to -2.0° , the relative humidity in the surface layer was 80%-97%; the windspeed varied over wide limits (4-20 m/sec) as a function of distance from the center and the wave height reached 4.5 meters. Snow fell from time to time, fog formed and minor ship icing was observed. Due to the flow of air from the ocean into the frontal portion of the cyclone, the temperature increased considerably, together with the humidity. This brought about a sharp change in the vertical temperature- and humidity-field structure. The vertical temperature gradient in the lower 500-meter layer decreased (down to $0.6-0.9$ deg/100 m), the inversion disappeared and the relative humidity increased at all levels (90% at 4 km). On 22-23 February, substantial horizontal temperature gradients were observed in the upper troposphere, air-flow convergence with close to jet velocities (25-28 m/sec), a sharp fall in tropopause height — i.e. conditions close to those in which tropopause disruption is observed. This gives reason to assume that there actually was a disruption in the polar tropopause above the northern Bering Sea during this period. The marked warming up in the lower 3-4 km layer of the stratosphere is then clarified. It could have occurred as a result of the injection of warm troposphere air into the stratosphere at the site of the tropopause break. At 0000 GMT, at the end of the day 26 February, the ship was at the far edge of a deep cyclonic system, in its frontal section. A low with a center pressure of 953 mb was located near the SE coast of Kamchatka. During 26 February the low was filled in by almost 20 mb and moved NW toward the Kamchatka coast. On 27 February the ship was stationed ahead of an occluded front, at the boundary between this cyclonic region to the SW and a ridge to the NE (Fig. 2.6). The ridge began to intensify on 27 February and extended to the rear side of the eastern cyclonic region from the north to the Bering Sea. These systems governed the weather from 28 February-2 March in the cruising region (Fig. 2.7). Notwithstanding the outflow of air masses from Alaska, the air temperature did not fall below -10° , which can be explained as follows. The air mass circulation was governed by a cyclonic system that had entered Alaska. The warm air masses in the leading portion of the cyclone were not cooled due to their short stay over the continent and were subsequently further warmed by $8^{\circ}-10^{\circ}$ above the open sea. Circulation in the middle and upper troposphere was governed by two high-altitude barometric centers — a low-pressure area over the southern Sea of Okhotsk, and a slowly-moving anticyclone over Alaska. The transport of warm air from the edges of the high trough and the cold air masses from the SW edge of the anticyclone from N. America accentuated the high frontal zone. Large horizontal temperature contrasts were observed throughout the troposphere, amounting to as much as $1.13^{\circ}-13.7^{\circ}$ at 4-5 km in the warm-front zone. The tropospheric wind system changed markedly. On 25 February, in the upper troposphere ahead of the warm front, a polar

jet-stream was noted, with a vertical extension of about 4 km. The maximum wind-speed on the jet axis (at an altitude of 6.7 km) reached 45 m/sec. In and behind the frontal zone the velocity fell off to 10-5 m/sec. After passing through the cold region of the high frontal zone (during the night of 26-27 February), increased wind intensity throughout the troposphere was again observed, and the jet stream again formed, with the axis of the newly-formed jet lower by 5 km and with a lower flow velocity (32 m/sec). High temperatures ($+0.2^{\circ}$ to -0.7°) and humidity (90-96%) were maintained in the 1-km surface layer (Fig. 2.8).

The vertical distributions of these parameters exhibited features characteristic of anticyclonic weather; however, they were less pronounced than at the beginning of the experiment. The average height of the layer with superadiabatic gradients remained the same, but the gradients themselves were reduced to 1.03 deg/100 m. The thickness of the inversion layer (with a gradient of 0.95 deg/100 m) was lower by a factor of two (0.31 km). And, finally, during the end of the period, the experimental area again came under the influence of cyclonic activity. From 3-8 March, two deep lows emerged in the SW region of the Bering Sea, with center pressures of 970 and 960 mb. Simultaneously, over the eastern section of the sea or over the Gulf of Alaska, shallow secondary lows were produced, forming a widened depression with the southern low that covered a very large area, including Alaska and the western portion of the Sea of Okhotsk (Fig. 2.9). /10

The weather in the navigation area was governed by the northern edge of this region. The windspeed varied over rather wide limits. The formation of the secondary lows led to increased barometric gradients at the edge of the depression, and resulted in an increase in windspeed up to 20 m/sec. As they filled in the wind moderated to 10-8 m/sec. With the prevailing NE winds, cold air masses from Alaska entered the water and wind direction, the temperature measured from shipboard fluctuated from -8° to -15° .

With the influx from southern Alaska the air temperature increased, but at the same time colder air masses arrived from the northern section of the peninsula. On 3-4 March, at the northern edge of the secondary low where the ship was stationed, 20 m/sec winds were noted, together with snowfall (visibility at times less than 1 km), weak steaming and heavy icing conditions.

On 7-8 March the ship was initially under the influence of the NW edge of the low, and later the NE edge. A windspeed of 21 m/sec formed waves up to 5 meters in height. The combination of the storm wind, heavy sea and low air temperature (-16°) caused heavy icing of the ship.

The lower boundary of the polar tropopause during 1-8 March averaged 10 km. Heat advection lifted it to 11 km, but in cold air it dropped to 7-8 km. The tropopause height remained constant with uniform flows (Fig. 2.10). /11

2.3. General features of the formation of ice cover in the Bering Sea. Ice formation in the Bering Sea usually begins at the end of September. If we exclude the Bering narrows, ice cover in the Bering Sea basin is observed over a 10-month period, from the end of September to the middle of July. Maximum ice-cover development is reached in March (Fig. 2.11). Ice begins to form in the northern section of the sea, usually in the gulfs of Anadyr, Kresta and in Norton Sound. Occasionally, ice from the Sea of Chukotsk is brought by winds and currents into the northern section of the sea, but the relative amount does not exceed 3%-5%. The main ice body is formed locally,

and during the course of the winter its boundaries move southward to 59° - 60° N in the central portion of the sea and to 55° - 57° N along the Asian and American coasts.

In the western Bering Sea, with the extension of the ice-cover from N to S due to natural formation, a steady migration of ice in the same direction takes place under the influence of the stable winds and currents. As a consequence, a stable ice window is formed along the southern coast of Chukotka, where the formation of new ice continues all winter. Toward March the width of the zone of newer ice reaches 250-300 km south of the coast of Chukotka. The advance of the ice edge to the south is due more to drift than to ice formation toward the open sea.

Toward the beginning of March thin, first-year (white) ice (thickness 30-70 cm) predominates in the Bering Sea. In the NW portion, and south of the Gulf of Anadyr, significant bodies of thicker first-year ice are encountered (average thickness 70-120 cm). The formation of such ice is related to the lower air temperature in the NW region of the sea, the considerable freshening of sea water due to the efflux of the Anadyr river and the rapid cooling of these relatively shallow regions of the sea. /12

The first-year ice is usually carried by the constant polar currents and winds into more southerly and easterly areas. Wedges of this ice can sometimes be found near the edges in western and central areas of the Bering Sea.

In the eastern Bering Sea the onset of freezing is about the same as in corresponding latitudes of the western portion. Norton Sound is a principal focus of ice formation. However, the regularity of ice drift in the eastern area of the sea is quite different from that in the western portion. Here the steady Pacific current, flowing from S to N, governs the drift of the ice in that direction. During the winter, with prevailing N winds, ice overcomes the steady current and gradually moves southward down to Bristol Bay.

Thus the ice cover in the Bering Sea is formed by the action of constant currents, strong tidal flow- and ebb-currents and winds. The steady currents create a relatively constant pattern of ice distribution, on which is superposed the action of meteorological factors. The role of the meteorological factors, which fluctuate more-or-less irregularly, usually show up as short-period changes in ice conditions.

2.4. Distribution and properties of sea ice in the microwave measurement test areas. To obtain the objective information on the quality and on the distribution of the ice-cover in the test areas needed for interpretation of the microwave surveys, an areal radar survey using side-looking radar was used, together with ship observations in the peripheral zone. The radar survey was made from an ice-survey AN-24 aircraft, which proceeded to the test areas as soon as the IL-18 and SU-990 aircraft had finished their operations. The maximum time interval between the radar and microwave surveys did not exceed 3 hours, and therefore they may be considered to be essentially synchronous.

The location of the ice that polygon (program option "C") was fixed on the basis of the possibility of cruising in ice of the Soviet weather research ship "Priboi"; according to the stated expedition program conditions this was to be in the SW sector of the Soviet quadrant during the entire survey period. During the survey period the "Priboi" served as an artificial reference point for the IL-18 aircraft. Simultaneously, oceanographic observation and physical investigations of the properties of the ice were made from ship-board. /13

For the subsequent joint analysis, data were selected from option "C" of 20 February and 5 March. Due to a lag in beginning operations, the radar survey was completed at the beginning of the following weeks — 21 February and 6 March, respectively. The radar survey of 21 February covered only 70% of the square test area. The survey of 6 March was of satisfactory quality and (at 20-30 km) covered the boundaries of the prescribed square.

The geographic location of both square test areas is fixed by the following coordinates:

21 February	Point -	61°21'	178°40' W
Time of survey	Point -	60 30	178 40
01.20 - 02.35	Point -	60 30	176 55
	Point -	61 21	176 54
6 March,	Point -	61 53	178 20
Time of survey	Point -	60 52	178 20
00.57 - 02.41	Point -	60 52	176 35
	Point -	61 53	176 31

From the above listing of coordinates it is seen that the test areas of 21 February and 6 March differed in latitude by only 22 miles. The ice conditions in the region of old ice also changed little during this time period.

The south portion of the test area of 21 February contained individual zones of cohering broken ice. The zones were 2-6 km in width with open 8-15 km water areas between them. The ice zones extended about parallel to the ice massive in the northern portion of the test area and were aligned NW-SE. The overall solidarity of the ice in the south sector of the test area was no more than three points. The north sector of the test polygon contained packed ice in the form of large hummocks of broken, thin, first-year ice (white ice). Among the pack ice many open water spaces were observed, whose orientation about coincided with that of the ice zones in the southern section of the polygon.

Packed ice predominated in the March 6 test polygon. The overall solidity of the ice did not exceed five points only in the SW portion, in the immediate vicinity of the edge. Along the diagonals of the polygon — from NW to SE — ran a chain of large open water areas, widths 2-10 km. The open water areas were in part filled with bands of finely broken fresh ice.

Let us consider the age makeup of the ice in the polygon areas and its morphological characteristics.

The ice cover in both polygons is typical for near-edge zones. It was formed by a process of gradual freezing of the sea from north to south under the constant action of wind and swell arriving from the open sea. Under these conditions the initial form of sea ice is usually "pancake" ice — glass ice. This ice is formed in the presence of sea waves and is found in the form of an accumulation of rounded floes of diameter 2-3 meters and thickness up to 10-15 cm. Along the edges of these floes are formed characteristic rollers of layered and deformed ice. As the thickness increases the pancake ice alters to gray-white and white ice; freezes together into larger floes and even into

an ice-field which is usually again broken down with an increase in wave state. Near the edge the processes of freezing and fracture of ice formations occurs constantly. The greater the thickness of the ice formations and the farther they are from open water, the larger are the frozen-together monolithic floes.

On 20 February at the Priboi's station, i.e. in the SW area of the polygon, in the near-edge zone, broken ice of solidarity up to 5 points (predominant size of floes less than 20 m), packed together in patches and zones of solidarity up to 9 points. The predominating ages of the ice were white (2 points) and grey-white (2 points) with minor inclusions of grey and glass ice (up to 1 point). Snow cover of the ice did not exceed 1 point (the thickness of the snow cover on the white ice was no more than 5 cm). /15

The ice situation in the vicinity of the ship's station on February 19-20 is given in Fig. 2.12, from data of the survey made by the IL-18 aircraft. Plotted are the many-year average of the edge of the drift ice and the ice edge from the aircraft radar data. Table 1 presents the symbology used in Figs. 2.12 and 2.13.

In the polygon surveyed on 6 March there were zones of packed ice along the edge, width of zones about 40-60 km, consisting of rounded floes, not frozen together, of diameter 15-20 meters. Each of the floes was formed by the freezing together of still smaller floes of rounded shape. The thickness of these frozen-together ice formations was not uniform and varied from 15 to 30-50 cm. Their surfaces were very rough; the contours of the frozen mosaic of smaller floes was clearly visible, with the edges of the swell waves penetrated freely through this zone of broken ice to hinder its freezing into larger ice formations.

With an average solidarity of ice in the open-pack zone of 3-5 points, the solidarity in patches reached 9 points. Under the influence of the strong wind waves and swell, together with the intrusion of warm Pacific water at a temperature up to +1.5°C, the glass ice formations almost completely disappeared in the zone of the open pack ice. White and gray ice retained their former ratio, but the thickness of the snow cover increased somewhat, reaching 7-10 cm on the white ice. Figure 2.13 shows the ice conditions in the vicinity of the ship for 5-6 March 1973.

In the northern portions of the polygons, where swell was substantially weakened, the processes of the freezing together of ice floes proceeded at a higher rate. Larger ice formations were observed in these areas, consisting also of larger floes of differing ages that had frozen together. The surface relief of these floes was quite complex and reflected the entire "history" of the formation of the ice cover from pancake ice up to the formation of large ice fields of first-year ice.

Thus the ice cover in the area of the microwave survey was formed in the immediate vicinity of the edge, which determined the complexity of its morphology and the diversity of its age gradations. The physical and chemical properties of these ices was non-uniform in space, and their parameters deviated widely from the parameters of the ice in other areas of the sea. /16

As noted earlier, the "Priboi" investigated the physical properties of all stages of growth of the drift ice — white, gray-white, gray and glass ice.

The measurements made of the salinity, density and temperature of these growth stages of the drift ice allowed establishing some general relationships which are

Table 2.2

Вид морского льда	Пределы измене- ния толщи- ны льда	Пределы измене- ния со- лености	Сред- няя $S\%$	Пределы изменения плотности	Сред- няя ρ	Примечание
a)	b) H_l	c) $S\%$	d)	e) ρ	f)	g)
Нилас h)	3-10 см	13-18	15,7	0,830-0,916 $\frac{\text{г}}{\text{см}^3}$	0,875	
Серый i)	10-15	7-10	8,0	0,810-0,890	0,830	
Серо- белый j)	15-30	2-7	-	0,780-0,890	-	S и ρ серо- белого и бе- лого льдов представлены графиками l)
Белый k)	30-70	2-7	-	0,700-0,900	-	

KEY: a) Type of sea ice; b) Ice thickness measurement limits H_l ; c) Salinity measurement limits, $S\%$; d) Average, $S\%$; e) Density measurement limits, ρ ; f) average, ρ ; g) Remarks; h) Glass ice; i) Gray; j) Gray-white; k) White; l) S and ρ for gray-white and white ice are shown graphically.

represented graphically and in tabular form (Figs. 2.4 and 2.15 and Table 2.2). The qualitative correlation between the nature of the vertical distribution of these parameters with those of arctic ice of corresponding age.

As can be seen from Figs. 2.14 and 2.15, the minimum salinity and density of the white and grey-white ices occurs in the upper layers of the above-water portion; this is a consequence of the migration of brine. The maximum salinity and density is observed in the upper layers of the underwater portion of the ice; this is explained by the accumulation of brine migrating from the above-water part of the ice. Below this layer these characteristics decrease somewhat and then smoothly increase. It can be seen from the graphs that these values scatter within certain limits. This can be explained by the large difference between the conditions of ice formation near the edge and in the ice massif, as well by certain inadequacies in the method of selecting ice samples from the ship. The salinity and density of the primary ices (gray and glass ice) also fluctuated within certain limits (Table 2.2); this is explained by the general difficulty and inadequately worked-out technique of taking samples.

The ice sample tests made during the experiment showed that three basic layers of characteristic texture (Fig. 2.16) can be distinguished from the external characteristics in white ice. The first layer (0-9 cm) was of white granular ice (water-snow type) with a large number of air inclusions in the form of bubbles (diameter 1-2 mm). The second layer (10-35 cm) was of darker ice, a layer of gradual transition to a more monolithic ice. In this case, as a rule, there are usually 1-2 clear dark seams of organic origin. The third layer (35-70 cm) is of still darker monolithic ice with a relatively small amount of chaotically oriented air inclusions. Two primary layers of characteristic texture are visible in the gray-white ice. The first layer (2-25 cm) is semi-transparent ice with a small number of air-bubble inclusions of diameter 1-2 mm. The texture of the earlier ice formations (grey and glass ice) were uniform over their entire thickness. The color was cloudy white. A large number of minute, mainly spherical, air inclusions were noted. Photographs of the crystal structure (Fig. 2.16) show that all ice age stages investigated possess a uniform, fine-grain structure; the crystals were isometric, of irregular shape, growing uniformly in all directions, the predominant crystal size was 0.5-1.0 cm.

In conclusion we should note that these properties of ice describe most completely the ice in the near-edge zone.

Appendices II.1 and II.2 contain tables of the radio-sounding of the atmosphere and tables of the more frequent meteorological observations made during the flight periods from the "Pribor". As a rule, two radiosondes were launched during a flight period — one prior to the flight and a second immediately afterward.

CHAPTER 3

/19

INFRARED MEASUREMENTS OF THE RADIATION TEMPERATURE OF WATER AND ICE AND WAVE MEASUREMENTS

3.1. Instrumentation and measuring techniques. One of the basic characteristics of the dynamic state of a water mass is its heat content. Therefore an infrared radiometer was selected to give an indication of the temperature of the underlying sea surface. This instrument has a number of advantages as compared with available standard instruments: first, it allows defining the thermal state of the upper layer of water, which interacts directly with the adjacent layers of the atmosphere, while ship temperature-measuring instruments are submerged to a depth of 0.5-1.0 meters or more; second, the non-contact method of measurement is identical with the aircraft (or satellite) method and allows defining the temperature in the natural state without various disturbances due to noise and distortions attributable to the ship. And, finally, the temperature of the ice surface with the ship underway can generally be found in practice only by non-contact methods of measurements in the microwave or infrared bands. A shipboard infrared radiometer was used for the non-contact surface-temperature measurement; the instrument had the following technical characteristics:

— water temperature-measuring range	-3° to +37°C
— sensitivity threshold	0.05°C
— measuring accuracy	±0.2°C
— viewing angle of optics	12°

The measuring circuit of the IR-radiometer is based on the principle of direct measurement of the infrared radiation of water, whose emissivity amounts to 0.98, with maximum radiation at a wavelength of about 10μ . The required spectral range is provided by an interference filter with a pass-band of $8-13\mu$.

The radiometer pickup was installed in the bow section of the ship, about 5 meters above the sea surface; this corresponds to a spatial resolution of 2×2 meters. /20

The accuracy of operation of the IR-radiometer was systematically checked using a calibration device. For ice temperature measurements the calibration curve was linearly extrapolated in the low-temperature range, with an accuracy within $\pm 0.5^\circ$.

In all, 200 synchronous measurements were made on water. Since the measuring accuracy of the IR-radiometer amounts to about $\pm 0.2^\circ$ C for water, periodic checks were made during the measurements to eliminate random errors, using the calibration device to establish the operating temperature point. This allowed making reliable measurements of surface temperature to 0.1° C.

The differences between the IR-radiometer indications and simultaneous mercury thermometer readings did not exceed $0-0.2^\circ$ (50% of all observations). The distribution of the IR-radiometer readings from the ship measurements is given in the form of a histogram in Fig. 3.1.

The greatest deviations of the IR-radiometer readings from simultaneous mercury-thermometer readings are caused by methodological aspects of the measurement, and

are not due to instrumental inaccuracies. These deviations are as a rule associated with daytime measurements with low air temperatures and strong winds, when it is usually difficult to make temperature measurements using contact methods.

3.2. Results of water surface temperature measurements. The thermal regime of the northern portion of the Bering Sea was most affected by the transport of the warm and humid sea air masses of middle latitudes in a system of southern lows and by the action of high-pressure regions of cold arctic air masses from the Chukatka and Kalyma regions. The air temperature upon the entry of warm air masses increased to $0 \pm 0.3^{\circ}$ and with the intrusion of arctic air it was lowered to -15° to -20°C . In the test polygon area, below-zero water temperatures prevailed (-1.7° , -1.8° , latitude 61°N). Due to the cyclonic circulation of 22-25 February and 1-8 March the water surface temperature in the experimental area rose to $+0.1^{\circ}$ to $+0.4^{\circ}\text{C}$ or more.

In two instances of tests in more southerly regions of the sea (58 - 59° N) the water surface temperature amounted to 0° - 1.7° .

The winter convective- and wind-mixing had equalized the vertical water-temperature trend to the bottom (-1.5°), making it thermally homogeneous. Spatial temperature measurements were not made during the course of ship maneuvers in the experimental area, and observations were made only near accumulations of floating ice.

An influence of hydrometeorological processes (internal waves, currents, etc) to alter the temperature distribution was not observed. No diurnal trend in water surface temperature was observed. Therefore the statistical treatment of the data was limited to the computation of averages (15-min samples), the calculation of average temperatures T over the aircraft operating time, computation of their mean-square deviations from the average S' and the dispersion σ' .

In Table 3-1 and in the Appendix are given water temperature measurements made during aircraft flights. Table 3-1 gives values over the entire flight; in Appendix III-1 these quantities are given for each 15-minutes.

As indicated by the observed data, the fine-scale variability of the water surface temperature, both spatially and in time, was negligible in the experimental area. The average water temperature over the operational area was above the average multi-year figure by 1.0° - 1.5°C (Figs. 3-2, 3-3). Temperature variations were mainly caused by the type of atmospheric circulation: the variance of its fluctuations amounted to $0.0-0.04^{\circ}$; the mean-square deviations were $0.0-0.2^{\circ}$, related to air-water temperature contrasts and significant wind speeds. The minimum surface temperature variability was observed with weak winds and air temperatures close to the water temperature.

In the analysis of the infrared radiometer records attention was given to the large variability in surface temperature as compared with simultaneous measurements from shipboard using a mercury thermometer: in most of them the dispersion was larger by a factor of 1.5 or even 2 than that for the contact thermometer measurements. This is evidence of the larger variability of the thermal processes at the water-air interface as compared with the deeper layers and of the higher sensitivity of IR-radiometers.

3.3. Radiation temperature measurements of the ice surface. Local ice forms in the northern region of the Bering Sea during the autumn. The ice cover of the northern Bering Sea in the experimental area was an accumulation of fine broken ice. This was

TABLE 3.1. Simultaneous Measurements of Surface Temperature (GMT) by the IR-Radiometer (TIR) and a Mercury Thermometer, their mean-square deviations s' and Dispersions σ

Date	Time (Greenwich)	T _{IR} ($^{\circ}$ C)	s'	σ	T _o ($^{\circ}$ C)	s'	σ
15-16.II	22.30-08.50	-0.14	0.16	0.02	-0.43	0.05	0.002
16-17.II	21.30-01.00	0.0	0.14	0.02	-0.1	0.08	0.006
19-20.II	21.30-01.00	-0.1	0.1	0.01	0.0	0.08	0.006
20-21.II	21.30-01.30	0.3	0.1	0.01	0.32	0.1	0.01
22-23.II	21.30-01.30	-0.8	0.21	0.04	-0.44	0.1	0.01
23-24.II	21.30-01.45	0.0	0.14	0.02	0.2	0.12	0.01
26-27.II	23.15-01.30	1.7	0.0	0.00	1.7	0.03	0.00
28.II -							
I.III	21.30-04.00	-1.45	0.1	0.01	-1.1	0.1	0.01
2-3.III	23.00-02.15	*)	-	-	0.2	0.15	0.02
5-6.III	21.30-02.15	-1.65	0.13	0.01	-1.3	0.1	0.01
7-8.III	23.00-03.00	*)	-	-	1.3	0.23	0.05

*Shipboard IR-measurements were not made due to stormy weather.

autumn-winter ice, with all stages of its development, from glass-ice to white ice with individual inclusions (1-2 points) of ice of autumn origin. The ice surface was usually covered by 5-7 cms of snow; however fields of fine broken ice and gray ice were found without snow cover, water-permeated.

The most widely-distributed ice forms (age-wise), were the gray and gray-white formations. Young forms (glass-ice, floating snow accretions) which had been formed in open areas of pure water due to its drift in marginal regions caused by currents and, in past, by winds. The overall amount of young forms did not exceed 3 points. Finely-broken ice predominated in the experimental area (floes of size less than 20 m); this is attributable to their breakup by wind and buckling.

As a consequence of the comparatively large influx of warm air from the southern regions of the sea and its overall warm-up, the southern edge of the ice was 90-100 miles north of the many-year average (Figs. 3.2, 3.3). The frequent outflow of southern storm winds into the experimental area and the shift to the north promoted a considerable ice drift, whose velocity (daily average) reached 20 miles/day. This yielded a variety of ice formations, from glass ice to autumn ice of thickness greater than one meter.

The temperature of the ice surface is an important quantity characterizing the physical state. Many IR-records were made of the surface temperature of various ice

formations, which may be the characteristic defining the temperature of the ice, particularly when considering the relative temperature variations.

/24

Ice thickness measurements were made together with the radiation temperature measurements with the ship (not underway) in drift ice.

Based on an analysis of all ice-surface radiation temperature measurements, Table 3.2 presents the data ordered in terms of the various age characteristics of the ice.

We note that if the air temperature is close to that of the sea water (-1.7° to 1.8°C), the ice-air thermal contrast almost disappears (not more than 0.2°C), while with air temperatures below zero this contrast is increased to 15° - 20°C . This calls attention to the fact that near the edges of the ice field there is considerable variation in the radiation temperature of the ice. This diversity is greater the more diverse the developmental forms caused by dynamic factors. In connection with the fact that the age characteristics of ice are closely related to its thickness, it seems possible to judge its thickness from radiation temperature measurements (Fig. 3.4).

It should be noted that the thermal contrasts at the ice-air interface can only yield correct information related to the growth and structure of the ice if they are determined under conditions of stable ambient air temperature; otherwise we must obtain a relationship for the transition to different temperatures.

3.4. Wave characteristics from weather ship "Priboi" data. The sea wave characteristics in the operational area of the Bering expedition were established directly from on board the weather research ship "Priboi" and from a radar survey.

The sea state at the "Priboi" position was recorded on two wave-gages. The mean value of wave height and period were established at the end of each measuring period with a special device and a method of accelerated reduction of wave records. The wave records in the Berlin expedition were taken during aircraft operations above the ship, when it was in open water. In view of the fact that the wave processes remained essentially unchanged over the time of each flight, the measurements were made once, over a long enough period to yield satisfactory statistical characteristics. Average values of wave height and period were established during each measuring period, using a device specially developed for this purpose. After ending each record the wave records were reduced using an accelerated technique and transmitted to the aircraft by radio (mean wave height, 5%-expectation height, mean period).

Initial reduction of wave records obtained in the experiment was carried out aboard ship. The differential functions of wave height and period shown in Fig. 3.5 were constructed from the wave records.

Table 3.3 gives sea state measurements from the wave-recorder data. Included are the wave heights and periods, the 15% expectation, the ratio of wave height to period and the wave and wind characteristics as established by visual observation.

The data in the table indicate that in most cases the sea state was combined with the prevailing swell.

Statistical processing of the measurements was accomplished on a computer, after the cruise; the results are given in Table 3.4, where data are given on the average

TABLE 3.2. Radiation Characteristics of the Bering Sea Ice-Cover in the Infrared Range

Дата 1)	время 2)	Характеристика льда 3)	Толщи- на (см) 4)	Радиа- цион- ная тем- перату- ра льда 5) (°C)	Темпе- ратура возду- ха 6) (°C)
I. III	09.00	Шуга, ледяная каша (9 баллов)	7)	-	-1,7
15. II	15.00	Ледяная каша	8)	-	-3,0
19. II	16.00	Снегухра	9)	5	-3,8
14. II	15.00	Тонкий нилас	10)	-	-3,4
15. II	10.10	Мелко-битый лёд с шугой	11)	15	-5,0
21. II	16.30	Мелко-битый серый лёд пропитан водой	12)	10	-4,5
21. II	16.50	Мелко-битый лёд, пропитан водой	13)	-	-3,6
15. II	08.50	Мелко-битый и блинчатый лед 9 баллов	14)	30	-5,0
15. II	09.10	Мелко-битый лёд 9 баллов	15)	-	-6,4
14. II	13.45	Молодой слаботоросистый лёд	16)	-	-6,1
15. II	08.35	Мелко-битый лёд (более крупные льдины)	17)	30	-6,2
15. II	03.42	Мелко-битый и блинчатый лёд	18)	50	-7,4
15. II	14.41	Блинчатый лёд (серый)	19)	-	-7,3
21. II	16.58	Мелко-битый лёд, серый 6-7 баллов	20)	30	-7,5
15. II	18.05	Льдина (до 20 м)	21)	50	-11,0
6. III	12.00	Мелкобитный лёд с белым снегом 10 см	22)	50	-7,0
6. III	11.00	Т о ж е 30 см	23)	70-80	-11,0
6. III	10.00	Т о ж е 20-30 см	24)	50	-6,8
22. II	12.00	Битый лёд со снегом (5-6 см)	25)	120	-11,3

KEY: 1) Date; 2) time; 3) ice characteristics; 4) thickness (cm);
 5) Radiation temperature of ice (°C); 6) air temperature (°C);
 7) sludge ice, crushed ice; 8) crushed ice; 9) floating snow concretion;
 10) thin glass ice; 11) finely broken ice with sludge; 12) finely-
 broken white ice permeated by water; 13) finely-broken white ice
 permeated by water; 14) fine-white and pancake ice, 9 points;
 15) finely-broken ice, 9 points; 16) fresh ice hummocks; 17) finely-
 broken ice (layer blocks); 18) finely broken and pancake ice; 19) pan-
 cake ice (gray); 20) finely-broken ice; gray, 6-7 points; 21) floes (up
 to 20 m); 22) finely-broken ice with white snow 10 cm; 23) same, 30
 cm; 24) same, 20-30 cm; 25) broken ice with snow (5-6 cm).

TABLE 3.3. Wave-Recorder and Visual Data on Sea State

1) Дата	2) Часы	3) Волнографные из- мерения			4) Визуальные наблюдения						7) Знобъ	
		$\frac{h}{15\%}$ см	τ sec	$\frac{h}{\tau}$ см/sec	5) Волнение			7) Знобъ			Ветер 8)	
					ветро- вое 6) 9) м	Высо- та 9) м	Напра- вление 10) град.	Напра- вление град.	Ско- рость 10) м/сек	11)		
I6.II	2.25	208	5,4	38,5	2,5				20	I4		
I6.II	23.31	237	7,2	33	2	$\frac{4}{2}$	$\frac{30}{80}$		20	I2		
20.II	22.36	I7I	7,I	24,I	2,5				350	I2		
22.II	23.00	293	I2,2	24	0,5	$\frac{4,5}{3}$	$\frac{200}{130}$	I00	I00	9		
23.II	6.13	280	I2,4	22,6	I,5	$\frac{4,5}{2}$	$\frac{200}{130}$	I00	I00	I0		
23.II	21.26	245	I2,8	I9,I	0,5	$\frac{4}{3}$	$\frac{230}{150}$	20		5		
26.II	23.30	343	9,8	35	2,5	4,5	I50	II0	I5			
27.II	3.21	303	I0,2	30,2	2,5	4,5	I50	90	I4			

KEY: 1) Date; 2) time; 3) wave-recorder measurements; 4) visual observations; 5) wave state; 6) wind-wave; 7) swell; 8) wind; 9) height (m); 10) direction (deg.); 11) velocity (m/sec).

values x_{ave} , the variance D, the mean-square deviation σ and the maximum heights x_{max} and periods of the waves.

As can be seen from the table, the sea state during the experiment was quite uniform. Clearly, to study the microwave radiation of the water surface and the effect on it of different stages of wave development, special experiments, with the measurement of wave slopes or stereo photo wave surveys are required.

3.5. Characteristics of the horizontal parameters of sea waves in the Bering experimental region. A radar picture of the sea surface was obtained by a side-looking radar installed aboard an AN-24 ice-survey aircraft. Flights were made at an altitude of 3000 meters, the survey was made at a 1:100,000 scale. In two flights made in accordance with the program "B" option (Feb. 16, 1973 and March 7, 1973) 30 pictures of a 15 x 30 km area were obtained. The flight plans and survey coordinates are shown in Figs. 3.6 and 3.7. The flight paths were selected so that three radar pictures with directions of illumination differing by 90° were obtained for the same section of the sea surface.

A visual analysis of the radar pictures of the wave surface showed that the nature of the picture depended only slightly on the direction of illumination, but for wind waves the

TABLE 3.4. Statistical Reduction of Wave-Records

№ волно-грамм 1)	Дата 2)	Часы 3)	Р е т е р		Число волн 7)	Высоты волн				Периоды волн			
			направление град. 5)	скорость м/сек 6)		h _{ave} м	D _h m ²	σ _h м	h _{max} м	τ _{ave} sec	D _τ sec ²	σ _τ sec	τ _{max} sec
I	16.II	2.00	20	14	76	1,35	2,40	1,55	3,41	3,5	13,7	3,7	5,9
2	16.II	2.25	20	14	226	1,27	2,31	1,52	3,17	4,1	23,5	4,9	9,1
3	16.II	23.31	20	12	137	1,59	3,19	1,78	3,30	3,79	16,8	4,1	7,7
4	20.II	22.36	350	12	206	1,14	1,69	1,3	2,35	5,2	30,7	5,6	13,1
5	20.II	23.20	350	12	183	1,13	1,58	1,26	3,06	5,17	30,3	5,5	10,9
6	22.II	23.00	100	9	130	1,84	4,75	2,18	4,74	6,1	47,5	6,9	12,5
7	23.II	6.13	100	10	131	1,82	4,32	2,08	5,39	7,4	35,8	6,0	18,15
8	23.II	21.26	20	5	63	1,57	3,26	1,8	4,02	8,4	82,8	9,1	16,8
9	26.II	23.30	110	15	152	2,12	5,87	2,42	6,02	7,1	52,8	7,3	13,9
10	27.II	3.21	90	14	148	1,87	4,54	2,13	4,19	7,2	62,1	7,9	14,4

KEY: 1) Wave-record; 2) date; 3) time; 4) wind; 5) direction (deg.); 6) velocity (m/sec);
 7) number of waves; 8) wave height; 9) wave period.

best relief was obtained with the direction of illumination toward the direction of motion of the waves. Analysis of the two-dimensional spectra obtained by optical processing of the radar pictures also agreed with this conclusion.

The radar spectra reflected to some extent the spectra of the wave slopes in the direction of illumination. However, due to the narrow-band spectra of the wind waves and swell (in frequency and amplitude), there is little difference between the wave-relief and wave-slope spectra normalized to the maximum. Hence the wave parameters were established directly from the radar picture spectra.

An analysis of the radar pictures of the sea surface obtained in the flight of March 7-8, 1973 and their 2-dimensional spectra show that a complex spatial structure of the agitated sea surface existed at the time of survey. The wind system had two clearly-expressed maxima in the wave-number plane; each of the sub-systems was very narrow-band and differed in frequency and direction. The main directions of these wind-wave systems are shown in Fig. 3.8. The first wave-system forms an angle of -26° with the direction of illumination (U-axis in Fig. 3.8) and the second an angle of $\pm 11^\circ$. Thus the main directions of these systems are developed with an angle between them of 37° . The direction of the bands of foam is clearly seen on the radar pictures. They coincide in direction with the second system of waves. The wind direction at the time of survey can be established from the direction of the foam zones. The first wave system, which deviates by -37° from the wind direction, was evidently formed somewhat earlier, when the wind was from a different direction. The wind then changed direction to form the second wave system. Therefore the first wave system has the nature of swell waves. /30

The wave length corresponding to the maximum of the spectral density of the first system is $\bar{\lambda}_1 = 119$ m, and the wave length of the second system is $\bar{\lambda}_2 = 101$ m. In the approximation of the integral, one-dimensional angle-spectrum by a function of the form $(\cos^m \theta)$, the coefficients of the angle spectrum for the first and second systems are $m_1 = 30$ and $m_2 = 10$, respectively. Cross-sections of the two-dimensional spectra, normalized to the maximum and extending in the main directions of each system are shown in Fig. 3.8b.

Due to the interaction of these two systems, the group wave structure is clearly expressed on the sea surface. The direction of movement of the wave groups, as established from both the radar picture and the two-dimensional spectrum of the picture, deviate by 17° from the first wave system and by 20° from the second, i.e. about midway between them. By averaging the group wave lengths, as determined from the picture and its spectrum, we get the same value, $\bar{\lambda}_{gr} = 640$ m.

In a direction perpendicular to the wind at the time of survey, a weak swell wave system was detected.

However, in the optical processing of its spectrum, the spectrum of the foam zones was superposed, which ruled out the possibility of accurate measurement. The average swell wavelength was approximately $\bar{\lambda}_s = 200$ m.

A picture of the sea wave stage on tack 7 (see Fig. 3.6) was prepared from the radar wave-survey data (16-17 February 1937). An analysis of the radar pictures and their two-dimensional spectra indicated that several wave systems were observed on the sea surface in this flight: the first system of wind-waves had $\bar{\lambda}_1 = 91$ m and angle $\alpha_1 = -34^\circ$ with the direction of illumination; the second system of wind-waves had

$\bar{\lambda}_2 = 93$ m and an angle $\alpha_2 = +10^\circ$; the first system of swell waves had $\bar{\lambda}_3 = 210$ m and an angle $\alpha_3 = -34^\circ$; the second system of swell waves had $\bar{\lambda}_4 = 230$ m and an angle $\alpha_4 = +26^\circ$.

A diagram of the wave system directions is shown in Fig. 3.9a; Fig. 3.9b shows sections of the two-dimensional spectra over the main directions of each wave system.

In analyzing the radar picture obtained during the flight of 16-17 February 1973, a group structure of the wind waves was not observed. However the radar picture of the sea surface was spotty in nature, which is possibly attributable to the interference of all form sea-wave systems observed in the survey.

TABLE 3.5. Salinity and Chlorine Content of the Surface Layer of the Sea

/33

a) дата	b) время (гри- вича)	c) координаты		темпер- атура по- верхнос- ти воды f) °C	хлор- ность g) ‰	соле- ность h) ‰
		сев. широта d)	зап. долгота e)			
I	2	3	4	5	6	7
15. II	II-43	61°07'	178°36'	-00.77	17.91	32.360
16. II	II-40	61 30	177 07	-01.02	18.04	32.590
17. II	5-52	60 28	177 19	-00.16	18.13	32.750
17. II	18-00	60 27	177 11	-00.18	18.19	32.860
18. II	II-52	60 27	177 23	-00.28	18.23	32.940
18. II	17-49	60 24	177 33	-00.31	18.20	32.880
19. II	5-53	60 57	178 29	-00.51	18.18	32.840
19. II	II-40	60 50	178 23	-00.08	18.21	32.900
20. II	0-00	60 43	178 32	00.14	18.27	33.010
20. II	II-40	60 36	178 40	00.05	18.23	32.940
21. II	II-35	60 50	178 36	-00.62	18.16	32.810
21. II	6-03	60 28	178 06	-00.50	18.13	32.750
22. II	23-40	60 20	177 05	-00.46	18.13	32.750
23. II	I7-51	59 33	177 38	01.02	18.28	33.030
23. II	23-25	59 30	177 00	00.10	18.21	32.900
24. II	II-35	60 28	178 12	-00.34	18.15	32.790
24. II	I8-04	60 25	178 13	00.10	18.19	32.860
24. II	23-50	61 03	178 32	-01.28	18.05	32.610
25. II	5-59	61 12	178 35	-01.26	18.05	32.610
25. II	II-40	61 10	178 54	00.70	18.22	32.920
26. II	I7-49	61 08	178 54	00.56	18.25	32.970
26. II	23-57	59 28	178 04	01.71	18.28	33.030
27. II	5-42	59 35	177 59	01.01	18.25	32.970
27. II	II-42	60 10	177 00	-00.56	18.11	32.720
28. II	5-33	60 23	177 02	-00.82	18.15	32.790
28. II	23-45	60 42	177 46	-01.12	18.09	32.680
I. III	5-43	60 24	177 55	-00.52	18.12	32.740

See key at end of table.

TABLE 3.5. (Continued)

I	2	3	4	5	6	7
I.III	II-40	60°17'	I78°04'	-00.49	I8.18	32.840
I.III	I7-52	60 07	I78 02	-00.46	I8.18	32.840
I.III	23-46	60 08	I77 59	-00.42	I8.20	32.880
2.III	6-00	60 01	I78 09	-00.40	I8.15	32.790
3.III	I7-51	59 40	I77 07	00.18	I8.22	32.920
3.III	23-40	60 20	I78 06	-00.58	I8.14	32.770
4.III	5-52	60 18	I78 21	-00.10		
4.III	23-45	60 14	I78 48	01.22	I8.32	33.100
5.III	I-42	60 35	I78 39	-00.62	I8.18	32.840
5.III	I8-03	60 32	I78 50	00.04	I8.21	32.900

KEY: a) Date; b) time (GMT); c) coordinates; d) N. lat.;
 e) W. Long; f) water surface temperature °C; g) chlorine content (%); h) salinity (%).

In this way, two-dimensional spectral analysis of the radar pictures allowed us to establish the number of systems of waves, the location of the maxima of the spectra in the wave-number plane and, from them, the directions and mean wavelength of each system, and to estimate the one-dimensional angular- and frequency-spectra of the waves.

3.6. Data on salinity, chlorine content and degree of surface foam coverage. The tasks of the oceanographic- and hydromechanical-complement of the "Priboi" specified the establishment of operational stations down to a depth of 500 meters along the ship's course.

In connection with the fact that only data on the surface layer of water are needed for interpretation of the microwave measurements, Table 3.5 gives the results of the measurements of temperature, salinity and chlorine content of the surface layer of the sea water in the experimental area.

The data of Table 3.5 indicate that the salinity and chlorine content can be taken to be constant and equal to 33 and 18 parts per thousand, respectively, with accuracy good enough for interpreting the microwave measurements of the emissivity of the sea surface.

Small-scale formations connected with the collapse of waves during storms (foam, spray) introduced a significant contribution into the microwave emission. The degree of foam coverage of the sea can serve as a characteristic directly related to the wind speed, with the condition that the relationship between these quantities is known. Data in the literature indicate that the percentage of surface covered by foam is proportional to the square of the wind speed. Therefore a visual estimate of the degree of foam coverage of the sea surface was made aboard the "Priboi" and attempts were made to develop the relationship between wind speed and amount of foam. /32

TABLE 3.6. Degree of Foam Coverage of Sea Surface

Дата a)	b) Время		Степень покрытия моря пе- ной e) %	Скорость ветра м/сек f)
	начала измере- ния c) НИИ	конца измере- ния d) НИИ		
I5-I6.II	22 30	00 30	20	I4-I5
	00 45	03 00	15	I3-I5
I6-I7.II	21 30	01 00	15	I2-I4
20-21.II	21 30	01 30	5	II-I4
23-24.II	21 30	01 45	0	4-5
26-27.II	23 15	01-30	15	I4-I5
28.II - I.III	21 30	02 15	5	I0-I2
28.II - I.III	02 30	04 00	3	I0-II
2-3.III	23 00	02 15	20	I7-I9
5-6.III	21 30	22-15	3	I2-I4
7-8.III	23 00	23 45	10	I1-I2
7-8.III	00 00	02 15	15	I8-I9
7-8.III	02 30	03 00	10	I9

KEY: a) Date; b) time; c) start of measurement;
 d) end of measurement; e) degree of foam coverage
 (%) ; f) wind speed m/sec.

Figure 3.10 is a plot of the visual estimates of the area of the sea surface covered by foam (in %) made during the Bering expedition and the corresponding wind speeds. Although the number of points is not large and they exhibit considerable scatter, the main region in which they are concentrated can be bounded by the following analytic curves:

$$S = 0.096 V^2$$

$$S = 0.028 V^2$$

Although this is a rather crude approximation, the very fact that it is possible to describe the link between wind speed and degree of foam coverage of the surface by a quadratic relationship is encouraging.

Tables 3-6 give data on the visual observation of the degree of foam coverage of the sea surface made on board the "Priboi" during the experiment.

CHAPTER 4

/36

AIRCRAFT MEASUREMENTS

4.1. Brief resume' of airborne microwave instrumentation and measurement procedure. A four-channel radiometer, operating at wavelengths of 3.0-1.6-, 1.35- and 0.8-cm, was installed aboard an IL-18 aircraft.

In view of the experimental task — measurement of the sea state, ice cover and precipitation zones — the measurements on three of the wavelengths (3.0, 1.6- and 0.8-cm) were used in the initial processing. The measurements at these wavelengths during operations in program options A and B were made in a non-scanning mode. In option B the viewing angle θ was held constant over the entire time of measurement. In option B the measurements were made with a variable viewing angle: at 3.0-cm the viewing angle was varied between 0° - 75° (from the nadir), and at 1.6- and 0.8-cm between 0° and 85° .

In program option C operations (ice-survey) the radiometer operated at 3.0-cm in a scanning mode, and the maximum temperature contrasts were simultaneously recorded along each line. The 1.6- and 0.8-cm radiometers operated at the nadir ($\theta = 0$) in a non-scanning mode.

When determining the sea state (wave-state-option B) the measurements were made during turns to obtain data at the largest sighting angles, which are of most interest in terms of the effect of waves on the radio radiation. In this case the sighting angle was defined as the sum of the antenna setting angle and the angle of bank of the aircraft. This measuring technique yielded data on the relationship between radio brightness temperature and wave state that is averaged over azimuth (when banking, the aircraft actually moves over a small-radius perimeter) and it does not seem possible to separate out the influence of the direction of wave propagation.

Option B measurements at 3.0-cm were made with two polarizations: at 1.6- and 0.8-cm measurements were made with horizontal polarization only. In all other cases measurements were made only with horizontal polarization.

4.2. Results of aircraft microwave measurements. In accordance with the mutually-adopted technical plan for conduct of the experiment, the measurements made with the non-scanning radiometers are presented graphically (Appendix IV.2). These graphs show the dependence of the radio brightness temperature in degrees absolute (ordinate, scale 0.5 deg/mm) on time (GMT, on abscissa, scale 3 sec/mm). Plotting in the time coordinate was made possible by the fact that the times of passing all check points were shown on the preliminary charts. In option B operation, as pointed out above, in addition to horizontal passes there are rotations in turns above one point (selected as point "C" near the position of the "Priboi"). In this case the time coordinate bears a conditional nature. The instantaneous values of radio-brightness temperatures cited in Appendix IV.2 are not time-averaged and their mean values are determined only by the time-constant of the gear. In subsequent averaging and interpretation we shall use an average based on the specific option of the measurement program.

/37

Combined chart-diagrams, coordinate tables for check points and times of passage over them as plotted from chart-diagrams obtained in a preliminary calculation by the American side, are given in Appendix IV. 1.

In view of the fact that scale reduction occurs when reproducing graphical material, an album of charts in the specified technical plan scale is appended to the report as working data.

In program option C operations, using a 3.0-cm scanning radiometer (horizontal polarization) in accordance with the technical plan, ice-field pictures are obtained to a 1:1000,000 scale. Figures 4-1 and 4-2 show plots of the microwave surveys of 20 February and 5 March. Since reproduction degrades the quality of the plots, the original plots (to working scale) are given in the Appendix.

4.3. Results of radar survey with the AN-24 aircraft. An areal radar survey with a side-looking radar was conducted to gather objective information on the properties and distribution of the ice-cover in the ice test areas during program option C operations. The survey was made with the AN-24 ice-survey aircraft, which entered the test area as soon as both the IL-18 and CV-990 aircraft had completed their operations. The maximum time interval between the radar and microwave surveys was no more than 3 hours. In view of the small variability of the ice state over this time interval, the surveys can be considered to be essentially simultaneous. For interpretation of the microwave survey plots, Figs. 4-3 and 4-4 give plots of the radar survey relating, respectively, to 21 February and 6 March. The radar survey of 21 February covers only 70% of the area of the test polygon. The survey of 6 March is of satisfactory quality and covers the boundaries of the assigned square at 20-30 km. A detailed analysis of the ice conditions from the radar survey is given in Chapter 2 of this report. The radar survey plot is to a 1:1000,000 scale.

4.4. Airborne thermo-hygrometer measurements. The airborne thermo-hygrometer is designed for the measurement and recording of atmospheric humidity at the dew-point and at air temperature. The humidity measurement is made using the "dew-point" method, which consists of measuring the temperature at which the water vapor concentration in the air is the saturation concentration.

The air temperature measuring limits are -65°C-40°C and the relative humidity limits 20-100%, with instrumental measuring errors of $\pm 0.3^\circ$ in temperature and $\pm 5\%$ in relative humidity. The thermometer lag, when measuring the air temperature, is no more than 1 second. For technical reasons, humidity measurements were made only up until 20 February, 1973. Tables of airborne sounding of the atmosphere are presented in Appendix IV. 3.

4.5. Measurements of cloud water content. Measurements of the water content of clouds were made using an instrument operating on the calorimetric principle of

/39

TABLE IV. 1

H km	0,5	0,6	2,0	3,57	4,10	4,30	4,60	4,80	5,50
W g/m ³	0,11	0,26	1,60	1,03	0,13	0,47	0,30	0,07	0,05

measuring water content ("hot-wire" method). The essence of the method consists of comparing the temperatures of two heated bodies, one of which is in a stream of cloud aerosol and the other is screened from the cloud particles. Profiles of the cloud water content changes were measured in the flight of 2 March, according to option A.

Table IV.1 gives the data for water content as a function of altitude, and Fig. 4.5 shows the plot of its variation with altitude, with the types of clouds indicated.

The equipment was inoperative during the first flight (option A) of 26 March due to strong icing conditions.

4.6. Results of airborne heat-scanner measurements. The airborne heat-scanning infrared radiometer operating in the spectral region 3.4-4.1 microns. The heat-scanner yielded black-white pictures of the radiation temperature of the underlying surface and of the upper edges of clouds. The momentary angular field of view of the instrument was 0.2° , and the angle of scan was 60° . The scanning band was to the left of the flight direction. Thus, when flying in accordance with program option C, a continuous areal survey was not obtained with the heat-scanner, but only individual passes. Figure 4.6 shows a plot of the IR-survey of the ice-fields from the passes of 20 February, and Figs. 4.7 and 4.8 are illustrations of individual passes from other program options. The IR-picture is given to standard scale 1:1000,000. /40

4.7. Infrared radiometer measurements (8-12 μ). The infrared radiometer is designed to measure the radiation temperature of the surface and clouds. Measurements were made in the $8-12\mu$ window, with a linear field-of-view angle of 22° . The sensitivity of the instrument was about 0.1° , accuracy $\pm 5\%$.

Radiometer measurements were made on 15 February and 2 March. Option C measurements were made on 15 February, and option A measurements on 2 March. The

TABLE IV.2
15 February 1973

Время ГМТ			Высо- та (м)			Радиа- ционная темпере- ратура ($^{\circ}$ С)			Время ГМТ			Высо- та (м)			Радиа- ционная темпере- ратура ($^{\circ}$ С)			Время ГМТ			Высо- та (м)			Радиа- ционная темпере- ратура ($^{\circ}$ С)		
1)	2)	3)	1)	2)	3)	I	2	3	1)	2)	3)	I	2	3	1)	2)	3)	I	2	3	1)	2)	3)	I	2	3
22 21	9000	-15,9	22 38	9000	-21,9	22 54	9000	-11,6	22 38	9000	-19,5	55	9000	-13,5	23 22	9000	-19,4	23 22	9000	-10,2	23 22	9000	-12,8	23 22	9000	-19,2
22	9000	-18,5	39	9000	-19,5	56	9000	-14,8	44	9000	-14,2	58	9000	-19,2	46	9000	-13,5	24	9000	-11,2	59	9000	-19,4	59	9000	-10,2
24	9000	-17,9	40	9000	-9,8	55	9000	-13,5	42	9000	-12,9	57	9000	-19,4	45	9000	-18,5	25	9000	-9,4	57	9000	-19,2	57	9000	-12,8
25	9000	-18,6	42	9000	-12,9	58	9000	-19,2	44	9000	-14,2	59	9000	-10,2	46	9000	-13,5	26	9000	-11,2	59	9000	-19,4	59	9000	-12,8
26	9000	-15,7	44	9000	-14,2	23	9000	-19,4	45	9000	-18,5	23	9000	-10,2	47	9000	-13,5	27	9000	-11,2	59	9000	-19,4	59	9000	-12,8
27	9000	-18,3	45	9000	-18,5	23	9000	-19,4	46	9000	-13,5	23	9000	-10,2	48	9000	-13,5	28	9000	-11,2	59	9000	-19,4	59	9000	-12,8
85	9000	-17,1	46	9000	-13,5	23	9000	-19,4	47	9000	-13,5	23	9000	-10,2	49	9000	-13,5	29	9000	-11,2	59	9000	-19,4	59	9000	-12,8
36	9000	-16,0	51	9000	-13,4	24	9000	-11,2	48	9000	-13,4	24	9000	-10,2	50	9000	-13,4	30	9000	-11,2	59	9000	-19,4	59	9000	-12,8
37	9000	-15,4	53	9000	-16,9	25	9000	-9,4	49	9000	-16,9	25	9000	-10,2	51	9000	-16,9	31	9000	-11,2	59	9000	-19,4	59	9000	-12,8

See key at end of table.

TABLE IV.2 (Continued)

1	2	3	1	2	3	1	2	3	
23	26	9000	-II,6	22	55	9000	-I6,3	OI I2	4900 -I2,5
	27	9000	- 9,2		56	9000	-I5,7	I3	4900 -I2,5
	28	9000	-I4,I		57	9000	-I6,8	I4	5500 -I4,2
	29	9000	-I6,0		58	9000	-I6,9	I5	5500 -I7,8
	37	9000	-I5,3		59	9000	-I7,I	I6	5500 -20,I
	38	9000	-I2,8	23	00	9000	-2I,3	25	5500 -I4,8
	41	9000	- 8,7		OI	9000	-I6,I	26	5500 -I5,7
	42	9000	-II,9		02	9000	-I5,5	27	5500 -I7,5
	43	9000	-II,6		03	9000	-I6,3	28	5500 -I6,9
	44	9000	-I0,9		04	9000	-I8,2	29	5500 -I8,I
	45	9000	-I4,2		05	9000	-2I,9	30	5500 -I2,8
OI	I9	9000	-22,8		06	9000	-I7,7	31	5500 -I3,8
	20	9000	-20,0		07	9000	-I5,5	32	5500 -II,6
	21	9000	-I7,6		08	9000	-I3,2	33	5500 -I8,4
	22	9000	-I7,5	00	40	9000	-I9,0	34	5500 -I4,4
	23	9000	-I8,3		41	9000	-I8,5	35	5500 -I3,9
	25	9000	-I6,5		42	9000	-20,9	36	5500 -I4,3
	26	9000	-I5,3		43	9000	-I4,I	37	5500 -II,8
	27	9000	-20,0		44	9000	-I8,4	38	5500 -I7,I
	28	9000	-I7,8		45	9000	-20,3	39	5500 -II,I
02	25	700	- 7,9		46	9000	-I8,4	51	5500 3,8
	26	700	-I0,4		47	9000	-24,5	52	5500 5,8
	27	700	-I0,7		48	9000	-I8,5	53	5500 4,I
	28	700	-II,8		49	9000	-I7,3	54	5500 4,2
					51	9000	-I8,I	55	5500 4,0
4)	<u>2 марта 1973 г</u>		OI OI	3600	-I2,2		56	5500 3,I	
				02	3600	-I6,4	57	5500 3,8	
22	46	9000	-2I,0		03	3600	-I4,I	58	5500 3,I
	47	9000	-20,2		04	3600	-2I,2	59	5500 2,7
	48	9000	-20,9		05	3600	-I6,4	02	00 5500 I,I
	49	9000	-I9,I		06	4000	-I6,2	OI	5500 2,7
	50	9000	-20,2		07	4000	-I6,9	02	5500 2,5
	51	9000	-I5,0		08	4000	-I4,9	03	5500 2,2
	52	9000	-20,2		10	4250	-II,2	04	5500 2,2
	53	9000	-I9,3		II	4250	-I6,5	07	5500 I,5
	54	9000	-I5,7						

KEY: 1) Time (GMT); 2) altitude (m); 3) radiation temperature ($^{\circ}\text{C}$); 4) 2 March 1973.

nature of the cloudiness is given in the airborne sounding tables (section 4.4). Table IV.2 gives the radiation temperatures as a function of time for these two days.

/42

4.8. Aerial photo-survey data. The aero-photo survey (IL-18 aircraft) was made using standard aerial camera equipment of focal length 70 mm and frame size 180 x 180 mm.

The aerial photo-survey was made for interpreting the results of the microwave ice-cover survey in the presence of suitable weather conditions. The aero-photo survey of 20 February covered only part of the test area, since the surface was screened by cloud-cover. The survey of 5 March was made entirely over the ice test polygon. In addition, on 7 March (option B - sea waves) an optimal frame-by-frame aero-photo survey was made; the areal characteristics of the sea state can be established from these pictures, together with an estimate of the percentage of foam-covered surface. Both plots, 20 February and 5 March, together with the frame-by-frame survey of 7 March are shown to standard scale, 1:1000,000.

CONCLUSIONS

This report contains the results of a preliminary reduction of the airborne microwave measurements and of the auxiliary airborne- and ship-measurements needed for subsequent interpretation.

Certain of the data relating to airborne actionmetric- and aerosol-measurements are not presented in this report since they have not yet been completely processed.

Subsequent processing will consist of an analysis of the results obtained, comparison with theoretical calculations and a determination of the basic meteorological parameters that describe the state of the sea surface and atmosphere. Comparison with the analogous results of the American measurements will be made for overlapping portions of the courses.

APPENDIX II, 1

/43

RADIOSOUNDING DATA TABLES

Coordinates:

61.0° N

178.0° W

16 February 1973

Time - 11.3

Cloud cover - 10/10 cb

/44

H	P	T	U	V	
I	2	3	4	5	6
0	I007	-9.9	81	020	I3
0.2	961	-14.0	96	040	I3
0.5	943	-17.5	89	043	I4
1.0	882	-21.0	88	055	I6
1.5	824	-25.2	85	040	I7
2.0	769	-27.9	74	043	I3
3	669	-31.9	65	029	I0
4	579	-38.3	34	035	06
5	500	-43.8	54	260	05
6	431	-45.8	46	338	02
7	370	-48.8	43	338	03
8	318	-50.2	38	220	03
9	272	-50.2	37	220	03
10	234	-48.3	35	220	02
11	201	-47.2	32	205	04
12	173	-46.7	31	209	08
13	149	-46.6	30	212	I0
14	128	-47.0	28	200	I2
15	110	-47.3	27	I93	I3
16	95	-47.0	24	I92	I3
17	81	-45.9	25	206	I2
18	70	-45.6	25	I95	II
19	60	-46.5	23	I80	I0
20	52	-46.6	23	I80	I0
21	45	-46.8	22	I80	I0
22	38	-47.0	21	I79	II
23	33	-47.1	20	I65	08
24	28	-48.0	19	I44	07

Coordinates:

17 February 1973

/45

60.6 N

Time - 9h 18 min

178.0 W

Cloud cover - 8/8 cb

H	P	T	u	d	v
0	I009	-I2,9	90	040	
0,2	983	-I5,6	90		
0,5	944	-I9,0	89		
I,0	883	-20,8	79		
I,5	825	-I9,8	67	045	I6
2,0	77I	-23,I	60	044	I2
3	67I	-30,5	66	045	09
4	582	-35,0	59	045	05
5	504	-42,4	58	I63	06
6	434	-44,7	49	I10	I2
7	373	-49,0	44	208	II
8	320	-51,4	41	I98	08
9	275	-49,8	39	I80	06
I0	236	-48,3	36	I80	05
I1	203	-47,2	34	I78	06
I2	I74	-47,6	32	I75	07
I3	I50	-47,3	31	I75	I0
I4	I29	-45,2	28	I60	I0
I5	III	-45,3	27	I60	09
I6				I70	I3
I7				I73	08
I8				I75	07
I9				I75	08
20				I75	09
21				I72	08
22				I42	06
23				I23	06
24				I73	09

Coordinates:

17 February 1973

60.0 N
178.0 WTime - 14 h 06 min
Cloud cover - 9/9 cb

H	P	T	U	d	V
0	I007	-II,8	80	020	I2
0,2	98I	-I5,0	82	030	I4
0,5	943	-I8,I	83	030	I3
I,0	882	-20,6	73	033	I2
I,5	824	-21,2	64	030	I2
2,0	770	-24,7	62	028	I0
3,0	670	-33,0	53	035	06
4	580	-36,6	46	I54	01
5	502	-42,3	48	2I6	07
6	432	-47,0	48	2I0	I2
7	37I	-50,2	47	20I	I4
8	3I8	-5I,6	46	208	II
9	273	-5I,6	44	2I0	09
I0	234	-49,2	43	I99	08
II	20I	-48,9	43	I97	08
I2	I73	-48,7	41	I92	07
I3	I48	-46,6	40	I85	I0
I4	I28	-47,7	40	I8I	I0
I5	IIO	-46,9	40	I80	I0
I6	94	-47,I	39	I80	09
I7	8I	-47,0	38	I80	I0
I8	70	-46,6	37	I92	09
I9	60	-46,7	36	208	08
20	52	-46,4	36	I83	07
2I	44	-47,6	35	I70	06
22	38	-47,5	34	I70	05
23	33	-48,0	34	I6I	06
24	28	-48,I	34	I7I	08

/47

Coordinates:

60.5 N
178.7 W

21 February 1973

Time - 11 hr 42 min
Cloud cover - 9/9 cb

H	P	T	u	d	v
0	1010	-12,0	92	350	I2
0,2	983	-14,4	97	360	I2
0,5	945	-17,0	97	007	II
1,0	884	-13,8	96	015	I4
1,5	828	-12,4	85	021	04
2	776	-13,1	83	025	07
3	680	-21,6	90	338	07
4	593	-27,1	89	041	04
5	515	-34,2	72	010	05
6	445	-41,2	67	034	06
7	383	-48,2	69	I2I	06
8	329	-54,8	68	254	03
9	281	-53,7	63	298	I0
I0	241	-51,4	57	280	II
I1	206	-50,3	57	265	I0
I2	I77	-48,6	57	265	I2
I3	I52	-48,2	56	268	I2
I4	I31	-46,5	55	272	II
I5	II3	-48,7	54	275	08
I6	97	-48,7	49	250	08
I7	83	-49,4	47	203	07

Coordinates:

60.9 N
178.3 W

22 February 1973

Time - 11 h 36 min
Cloud cover - 6/6 Cu

H	P	T	μ	d	V
0	I0II	-9,6	8I	090	I0
0,2	985	-I2,3	82	085	I3
0,5	947	-I3,7	84	085	I4
I,0	887	-II,I	83	092	I4
I,5	83I	-II,I	80	III	I4
2	779	-I2,6	78	I30	I6
3	682	-I9,2	72	I40	I4
4	596	-24,5	54	I40	09
5	519	-26,6	33	I64	03
6	45I	-3I,3	29	230	06
7	39I	-38,I	30	230	07
8	338	-45,9	34	245	09
9	290	-53,8	38	245	II
I0	248	-58,6	4I	247	I6
II	2II	-59,5	40	23I	I5
I2	I8I	-52,4	38	235	I9
I3	I55	-5I,9	35	235	I6
I4	I33	-50,7	32	235	I8
I5	II4	-5I,4	30	23I	I8
I6	98	-5I,4	30	225	I6
I7	84	-49,I	29	225	I5
I8	72	-48,7	28	225	I4
I9	62	-49,4	27	224	I3
20	53	-50,3	27	2I7	II
2I	46	-50,3	26	2I5	I0
22	39	-5I,4	26	2I0	09
23	33	-5I,7		I95	07
24	29	-53,3		I90	07

Coordinates:

24 February 1973

59.5 N
177.0 WTime - 09 h 06 min
Cloud cover - 10/6 Cb, As

H	P	T	U	d	V
0	I003	-0,6	91	020	05
0,2	978	-2,0	91	015	06
0,5	94I	-4,1	91	005	08
1,0	883	-6,9	92	010	08
1,5	828	-10,4	92	045	03
2,0	775	-13,9	93	271	03
3	678	-18,8	88	I45	04
4	592	-25,7	89	I45	07
5	514	-32,4	88	I40	10
6	446	-39,7	87	I54	I7
7	384	-45,1	79	I50	28
8	330	-48,2	66	I49	32
9	284	-49,5	57	I55	31
10	244	-49,3	51	I60	22
11	209	-48,3	48	I62	20
12	180	-48,8	45	I66	I8
13	154	-47,6	42	I68	I8
14	133	-48,0	40	I67	I9
15	II4	-44,7	39	I75	I7
16	98	-47,5	37	I75	I8
17	84	-46,2	36	I75	20
18	73	-45,5	35	I62	I8
19	63	-47,4	35	I59	I8
20	54	-50,4	35	I76	I8
21	46	-50,7	35	I80	I3
22	39	-52,5	35	I75	07
23	34	-51,9		I60	07
24	29	-51,7		I55	08

Coordinates:

24 February 1973

/50

59.5 N

177.0 W

Time - 13 h 00 min

Cloud cover - 10/7 Cb, As

H	P	T	u	d	v
0	I005	0,2	88	360	05
0,2	980	-2,9	90	360	05
0,5	944	-4,8	92	018	05
1,0	886	-7,0	90	343	06
1,5	831	-9,9	88	330	06
2,0	778	-13,4	88	035	03
3	682	-18,8	87	093	02
4	595	-25,9	86	130	02
5	517	-32,7	85	145	10
6	448	-38,5	83	145	13
7	387	-43,8	70	145	25
8	333	-46,1	55	147	29
9	286	-48,2	46	158	26
10	246	-48,1	42	160	20
II	211	-50,5	39	160	20
I2	181	-50,1	36	169	17
I3	155	-49,4	35	177	18
I4	134	-48,1	33	169	19
I5	115	-46,2	31	195	16
I6	99	-49,4	30	179	17
I7	85	-45,6	29	172	21
I8	73	-47,9	29	166	21
I9	63	-47,0	28	166	17
20	54	-48,1	27	190	16
21	46	-51,0	25	190	13
22	40	-52,7	24	190	09
23	34	-53,3	25	182	08
24	29	-53,0		175	08

Coordinates:

27 February 1973

/51

59.6 N
178.1 WTime - 09 hr 42 min
Cloud Cover - 10/10 Sc

H	P	T	U	d	V
0	I00I	0,2	9I	070	I8
0,2	976	-I,5	92	I00	I9
0,5	940	-4,6	94	II5	I9
I,0	882	-8,2	72	I40	I2
I,5	827	-II,4	49	I20	I4
2	775	-II,4	3I	I20	I3
3	679	-I6,4	23	II6	I8
4	594	-2I,0	I9	I34	23
5	518	-27,I	I8	II5	32
6	450	-33,8	20	II5	24
7	389	-40,8	2I	II0	I7
8	335	-48,6	2I	II0	20
9	287	-55,2	2I	I24	20
I0	246	-55,8	22	I23	26
I1	210	-48,8	22	I2I	22
I2	I8I	-47,8	2I	I25	II
I3	I55	-47,0	20	I2I	II
I4	I34	-46,0	20	II5	09
I5	II5	-48,6	I9	II5	09
I6	99	-49,4	I9	II5	08
I7	85	-49,I	I8	II5	09
I8	73	-5I,2	I9	II0	II
I9	62	-52,3	I8	I05	I0
I0	53	-52,6	I7	096	07
I1	46	-54,0	I7	093	05
I2	39	-53,9	I6	II0	03
I3	33	-54,2	I6	II0	08
I4	29	-55,9	I6	I0I	II

27 February 1973

Coordinates:

59.4 N
178.2 WTime - 13 hr 06 min
Cloud cover - 10/10 Sc, Cu

H	P	T	u	d	v
0	I002	0,2	92	II0	I5
0,2	977	-I,8	95	I00	I6
0,5	94I	-3,8	94	I20	I6
I,0	884	-6,5	95	I35	I4
I,5	828	-9,4	95	I37	I2
2,0	776	-II,8	94	I45	II
3	680	-I7,0	47	II5	I5
4	595	-I9,8	32	I25	20
5	519	-24,7	30	I25	28
6	452	-3I,7	33	I20	30
7	39I	-39,0	3I	II8	28
8	338	-45,6	30	II5	22
9	290	-5I,6	30	II6	22
I0	248	-54,2	30	I20	26
I1	2I3	-5I,0	30	I29	25
I2	I83	-47,8	30	I30	I5
I3	I57	-47,2	30	I36	I3
I4	I35	-46,0	29	I40	I0
I5	II6	-47,4	28	I40	07
I6	I00	-48,5	28	I39	08
I7	86	-49,I	28	I29	06
I8	74	-50,7	28	I25	07
I9	63	-52,0	28	I25	08
20	54	-52,0	28	I25	06
21	46	-53,3	28	I25	04
22	40	-53,8	28	I25	03
23	34	-54,0		II4	05
24	29	-55,0		I05	07

Coordinates:

1 March 1973

60.7 N
177.8 WTime - 8 hr 54 min
Cloud cover - 5/1 Cu, Ci

H	P	T	u	d	v
0	I0I5	-7,4	78	040	II
0,2	990	-9,6	77	055	I6
0,5	952	-I2,6	76	055	I4
I,0	892	-9,2	63	070	I4
I,5	836	-8,8	4I	070	I0
2,0	784	-I0,5	30	070	I2
3	688	-I5,6	40	050	I3
4	602	-20,0	39	060	I2
5	524	-28,6	44	060	I7
6	455	-36,0	58	060	I8
7	393	-43,0	47	05I	I3
8	338	-50,2	49	060	I6
9	289	-59,0	54	059	I9
I0	246	-62,4	55	059	I2
II	210	-54,9	47	C70	I2
I2	180	-5I,7	37	C85	05
I3	I54	-49,7	3I	085	06
I4	I32	-48,6	26	088	07
I5	II4	-48,3	24	I25	08
I6	98	-48,6	22	I35	08
I7	84	-49,3	22	II3	08
I8	72	-5I,6	2I	I2I	08
I9	62	-50,9	2I	I50	I0
I0	53	-5I,0	2I	II3	08
I1	45	-52,0	20	I00	09
I2	39	-52,2	I8	II5	I2
I3	33	-53,0	I9	II7	II
I4	28	-53,I	I20	I0	

Coordinates:

1 March 1973

/54

60.7 N
177.8 WTime - 14 hr 30 min
Cloud cover - 10/1 Ci, Cu

H	P	T	U	d	V
0	I015	-5,8	8I	050	I2
0,2	989	-7,3	80	040	I2
0,5	952	-9,5	80	050	I3
I,0	892	-9,2	69	050	II
I,5	837	-10,0	58	053	I2
2	784	-9,6	5I	065	09
3	688	-15,0	5I	060	07
4	602	-22,3	52	05I	09
5	524	-30,0	59	030	II
6	454	-35,6	70	040	I2
7	393	-41,9	72	043	I5
8	338	-49,9	72	045	I6
9	289	-59,0	73	045	I8
I0	246	-63,2	72	039	I4
I1	210	-53,5	68	035	07
I2	I80	-52,7	60	035	0I
I3	I54	-50,9	54	065	02
I4	I32	-49,6	49	I45	03
I5	II4	-48,8	46	I45	02
I6	97	-47,8	43	I3I	05
I7	84	-50,3	42	I30	07
I8	72	-50,3	40	I3I	06
I9	62	-5I,5	39	II8	06
20	53	-52,7	38	I03	I0
2I	45	-52,8	38	I20	08
22	39	-5I,7	37	I28	08
23	33	-53,0	36	I20	09
24	28	-53,8		I07	I0

Coordinates:

58.8 N
173.9 W

3 March 1973

Time - 10 hr 30 min
Cloud cover - 9/6 Cb, Cu, Ci

H	P	T	α	d	V
0	999	-9,6	8I	080	I7
0,2	973	-12,2	8I	090	I6
0,5	935	-14,6	7I	094	I9
I,0	875	-15,8	4I	106	I7
I,5	819	-16,0	28	II5	I4
2	767	-15,6	20	I20	I2
3	67I	-18,I	II	I2I	I2
4	586	-25,I	55	I82	05
5	510	-27,3	78	2I0	II
6	444	-32,0	79	2I0	I8
7	384	-39,6	78	2I0	I6
8	33I	-47,5	77	2I0	I9
9	284	-55,I	76	206	27
I0	242	-60,5	74	2I5	22
I1	207	-53,0	66	226	I8
I2	177	-52,0	59	215	I5
I3	152	-50,I	5I	245	I4
I4	130	-52,0	43	245	I0
I5	II2	-52,9	39	245	I0
I6	96	-54,0	36	223	I0
I7	82	-5I,6	36	200	09
I8	70	-49,7	33	I70	06
I9	60	-5I,4	29	I60	06
20	52	-5I,0	27	I60	09
2I	44	-52,2	25	I53	09
22	38	-5I,9	24	I45	09
23	32	-53,6	22	I42	I0
24	28	-53,0	20	I40	II

Coordinates:

3 March 1973

/56

58.2 N
172.8 WTime - 14 hr 48 min
Cloud cover - 10/10 NS, *

H	P	T	μ	d	V
0	993	- 9,6	85	080	I7
0,2	967	-12,0	85	080	I8
0,5	930	-14,5	85	097	I5
I,0	87I	-13,7	85	II7	I3
I,5	816	-13,3	86	I43	I2
2	764	-14,8	85	I78	II
3	668	-19,0	83	I62	07
4	583	-23,0	81	I92	II
5	508	-28,7	81	I80	II
6	44I	-33,6	74	I80	II
7	382	-40,0	50	I69	I4
8	339	-48,0	49	I62	II
9	282	-52,2	49	I86	I5
I0	242	-51,4	46	I99	I5
II	208	-48,2	45	2II	I4
I2	I78	-48,2	43	208	I5
I3	I53	-48,2	41	226	I7
I4	I32	-50,0	39	225	I4
I5	II3	-50,9	39	225	I3
I6	97	-50,8	40	225	I4
I7	83	-52,2	40	225	I4
I8	7I	-52,4	40	225	II
I9	6I	-50,7	40	207	II
20	52	-51,2	39	I75	I3
2I	45	-51,0	39	I75	09
22	38	-52,0	39	I75	08
23	33	-52,2		I75	07
24	28	-52,2		I5I	08

Coordinates:

60.7 N
178.6 W

6 March 1973

Time - 09 hr 06 min
Cloud cover - 1/1 Cu

H	P	T	u	d	v
0	I007	-I3,8	77	060	II
0,2	980	-16,4	81	054	I7
0,5	942	-18,0	81	056	I6
I,0	881	-16,2	59	070	I8
I,5	825	-15,8	37	070	08
2	772	-I7,6	35	052	05
3	674	-24,0	62	I60	02
4	587	-28,6	47	062	04
5	510	-34,6	36	210	03
6	441	-38,0	35	260	I4
7	381	-43,5	47	247	28
8	328	-47,6	58	240	32
9	281	-54,0	61	240	38
I0	240	-60,9	61	231	30
I1	204	-59,6	58	225	I7
I2	I74	-56,2	53	225	I6
I3	I49	-54,5	47	225	I4
I4	I28	-52,0	39	225	I5
I5	I10	-52,0	37	225	I7
I6	94	-51,4	36	225	21
I7	80	-50,6	34	231	21
I8	69	-50,6	31	235	I8
I9	59	-50,8	30	235	I5
20	51	-52,9	29	234	I4
21	43	-51,9	29	227	I4
22	37	-52,7		237	12
23	32	-52,2		250	I0
24	27	-51,3		250	I0

Coordinates:

6 March 1973

/58

60.9 N
178.6 WTime - 13 hr 36 min
Cloud cover - 5/2 Ci, Ac, Cu

H	P	T	u	d	v
0	I006	-I4,8	85	050	I0
0,2	980	-I6,8	86	045	II
0,5	94I	-I6,4	75	069	I2
I,0	88I	-I4,3	46	075	09
I,5	825	-I4,3	36	070	06
2	772	-I6,8	32	030	03
3	675	-21,0	52	I60	02
4	589	-26,6	40	I35	03
5	512	-32,3	35	I85	02
6	444	-36,4	32	266	I7
7	383	-40,6	42	254	26
8	330	-47,0	39	245	27
9	283	-53,9	55	239	27
I0	242	-61,I	55	235	29
II	206	-57,2	55	235	I7
I2	I76	-53,8	48	235	I7
I3	I5I	-51,0	40	230	I6
I4	I30	-50,2	37	230	I6
I5	III	-50,4	32	230	I7
I6	95	-46,5	30	23I	I8
I7	82	-47,6	29	235	I7
I8	70	-50,8	25	235	I8
I9	60	-50,I	27	235	I7
20	52	-49,6	27	235	I3
21	45	-48,I	27	235	I2
22	38	-49,5	24	235	I0
23	33	-49,2		239	I0
24	28	-47,5		253	II

Coordinates:

8 March 1973

60.3 N
179.3 WTime - 09 hr 48 min
Cloud cover - 10/10 Cb, V

H	P	T	u	α	v
0	998	-14,8	95	040	20
0,2	972	-17,8	96		
0,5	934	-21,6	97	050	24
1,0	873	-15,0	85	070	24
1,5	817	-14,2	70	075	I7
2	765	-16,4	77	075	I7
3	670	-18,3	82	085	II
4	585	-21,4	54	084	07
5	510	-26,0	59	075	04
6	443	-33,3	68	169	06
7	384	-40,7	75	191	08
8	331	-48,2	74	196	09
9	283	-56,1	72	220	10
10	242	-64,5	70	217	10
11	206	-57,3	67	211	10
12	176	-50,7	61	220	II
13	151	-52,5	56	220	12
14	129	-52,4	51	220	I3
15	III	-51,6	49	220	I5
16	95	-50,0	46	220	I7
17	82	-49,7	45	220	I9
18	70	-47,9	44	220	I4
19	60	-49,6	43	218	I2
20	52	-48,2	42	216	I2
21	44	-49,3		205	II

APPENDIX II. 2

/60

TABLES OF STANDARD METEOROLOGICAL OBSERVATIONS AT 15-MIN INTERVALS

/61

Время границы a)	Местоположение судна (град. мин.)		Количество облаков одинаковой непрерывности (град.)	Истинный ² ветер		i) видимость км	j) Гидро- метеороло- гичес- кие явления (вспало- ковец)	k) корректируемое ат- мосферное давле- ние над морем мм	l) температура воздуха С°	m) температура воды С°	n) однозначность			o) влажность				
	Широта сев. с.)	Долгота зап.-д.)		направление (град.)	скорость (м/сек.)						w) облачность средней формы	q) высота нижней формы	r) высота средней формы	s) высота верхней формы	t) температура тумана С°	u) абсолютная мб	v) относитель- ная %	
I	2	3	4	5	6	7	8	9	10	11	12	13	14	15	16	17	18	19
15-16 February 1973																		
22 30	61°00'	178°00'	[10]	28	I5	2,0	4° П	755,4	-9,9	-0,4	[10]	C8	400	0	0	-12,0	2,2	77
22 45	61 00	178 00	10	40	I6	1,5	5° П	755,5	-9,7	-0,4	10	C6	400	x	x	-11,5	2,3	78
23 00	61 00	178 00	[10]	20	I3	2,0	5° П	755,5	-9,5	-0,4	[10]	C6	400	0	0	-11,5	2,3	78
23 15	61 00	178 00	10	30	I4	0,2	5° П	754,8	-10,1	-0,4	10	C6	400	x	x	-12,00	2,2	77
23 30	61 00	178 00	10	50	I4	0,1	5° П	755,4	-10,0	-0,4	10	C6	400	x	x	-12,0	2,2	77
23 45	61 00	178 00	10	40	I5	0,4	5° П	755,4	-9,7	-0,4	10	C6	400	x	x	-11,0	2,4	81
00 00	61 00	178,00	10	30	I3	0,4	5° П	755,5	-8,9	-0,4	10	C6	400	x	x	-10,1	2,6	83
00 15	61 00	178 00	[10]	30	I4	0,5	5° П	755,4	-9,7	-0,4	[10]	C6	400	x	x	-10,1	2,6	83
00 30	61 00	178 00	[10]	30	I5	0,8	5° П	755,6	-10,1	-0,4	[10]	C6	400	0	0	-10,1	2,6	83
00 45	61 00	178 00	10	30	I5	0,9	5° П	755,6	-10,1	-0,4	[10]	C6	400	0	0	-11,0	2,4	86
01 00	61 00	178 00	10	20	I5	0,3	5° П	755,6	-9,9	-0,4	10	C6	400	x	x	-11,5	2,3	81
01 15	61 00	178 00	[10]	20	I4	3,0	[5] П	755,6	-10,2	-0,4	10	C6	400	x	x	-11,5	2,3	81
01 30	61 00	178 00	[10]	20	I4	4,0	[5] П	755,6	-9,5	-0,4	[10]	C6	400	0	0	-11,0	2,4	82
01 45	61 00	178 00	10	10	I5	0,8	5° П	755,4	-9,8	-0,4	[10]	C6	400	0	0	-12,5	2,1	71
02 00	61 00	178 00	[10]	20	I5	2,0	[5] П	755,6	-10,1	-0,4	10	C6	400	x	x	-11,0	2,4	86
02 15	61 00	178 00	[10]	20	I5	2,0	[5] П	755,6	-10,2	-0,5	[10]	C6	400	0	0	-11,0	2,4	86
02 30	61 00	178 00	10	20	I4	1,0	[5] П	755,4	-9,9	-0,5	10	C6	400	0	0	-11,5	2,3	81
02 45	61 00	178 00	10	20	I3	0,7	5° П	755,5	-9,9	-0,5	10	C6	400	x	x	-11,5	2,3	81

KEY: a) Greenwich time; b) ship's position (deg. min); c) N. Lat.; d) W. long; e) overall sky cover; f) true wind; g) direction (deg); h) velocity (m/sec); i) visibility (km); j) hydrometeorological phenomena (start-finish); k) corrected atmospheric pressure above sea level (mm); l) air tem. C°; m) water tem. C°; n) cloudiness; o) humidity; p) form (lower); q) height (lower or upper); r) form (middle); s) form (upper); t) dew point temperature C°; u) absolute (mb); v) relative (%). w) amount

I	2	3	4	5	6	7	8	9	10	II	12	13	14	15	16	17	18	19
03 00	61 00	I78 00	10	10	II	0,5	8 0	755,5	-9,9	-0,5	10	Cb	400	x	x	-II,0	2,4	85
16-17 February 1973																		
21 30	60 31	I78 00	10	40	I4	I,5	8' 0	756,8	-12,7	-0,2	10	Cb	400	0	0	-12,0	2,2	95
21 45	60 28	I78 00	10	40	I4	I,0	8' 0	756,6	-12,4	-0,1	10	Cb	400	x	x	-12,0	2,2	95
22 00	60 25	I78 00	10	40	I4	I,5	8' 0	756,6	-12,7	0,0	10	Cb	400	0	0	-12,0	2,2	95
22 15	60 20	I78 00	10	40	I4	I,5	8' 0	756,6	-12,7	0,0	10	Cb	400	0	0	-12,0	2,2	95
22 30	60 16	I78 00	10	50	I3	I,0	8' 0	756,6	-12,3	0,0	10	Cb	400	0	0	-12,0	2,2	95
22 45	60 13	I78 00	10	40	I2	I,5	8' 0	756,2	-12,0	-0,1	10	Cb	400	0	0	-12,0	2,2	91
23 00	60 10	I78 00	10	40	I2	2,0	8' 0	755,8	-12,5	-0,1	10	Cb	400	0	0	-II,5	2,3	97
23 15	60 10	I78 00	10	40	I2	2,0	8' 0	755,6	-12,3	-0,2	10	Cb	400	0	0	-12,0	2,2	94
23 30	60 09	I78 00	10	40	I2	2,0	8' 0	755,5	-12,1	-0,2	10	Cb	400	0	0	-12,0	2,2	92
23 45	60 00	I78 00	10	20	I2	2,0	8' 0	755,7	-11,8	-0,1	10	Cb	400	0	0	-12,0	2,2	90
00 00	60 00	I78 00	10	20	I2	2,0	8' 0	755,6	-12,5	0,0	10	Cb	400	0	0	-12,0	2,2	93
00 15	60 00	I78 00	10	20	I2	2,0	8' 0	755,4	-11,4	0,0	10	Cb	400	0	0	-12,0	2,2	85
00 30	60 00	I78 00	10	20	I2	3,0	[8] 0	755,2	-12,1	-0,1	10	Cb	400	0	0	-12,0	2,2	90
00 45	60 00	I78 00	8	30	I4	3,0	[8] 0	755,4	-12,1	-0,2	8	Cb	400	0	0	-12,0	2,2	90
01 00	60 00	I78 00	9	30	I4	I,0	[8] 0	755,5	-11,1	-0,2	9	Cb	400	0	0	-II,0	2,4	89
19-20 February 1973																		
21 30	60 43	I78 30	7	10	II	I,5	[[V]] 0	752,8	-15,2	-0,1	7	Cu _{avg}	500	0	0	-14,8	I,7	94
21 45	60 43	I78 30	8	10	II	I,0	[[V]] 0	752,5	-15,0	0,0	8	Cu _{avg}	500	0	0	-14,2	I,8	94
22 00	60 43	I78 30	8	20	II	I,0	[[V]]	752,7	-15,5	0,0	8	Cu _{avg}	500	0	0	-14,8	I,7	93
22 15	60 43	I78 30	7	20	II	I,0	[[V]] 0	752,4	-15,1	0,0	7	Cu _{med}	500	0	0	-14,8	I,7	89
22 30	60 43	I78 30	8	20	II	0,5	[[V]] 0	751,9	-15,1	0,0	8	Cu _{med}	500	0	0	-14,8	I,7	89
22 45	60 43	I78 30	8	20	II	I,0	[[V]] 0	752,2	-15,4	-0,2	8	Cu _{avg}	500	0	0	-15,5	I,6	89
23 00	60 43	I78 30	7	10	II	2,0	[[V]] 0	752,5	-14,9	-0,2	7	Cu _{hum}	500	0	0	-14,8	I,7	86
23 15	60 43	I78 30	7	10	II	I,5	[[V]] 0	752,1	-15,3	-0,2	7	Cu _{med}	500	0	0	-15,5	I,6	87

I	2	3	4	5	6	7	8	9	10	II	12	13	14	15	16	17	18	19
23 30	60 43	I78 30	7	IO	II	2,0	III v o	752,0	-15,3	-0,2	7	Cu fr Cu med	500	0	0	-14,8	I,7	91
23 45	60 43	I78 30	6	IO	II	1,5	III v o	751,9	-14,9	-0,2	6	Cu fr Cu med	500	0	0	-15,5	I,6	84
00 00	60 43	I78 30	6	IO	II	1,5	III v o	751,9	-14,7	-0,2	6	Cu med	500	0	0	-14,8	I,7	86
00 15	60 43	I78 30	8	IO	II	1,5	III v II	751,8	-14,9	0,0	8	Cu med Cu cong	500	0	0	-15,5	I,6	84
00 30	60 43	I78 30	8	IO	II	0,6	III v II	751,7	-15,1	+0,1	8	Cu med	500	0	0	-14,8	I,7	87
00 45	60 43	I78 30	9	IO	II	0,8	III v II	751,4	-14,5	0,1	9	Cu med Cu cong	500	0	0	-14,8	I,7	84
01 00	60 43	I78 30	6	IO	II	1,5	III v II	751,2	-14,5	0,1	6	Cu med Cu cong	500	0	0	-14,2	I,8	88

20-21 February 1973

21 30	60 30	I78 40	IO	360	I4	0,8	III v II	751,5	-12,7	-0,4	10	Cb Cu cong	400	x	x	-12,0	2,2	98
21 45	60 30	I78 40	IO	360	I2	0,8	III v II	751,7	-12,7	-0,4	10	Cb Cu cong	400	x	x	-12,0	2,2	98
22 00	60 30	I78 40	IO	360	I2	0,6	III v	751,8	-13,1	0,5	10	Cb	400	x	x	-12,5	2,1	95
22 15	60 30	I78 40	10	360	I2	0,6	III v	751,7	-12,8	0,5	10	Cb Sc	400	0	0	-12,5	2,1	93
22 30	60 30	I78 40	10	360	I2	0,6	III v	751,8	-12,7	0,5	10	Cb	400	0	0	-11,5	2,3	97
22 45	60 30	I78 40	10	360	I2	0,5	III II	751,8	-12,0	0,4	10	Cu cong Cb Sc	400	0	0	-12,0	2,2	91
23 00	60 30	I78 40	9	360	I2	1,0	III II	752,1	-12,7	0,4	9	Cb Cu cong	400	0	0	-12,0	2,2	92
23 15	60 30	I78 40	9	360	I2	1,0	III II	752,2	-12,5	0,4	8	Cb	400	0	0	-12,5	2,1	90
23 30	60 30	I78 40	8	360	I2	1,0	III II	752,4	-12,5	0,4	8	Cb	400	0	0	-12,0	2,2	94
23 45	60 30	I78 40	9	360	I2	1,5	III II	752,4	-12,2	0,4	8	Cb	400	0	0	-12,0	2,2	94
00 00	60 30	I78 40	9	360	I2	1,0	III II	652,6	-12,1	0,4	8	Cu cong	400	0	0	-11,5	2,3	94
00 15	60 30	I78 40	9	360	I2	1,0	III II	752,6	-12,0	0,3	8	Cu cong	400	0	0	-11,5	2,3	94
00 30	60 30	I78 40	10	360	II	1,0	III II	752,8	-12,0	0,3	10	Cu cong	400	0	0	-12,0	2,2	92
00 45	60 30	I78 40	10	360	II	1,0	III II	753,0	-11,7	0,3	9	Cu cong	400	0	0	-12,0	2,2	86
01 00	60 30	I78 40	10	360	II	1,0	III II	753,1	-12,3	0,4	9	Cu cong	400	0	0	-12,0	2,1	90
01 15	60 30	I78 40	9	360	II	1,0	o III	753,1	-12,2	0,4	8	Cu cong	400	0	0	-12,0	2,2	89
01 30	60 30	I78 40	7	360	II	1,0	o III	753,1	-11,8	0,1	7	Cu cong	400	0	0	-12,0	2,2	92

1	2	3	4	5	6	7	8	9	10	II	12	13	14	15	16	17	18	19	
23-24 February 1973																			
21 30	59°30'	177°00'	IO	350	4	10	⊕ *	○*	752,4	-0,8	0,I	I	Cu med	700	As As	C6	-2,0	5,2	9I
21 45	59 30	177 00	IO	350	4	10	⊕	○*	752,5	-0,7	0,I	4	Cu med	700	As	C5	-1,7	5,3	9I
22 00	59 30	177 00	IO	360	5	10	○*		752,7	-0,8	0,I	6	Cu med	700	As	C5	-2,0	5,2	9I
22 15	59 30	177 00	IO	360	5	10	○*		752,7	-0,7	0,I	6	Cu med	700	As	C5	-1,7	5,3	9I
22 30	59 30	177 00	IO	340	4	10	○*	**	752,7	-0,4	0,I	6	Cu med	700	As	x	-1,5	5,4	9I
22 45	59 30	177 00	IO	340	4	10	○*	**	752,8	-0,3	0,I	8	Cu med	700	As	x	-2,0	5,2	8I
23 00	59 30	177 00	IO	320	4	10	**	□	752,8	-0,3	0,I	7	Cu med	700	As	x	-1,5	5,4	9I
23 15	59 30	177 00	IO	320	5	10	**	□	753,3	-0,4	0,I	IO	Sc op	600	x	x	-1,7	5,3	89
23 30	59 30	177 00	IO	350	5	10	**	□	753,4	-0,5	0,I	IO	Cu med	600	x	x	-1,5	5,4	9I
23 45	59 30	177 00	IO	360	5	3,0	▽	○*	753,4	-0,5	0,I	8	Cb cap	600	Astr	x	-1,5	5,4	9I
00 00	59 30	177 00	IO	360	5	1,5	▽	○*	753,5	-0,7	0,I	8	Cb cap	600	Astr	x	-1,3	5,5	95
00 15	59 30	177 00	IO	360	4	1,5	▽	○*	753,6	-0,3	0,2	8	Cb	600	Astr	x	-1,5	5,4	9I
00 30	59 30	177 00	IO	360	4	1,5	▽	○*	753,6	-0,3	0,2	8	Cb	600	Astr	x	-1,5	5,4	9I
00 45	59 30	177 00	IO	340	5	2,0	▽	=*	753,6	-0,4	0,2	8	Cb	600	Astr	x	-1,5	5,4	9I
01 00	59 30	177 00	IO	340	5	3,0	▽		753,6	-1,0	0,3	6	Cb	600	Ac	x	-2,0	5,2	92
01 15	59 30	177 00	8	340	5	IO	○		753,6	-0,5	0,4	5	Cu cong	600	Ac	Ci	-2,0	5,2	89
01 30	59 30	177 00	8	340	5	IO	○*		753,6	-0,9	0,4	5	Cu cong	600	Ac	Ci	-2,0	5,2	90
01 45	59 30	177 00	8	340	5	IO	○*		753,6	-0,9	0,4	5	Cu cong	600	Ac	Ci	-1,7	5,3	93
26-27 February 1973																			
23 15	59 39	178 04	IO	II0	I4	15	□		751,4	0,2	1,7	IO	Sc,Cu _{tr}	500	x	x	-1,4	5,5	88
23 30	59 28	179 04	IO	II0	I4	15	□		751,2	0,2	1,7	IO	Sc _{tr}	500	x	x	-1,4	5,5	88
23 45	59 28	178 04	IO	II0	I4	15	□		751,2	0,3	1,7	IO	Sc _{tr}	500	x	x	-1,4	5,5	88
00 00	59 28	178 04	IO	II0	I4	15	□		751,4	0,1	1,7	IO	Sc _{tr}	500	x	x	-1,4	5,5	90
00 15	59 28	178 04	IO	II0	I4	15	□		751,5	0,1	1,7	IO	Sc _{tr}	500	x	x	-0,07	5,8	94
00 30	59 28	178 04	IO	II0	I4	15	□,*		751,5	0,1	1,7	IO	Sc _{tr}	500	x	x	-0,3	6,0	98

I	2	3	4	5	6	7	8	9	10	II	12	13	14	15	16	17	18	19
00 45	59°28'	I78°04'	10	90	15	15	II	75I.5	0,I	I,7	10	Sc	500	x	x	-1,4	5,5	90
01 00	59 28	I78 04	10	90	14	15	II	75I.4	0,3	I,7	10	Sc	500	x	x	-0,5	5,9	94
01 15	59 28	I78 04	10	110	14	15	II	75I.4	0,2	I,7	10	Sc	500	x	x	-0,3	6,0	96
01 30	59 28	I78 04	10	110	14	15	II	75I.4	0,2	I,6	10	Sc	500	x	x	-0,3	6,0	96

28 February - 1 March 1973

21 30	60 37	I77 54	4	40	II	30	O°	76I.6	-7,0	-I,2	2	Cu hum	400	x	Ci sp	-9,7	2,7	73
21 45	60 39	I77 50	5	40	II	30	O°	76I.7	-6,7	-I,2	2	Cu hum	400	o	Ci sp	-9,7	2,7	74
22 00	60 42	I77 46	3	50	10	30	O°	76I.8	-6,5	-I,2	2	Cu hum	600	o	Ci sp	-9,3	2,8	74
22 15	60 42	I77 46	5	50	10	30	O°	76I.8	-4,9	-I,2	I	Cu hum	600	o	Ci sp	-9,3	2,8	77
22 30	60 42	I77 46	5	50	10	30	O°	76I.7	-5,8	-I,2	I	Cu hum	600	o	Ci sp	-9,3	2,8	70
22 45	60 42	I77 46	5	50	10	30	O°	76I.5	-6,2	-I,0	2	Cu hum	600	o	Ci sp	-9,7	2,7	69
23 00	60 42	I77 46	6	50	II	30	O°	76I.5	-6,2	-I,0	I	Cu hum	600	o	Ci sp	-9,3	2,8	72
23 15	60 42	I77 46	8	40	II	30	O°	76I.5	-6,3	-I,0	I	Cu hum	600	o	Ci sp	-10,6	2,5	66
23 30	60 42	I77 46	10	50	II	30	O°	76I.3	-6,3	I,0	I	Cu hum	600	o	Ci sp	-10,I	2,6	69
23 45	60 42	I77 46	10	50	II	30	O°	76I.1	-6,6	-I,0	I	Cu hum	600	o	Ci sp	-11,0	2,4	65
00 00	60 42	I77 46	7	40	II	30	O°	76I.1	-6,7	-I,0	I	Cu hum	600	o	Ci sp	-10,I	2,6	71
00 15	60 42	I77 46	7	40	II	30	O°	76I.1	-6,6	-I,0	I	Cu hum	600	o	Ci sp	-10,I	2,6	68
00 30	60 40	I77 48	7	50	10	30	O°	76I.2	-6,5	-I,0	I	Cu hum	600	o	Ci sp	-9,7	2,7	72
00 45	60 41	I77 50	7	50	10	30	O°	76I.5	-6,7	-I,0	I	Cu hum	600	o	Ci sp	-10,I	2,6	71
01 00	60 37	I77 54	9	50	10	30	O°	76I.5	-6,7	-I,0	I	Cu hum	600	o	Ci sp	-10,I	2,6	71
01 15	60 37	I77 54	8	50	10	30	O°	76I.0	-6,6	-I,0	I	Cu hum	600	o	Ci sp	-9,3	2,8	74
01 30	60 37	I77 54	8	50	10	30	O°	76I.3	-6,5	-I,0	I	Cu hum	600	o	Ci sp	-10,6	2,5	66
01 45	60 37	I77 54	8	50	10	30	O°	76I.3	-6,2	-I,0	I	Cu hum	600	o	Ci sp	-11,0	2,4	64
02 00	60 37	I77 54	8	50	10	30	O°	76I.3	-5,9	-I,2	I	Cu hum	600	o	Ci sp	-11,0	2,4	62
02 15	60 37	I77 54	6	40	10	30	O°	76I.3	-6,1	-I,2	I	Cu hum	600	o	Ci sp	-9,7	2,7	70
02 30	60 37	I77 54	6	30	10	30	O°	76I.4	-6,1	-I,2	I	Cu hum	600	o	Ci sp	-9,3	2,8	72

1	2	3	4	5	6	7	8	9	10	II	12	13	14	15	16	17	18	19
02 45	60°37'	I77°54'	7	30	10	30	0°	761,4	-6,I	-I,2	I	Cu hum	600	0	Ci sp	-8,8	2,9	75
03 00	60 37	I77 54	8	30	10	30	0°	761,2	-6,I	-I,2	I	Cu hum	600	0	Ci sp	-9,7	2,7	70
03 15	60 37	I77 54	8	40	10	30	0°	760,9	-5,9	-I,I	0	0	600	0	Ci sp	-10,I	2,6	67
03 30	60 37	I77 54	8	40	10	30	0°	760,9	-5,7	-I,I	0	0	600	0	Ci sp	-9,7	2,7	68
03 45	60 37	I77 54	7	40	10	30	0°	750,9	-5,7	-I,I	I	Cu hum	600	0	Ci sp	-8,I	3,I	78
04 00	60 37	I77 54	7	40	10	30	0°	761,0	-6,0	-I,2	I	Cu hum	600	0	Ci sp	-8,5	3,0	78

2-3 March 1973

23 00	58 42	I73 45	10	80	21	5	0°	747,6	-9,7	0,2	7	Cu cong	500	Astr	x	-II,0	2,4	81
23 15	58 36	I73 32	10	80	21	4	0°	747,5	-9,5	0,4	7	Cu fr, Cb ap	500	As op	x	-IO,6	2,5	85
23 30	58 31	I73 32	10	70	20	4	0°	747,1	-9,6	0,4	7	Cu fr, Cb ap	500	As op	x	-IO,6	2,5	85
23 45	58 29	I73 26	10	80	20	4	0°	746,9	-9,6	0,4	10	Cu fr, Cb ap	500	As op	x	-IO,1	2,6	88
00 00	58 28	I73 19	10	70	18	4	0°	746,8	-10,I	0,4	10	Cu fr, Cb ap	500	As op	x	-II,0	2,4	85
00 15	58 28	I73 16	10	90	20	4	[5]	746,4	-10,3	0,4	10	Cu fr, Cb ap	500	x	x	-II,0	2,4	85
00 30	58 27	I73 13	10	90	20	4	[5]	746,3	-10,I	0,1	10	Cu fr, Cb ap	500	x	x	-IO,6	2,5	87
00 45	58 26	I73 10	10	90	20	4	[5]	746,2	-10,4	0,1	10	Cu fr, Cb ap	500	x	x	-II,0	2,4	85
01 00	58 25	I73 06	10	70	18	4	[5]	746,2	-10,4	0,1	10	Cb	500	x	x	-IO,6	2,5	89
01 15	58 23	I73 04	10	70	18	4	[5]	746,1	-10,5	0,1	10	Cb	500	x	x	-IO,6	2,5	91
01 30	58 18	I72 55	10	70	18	I	0°	746,0	-10,5	0,0	10	Cb	500	x	x	-IO,6	2,5	91
01 45	58 17	I72 52	10	60	20	I	*	744,5	-10,3	0,0	10	Ns	500	x	x	-10,I	2,6	90
02 00	58 16	I72 48	10	80	17	I	*	744,1	-10,5	0,1	10	Ns	500	x	x	-10,I	2,6	94
02 15	58 16	I72 48	10	80	17	I	*	744,2	-10,4	0,2	10	Ns	500	x	x	-10,I	2,6	89

5-6 March 1973

21 30	60 43	I78 38	2	60	12	30	0°	754,8	-14,0	-I,5	2	Cu hum	500	0	0			
21 45	60 46	I78 32	3	50	14	30	0°	754,7	-14,3	-I,5	2	Cu hum	500	0	0			
22 00	60 48	I78 28	3	50	14	30	0° III	754,9	-14,3	-I,5	2	Cu hum	500	0	0			

I	2	3	4	5	6	7	8	9	10	II	12	13	14	15	16	17	18	19
22 15	60°49'	I78°25'	3	50	14	30	○ M°	754,9	-14,6	-1,5	2	Cu hum	500	0	Ci fil			
22 30	60 50	I78 22	2	60	13	30	○ M°	754,9	-15,1	-1,5	1	Cu hum	500	0	Ci fil			
22 45	60 50	I78 22	4	60	13	30	○	755,2	-15,1	-1,5	2	Cu hum	500	0	Ci fil			
23 00	60 50	I78 21	5	60	13	30	○ M°	755,0	-14,5	-1,5	2	Cu hum	500	0	Ci fil			
23 15	60 51	I78 20	6	40	11	30	○ M°	754,9	-15,2	-1,5	1	Cu hum	500	0	Ci fil			
23 30	60 51	I78 20	6	40	9	30	○ M°	754,8	-15,2	-1,5	1	Cu hum	500	0	Ci fil			
23 45	60 51	I78 20	6	40	9	30	○ M°	754,8	-15,4	-1,5	2	Cu hum	500	0	Ci fil			
00 00	60 52	I78 I9	6	40	9	30	○ M°	754,6	-15,3	-1,5	2	Cu hum	500	Ac	Ci	-15,5	1,6	85
00 15	60 52	I78 I9	4	40	9	30	○ M°	754,6	-14,5	-1,4	3	Cu hum	500	Ac	Ci	-14,2	1,8	89
00 30	60 52	I78 I9	5	40	9	30	○ M°	754,5	-14,5	-1,3	3	Cu hum	500	Ac	Ci	-14,2	1,6	86
00 45	60 52	I78 I9	5	50	10	30	○ M°	754,1	-14,6	-1,3	3	Cu hum	500	Ac	Ci	-15,5	1,6	85
01 00	60 52	I78 I9	7	50	10	30	○ M°	754,0	-14,6	-1,3	4	Cu hum	500	Ac	Ci	-14,8	1,7	86
01 15	60 52	I78 I9	6	50	10	30	○ M°	753,6	-14,3	-1,3	4	Cu hum	500	Ac	Ci	-14,8	1,7	82
01 30	60 52	I78 I9	5	50	10	30	○ M°	753,6	-14,7	-1,3	2	Cu hum	500	Ac	Ci	-14,8	1,7	86
01 45	60 52	I78 I9	5	50	10	30	○ M°	753,6	-14,3	-1,3	2	Cu hum	500	Ac	Ci	-14,8	1,7	83
02 00	60 52	I78 I9	5	50	10	30	○ M°	753,5	-14,5	-1,3	2	Cu hum	500	Ac	Ci	-14,2	1,6	86
02 15	60 52	I78 I9	6	60	8	30	○ M°	753,5	-14,3	-1,3	2	Cu hum	500	Ac	Ci	-14,2	1,6	86

7-8 March 1973 -

23 00	60 I8	I79 20	[10]	40	22	0,I	$\text{M}^{\circ} \vee \text{P}^{\circ}$	747,2	-14,1	1,0	[10]	Cb, Cufr	400	0	0	-13,0	2,0	98
23 15	60 I8	I79 20	[10]	40	21	0,I	$\text{M}^{\circ} \vee \text{P}^{\circ}$	747,2	-14,0	0,9	[10]	Cb, Cufr	400	0	0	-13,0	2,0	97
23 30	60 I8	I79 20	[10]	40	21	0,I	$\text{M}^{\circ} \vee \text{P}^{\circ}$	747,2	-13,8	0,9	[10]	Cb, Cufr	400	0	0	-12,5	2,1	97
23 45	60 I8	I79 20	[10]	40	21	0,I	$\text{M}^{\circ} \vee \text{P}^{\circ}$	746,5	-14,1	0,9	[10]	Cb, Cufr	400	0	0	-13,0	2,0	97
00 00	60 I8	I79 20	[10]	40	21	0,I	$\text{M}^{\circ} \vee \text{P}^{\circ}$	747,2	-13,8	1,0	[10]	Cb, Cufr	400	0	0	-12,5	2,1	97
00 15	60 I8	I79 20	[10]	40	21	0,I	$\equiv \text{V}^{\circ}$	747,2	-14,1	1,2	[10]	Cu cong, Cufr	400	0	0	-13,0	2,0	97
00 30	60 I7	I79 23	[10]	40	21	0,I	$\equiv \text{V}^{\circ}$	746,8	-13,5	1,5	[10]	Cu cong, Cufr	400	0	0	-12,5	2,1	97
00 45	60 I7	I79 27	[10]	40	21	0,I	$\equiv \text{V}^{\circ}$	746,8	-13,3	1,5	[10]	Cu cong, Cufr	400	0	0	-12,5	2,1	96
01 00	60 I7	I79 27	[10]	40	21	0,I	$\equiv \text{V}^{\circ}$	746,8	-14,2	1,5	[10]	Cu cong, Cufr	400	0	0	-13,6	1,9	92

I	2	3	4	5	6	7	8	9	10	II	12	13	14	15	16	17	18	19
01 15	60°17'	I79°27'	[10]	40	20	0,I	$\equiv \text{V}^{\circ}$	746,9	-15,0	1,5	[10]	Cu cong, Cufr	400	0	0	-14,2	1,8	92
01 30	60 17	I79 27	[10]	40	19	0,I	$\equiv \text{V}^{\circ}$	747,2	-15,0	1,4	[10]	Cu cong, Cufr	400	0	0	-14,2	1,8	92
01 45	60 17	I79 28	[10]	40	19	0,I	$\equiv \text{V}^{\circ}$	746,8	-14,9	1,4	[10]	Cu cong, Cufr	400	0	0	-14,2	1,8	91
02 00	60 16	I79 29	[10]	40	18	0,I	$\equiv \text{V}^{\circ}$	746,2	-14,7	1,4	[10]	Cu cong, Cufr	400	0	0	-14,2	1,8	91
02 15	60 16	I79 32	[10]	40	18	0,I	$\equiv \text{V}^{\circ}$	745,9	-15,2	1,4	[10]	Cu cong, Cufr	400	0	0	-14,8	1,7	91
02 30	60 16	I79 32	[10]	40	19	0,I	$\equiv \text{V}^{\circ}$	746,1	-15,2	1,4	[10]	Cu cong, Cufr	400	0	0	-14,8	1,7	91
02 45	60 14	I79 32	[10]	40	19	0,I	$\equiv \text{V}^{\circ}$	745,9	-15,1	1,4	[10]	Cu cong, Cufr	400	0	0	-14,2	1,8	91
03 00	60 14	I79 32	[10]	40	19	0,I	$\equiv \text{V}^{\circ}$	745,8	-15,2	1,4	[10]	Cu cong, Cufr	400	0	0	-14,8	1,7	91

APPENDIX III. 1

/69

TABLES OF RADIATION TEMPERATURES OF WATER AND ICE SURFACES

15-16 February 1973

/70

a) Время (грин- вича)	b) Координаты		Темпера- тура воздуха (°C)	Влаж- ность относи- тельная (%) e)	Темпера- тура по- верхности воды по ртутному термомет- ру (°C)f)	Радиаци- онная темпере- тура во- да (°C) g)
	N. Lat.	W. Long	d)	e)	f)	g)
22.30	61°00'	178°00'	-9,9	77	-0,4	-0,2
22.45	61 00	178 00	-9,7	78	-0,4	-0,1
23.00	61 00	178 00	-9,5	78	-0,4-	0,1
23.15	61 00	178 00	-10,1	78	-0,4	-0,2
23.30	61 00	178 00	-10,0	77	-0,4	-0,3
23.45	61 00	178 00	-9,7	81	-0,4	-0,4
00 00	61 00	178 00	-8,9	83	-0,4	-0,1
00 15	61 00	178 00	-9,7	88	-0,4	-0,1
00 30	61 00	178 00	-10,1	-	-0,4	-0,4
00 45	61 00	178 00	-9,9	81	-0,4	-0,4
01 00	61 00	178 00	-10,2	-	-0,4	-0,2
01 15	61 00	178 00	-9,5	82	-0,4	0,0
01 30	61 00	178 00	-9,8	71	-0,4	-0,1
01 45	61 00	178 00	-10,1	-	-0,4	0,0
02 00	61 00	178 00	-10,2	81	-0,5	0,1
02 15	61 00	178 00	-9,9	81	-0,5	0,0
02 30	61 00	178 00	-9,9	77	-0,5	0,0
02 45	61 00	178 00	-9,9	81	-0,5	-
03 00	61 00	178 00	-9,9	85	-0,5	-
Average over flight			-9,8		-0,43	0,14
Mean-square deviation S					0,05	0,16
Dispersion $\hat{\sigma}^2$					0,002	0,02
Wind $10-50^0 = 13-16 \text{ m/sec}$						

KEY: a) Time (greenwich); b) coordinates; c) air temp. (°C);
d) relative humidity (%); e) water surface temperature (mercury thermometer) (°C); f) radiation temperature of water (°C).

16-17 February 1973

/71

a) Время (грин- вича)	b) Координаты		Темпера- тура воздуха (°C) c)	Влаж- ность относи- тельная d) (%)	Темпера- тура по- верхности воды по ртутному термометру e) (°C)	Радиа- ционная темпере- тура во- ды f) (°C)
	N. Lat.	W. Long				
21.30	60°31'	178°00'	-12,7	95	-0,2	-
21 45	60 28	178 00	-12,4	95	-0,1	-
22 00	60 25	178 00	-12,7	95	0,0	-
22 15	60 20	178 00	-12,7	95	0,0	-
22 30	60 16	178 00	-12,3	95	0,0	-
22 45	60 13	178 00	-12,0	91	-0,1	-
23 00	60 10	178 00	-12,5	97	-0,1	-
23 15	60 10	178 00	-12,3	94	-0,2	-
23 30	60 00	178 00	-12,1	92	-0,2	0,2
23 45	60 00	178 00	-11,8	90	-0,1	0,0
00 00	60 00	178 00	-12,5	93	0,0	0,1
00 15	60 00	178 00	-11,4	85	0,0	0,1
00 30	60 00	178 00	-12,1	90	-0,1	0,0
00 45	60 00	178 00	-12,1	90	-0,2	-0,3
01 00	60 00	178 00	-11,1	89	-0,2	-0,3

Average value over flight -12.1

-0,1 0,0

Mean-square deviation S

0,08 0,14

Dispersion $\hat{\sigma}^2$

0,006 0,02

Wind 20° - 40° = 12-14 m/sec

Note: IR radiometer did not operate until 2330.

KEY: a) Time (Greenwich); b) coordinates; c) air temp. (°C);
d) relative humidity (%); e) water surface temperature (mercury
thermometer) (°C); f) radiation temperature of water (°C).

19-20 February 1973

/72

a) Время (гри- вича)	b) Координаты		Темпе- ратура возду- ха (°C) c)	Влаж- ность относи- тельная (%) d)	Темпера- тура по- верхнос- ти воды по ртут- ному тер- мометру e) (°C)	Радиаци- онная темпере- тура во- ды (°C) f)
21.30	60°43'	178°30'	-15,2	94	-0,1	-0,1
21 45	60 43	178 30	-15,0	94	0,0	-0,1
22 00	60 43	178 30	-15,5	93	0,0	0,0
22 15	60 43	178 30	-15,1	89	0,0	0,1
22 30	60 43	178 30	-15,1	89	0,0	-0,3
22 45	60 43	178 30	-15,4	89	0,0	-0,2
23 00	60 43	178 30	-14,9	86	0,2	0,1
23 15	60 43	178 30	-15,3	87	0,2	-0,1
23 30	60 43	178 30	-15,3	91	0,1	0,0
23 45	60 43	178 30	-14,9	84	0,1	-0,1
00 00	60 43	178 30	-14,7	86	0,0	-0,1
00 15	60 43	178 30	-14,9	84	0,0	-0,2
00 30	60 43	178 30	-15,1	87	0,0	-0,1
00 45	60 43	178 30	-14,5	84	0,0	0,0
01 00	60 43	178 30	-14,5	88	0,0	-0,1
Average value over flight -15.0					0,0	-0,1
Mean-square deviation S					0,08	0,1
Dispersion σ^2					0,006	0,01
Wind $10^0\text{-}20^0 = \text{II-I2 m/sec}$						

KEY: a) Time (Greenwich); b) coordinates; c) air temp. (°C);
d) relative humidity (%); e) water surface temperature (mercury thermometer) (°C); f) radiation temperature of water (°C).

20-21 February

/73

a) Время (грин- вича)	b) Координаты		Темпе- ратура воздуха (°C) c)	Влаж- ность относи- тель- ная d) (%)	Темпе- ратура по- верхности воды по ртутному термомет- ру (°C)e)	Радиа- ционная темпере- тура воды f)
	N. Lat.	W. Long				
21.30	60°30'	178°40'	-12,7		0,4	0,5
21.45	60 30	178 40	-12,7			
22.00	60 30	178 40	-13,1	95	0,5	0,2
22.15	60 30	178 40	-12,8	93	0,5	0,5
22.30	60 30	178 40	-12,7	97	0,4	0,35
22.45	60 30	178 40	-12,0	91	0,4	0,2
23.00	60 30	178 40	-12,7	92	0,4	0,2
23.15	60 30	178 40	-12,5	90	0,4	0,2
23.30	60 30	178 40	-12,5	94	0,4	0,2
23.45	60 30	178 40	-12,2	94	0,4	0,3
00.00	60 30	178 40	-12,1	91	0,4	0,2
00.15	60 30	178 40	-12,0	94	0,3	0,4
00.30	60 30	178 40	-12,0	92	0,3	0,5
00.45	60 30	178 40	-11,7	86	0,3	0,4
01.00	60 30	178 40	-12,3	90	0,4	0,2
01.15	60 30	178 40	-12,2	89	0,4	0,2
01.30	60 30	178 40	-11,8	92	0,1	0,4
			12,4			

Average value over flight 0,32 0,3

Mean-square deviation S 0,1 0,1

Dispersion σ^2 0,01 0,01Wind $350^\circ\text{-}360^\circ = 11\text{-}14 \text{ m/sec}$

KEY: a) Time (Greenwich); b) coordinates; c) air temp. (°C);
 d) relative humidity (%); e) water surface temperature (mercury thermometer) (°C); f) radiation temperature of water (°C).

22-23 February 1973

/74

a) Время (грин- вича)	b) Координаты		Темпера- тура воздуха (°C) c)	Влаж- ность относи- тельная d) (%)	Темпера- тура по- верхности воды по ртутному термомет- ру (°C)e)	Радиаци- онная температура во- ды f) (°C)
	N. Lat	W. Long				
21 30	60°20'	177°00'	-0,2	92	-0,6	-0,7
21 45	60 20	177 00	-0,2	92	-0,6	-0,7
22 00	60 20	177 00	0,1	92	-0,6	-1,1
22 15	60 20	177 00	0,1	92	-0,6	-1,1
22 30	60 20	177 00	0,2	90	-0,6	-
22 45	60 20	177 00	0,1	90	-0,5	-0,8
23 00	60 20	177 00	-0,3	94	-0,4	-0,5
23 15	60 20	177 00	-0,8	98	-0,4	-0,4
23 30	60 20	177 00	-1,0	98	-0,4	-0,5
23 45	60 20	177 00	-1,0	98	-0,4	-0,6
00 00	60 20	177 00	-1,0	98	-0,4	-0,5
00 15	60 20	177 00	-0,2	92	-0,4	-0,6
00 30	60 20	177 00	-0,5	94	-0,4	-0,8
00 45	60 20	177 00	-0,5	94	-0,4	-0,8
01 00	60 20	177 00	-0,2	92	-0,4	-0,8
01 15	60 20	177 00	-0,4	92	-0,4	-0,8
01 30	60 20	177 00	-0,9	94	-0,5	-0,9
Average value over flight -0.4					-0,44	-0,8
Mean-square deviation S					0,1	0,21
Dispersion σ^2					0,01	0,04
Wind 100-120° 8-10 m/sec						

KEY: a) Time (Greenwich); b) coordinates; c) air temp. (°C);
 d) relative humidity (%); e) water surface temperature (mercury
 thermometer) (°C); f) radiation temperature of water (°C).

23-24 February 1973

/75

a) Время (грин- вич)	b) Координаты		Темпе- ратура возду- ха c) ($^{\circ}$ C)	Влаж- ность относи- тельная d) (%)	Темпера- тура по- верхности воды по ртутному термомет- ру e) ($^{\circ}$ C)	Радиаци- онная темпере- тура воды f) ($^{\circ}$ C)
	N. Lat	W. Long				
21 30	59 $^{\circ}$ 30'	177 $^{\circ}$ 00'	-0,8	91	0,1	0,0
21 45	59 30	177 00	-0,7	91	0,1	-0,2
22 00	59 30	177 00	-0,8	91	0,1	-0,2
22 15	59 30	177 00	-0,7	91	0,1	-0,3
22 30	59 30	177 00	-0,4	91	0,1	-
22 45	59 30	177 00	-0,3	87	0,1	0,3
23 00	59 30	177 00	-0,3	91	0,1	0,2
23 15	59 30	177 00	-0,4	89	0,1	0,2
23 30	59 30	177 00	-0,5	91	0,1	0,0
23 45	59 30	177 00	-0,5	91	0,1	0,1
00 00	59 30	177 00	-0,7	95	0,1	0,1
00 15	59 30	177 00	-0,3	91	0,2	0,1
00 30	59 30	177 00	-0,3	91	0,2	0,0
00 45	59 30	177 00	-0,4	91	0,2	0,0
01 00	59 30	177 00	-1,0	92	0,3	0,0
01 15	59 30	177 00	-0,5	89	0,4	0,0
01 30	59 30	177 00	-0,9	90	0,4	0,1
01 45	59 30	177 00	-0,9	93	0,4	0,1
Average value over flight -0,6					0,2	0,0
Mean-square deviation S					0,12	0,14
Dispersion $\hat{\sigma}^2$					0,01	0,02
Wind 320-360 $^{\circ}$ 4-5 m/sec						

KEY: a) Time (Greenwich); b) coordinates; c) air temp. ($^{\circ}$ C);
 d) relative humidity (%); e) water surface temperature (mercury thermometer) ($^{\circ}$ C); f) radiation temperature of water ($^{\circ}$ C).

26-27 February 1973

a) Время (гри- вича)	b) Координаты		Темпера- тура воздуха (°C) c)	Влаж- ность отно- ситель- ная d)(%)	Темпера- тура по- верхнос- ти воды по ртут- ному тер- мометру e) (°C)	Радиа- ционная температура воды (°C) f)
	N. Lat	W. Long				
23.15	59°37'	178°04'	0,2	88	1,7	-
23.30	59 28	178 04	0,2	88	1,7	1,7
23.45	59 28	178 04	0,3	88	1,7	1,7
00.00	59 28	178 04	0,1	90	1,7	1,7
00.15	59 28	178 04	0,1	94	1,7	1,7
00.30	59 28	178 04	0,1	98	1,7	1,7
00.45	59 28	178 04	0,1	90	1,7	1,6
01.00	59 28	178 04	0,3	94	1,7	1,7
01.15	59 28	178 04	0,2	96	1,7	1,7
01.30	59 28	178 04	0,2	96	1,6	1,7
			0,18			

Average value over flight	1,7	1,7
Mean-square deviation S	0,03	0,0
Dispersion σ^2	0,001	0,0

Wind 90-II10° = 14-15 m/sec

KEY: a) Time (Greenwich); b) coordinates; c) air temp. (°C);
 d) relative humidity (%); e) water surface temperature (mercury thermometer) (°C); f) radiation temperature of water (°C).

28 February - 1 March 1973

/77

a) Время (грин- вич)	b) Коор- динаты		Темпера- тура воз- духа (°C) c)	Влаж- ность относи- тельная (%) d)	Темпера- тура по- верхнос- ти воды по ртутя. термомет. e) (°C)	Радиаци- онная темпере- тура во- ды f) (°C)
	N. Lat	W. Long				
21.30	60°37'	177°54'	-7,0	73	-1,2	-1,5
21 45	60 39	177 50	-6,7	74	-1,2	-1,4
22 00	60 42	177 46	-6,5	74	-1,2	-1,2
22 15	60 42	177 46	-4,9	67	-1,2	-1,3
22 30	60 42	177 46	-5,8	70	-1,2	-1,3
22 45	60 42	177 46	-6,2	69	-1,0	-1,4
23 00	60 42	177 46	-6,2	72	-1,0	-1,3
23 15	60 42	177 46	-6,3	66	-1,0	-1,4
23 30	60 42	177 46	-6,3	69	-1,0	-1,4
23 45	60 42	177 46	-6,6	65	-1,0	-1,5
00 00	60 42	177 46	-6,7	71	-1,0	-1,4
00 15	60 42	177 46	-6,6	68	-1,0	-1,4
00 30	60 40	177 48	-6,5	72	-1,0	-1,4
00 45	60 41	177 50	-6,7	71	-1,0	-2,1
01 00	60 37	177 54	-6,7	71	-1,0	-1,4
01 15	60 37	177 54	-6,6	74	-1,0	-1,5
01 30	60 37	177 54	-6,5	66	-1,0	-1,4
01 45	60 37	177 54	-6,2	64	-1,0	-1,4
02 00	60 37	177 54	-5,9	62	-1,2	-1,5
02 15	60 37	177 54	-6,1	70	-1,2	-1,6
02 30	60 37	177 54	-6,1	72	-1,2	-1,6
02 45	60 37	177 54	-6,1	75	-1,2	-1,3
03 00	60 37	177 54	-6,1	70	-1,2	-1,4
03 15	60 37	177 54	-5,9	67	-1,1	-1,6
03 30	60 37	177 54	-5,7	68	-1,1	-1,5
03 45	60 37	177 54	-5,7	78	-1,1	-1,5
04 00	60 37	177 54	-6,0	78	-1,2	-1,4

Mean value over flight -6.2

-1,1 -1,5

Mean-square deviation S

0,034 0,31

Dispersion σ'

0,009 0,094

KEY: a) Time (Greenwich); b) coordinates; c) air temp. (°C);
d) relative humidity (%); e) water surface temperature (mercury
thermometer) (°C); f) radiation temperature of water (°C).

2-3 March

/78

a) Время (грин- вича)	b) Координаты		Темпера- тура воздуха (°C) c)	Влаж- ность отно- ситель- ная d) (%)	Темпера- тура по- верхнос- ти воды по ртут- ному тер- мометру e) (°C)	Радиаци- онная температура воды f) (°C)
	N. Lat	W. Long				
23.00	58°42'	173°45'	-9,7	81	0,2	-
23.15	58 36	173 32	-9,5	85	0,4	-
23.30	58 31	173 32	-9,6	85	0,4	-
23.45	58 29	173 26	-9,6	88	0,4	-
00.00	58 28	173 19	-10,1	85	0,4	-
00.15	58 28	173 16	-10,3	87	0,4	-
00.30	58 27	173 13	-10,1	85	0,1	-
00.45	58 26	173 10	-10,4	89	0,1	-
01.00	58 25	173 06	-10,5	91	0,1	-
01.15	58 23	173 04	-10,5	91	0,0	-
01.30	58 18	172 55	-10,3	90	0,0	-
01.45	58 17	172 52	-10,5	94	0,1	-
02.00	58 16	172 48	-10,2	89	0,2	-
02.15	58 16	172 48	-10,4	96	0,2	
			-10,1			

Mean value over flight 0,2

Mean-square deviation S 0,15

Dispersion σ^2 0,02Wind $70^\circ\text{-}90^\circ = 21\text{-}17 \text{ m/sec}$

KEY: a) Time (Greenwich); b) coordinates; c) air temp. (°C);
 d) relative humidity (%); e) water surface temperature (mercury thermometer) (°C); f) radiation temperature of water (°C).

5-6 March

/79

a) Время (грин- вича)	b) Координаты		Темпера- тура воз- духа	Влаж- ность относи- тель- ная	Темпера- тура по- верхнос- ти воды по ртут- ному термо- метру	Радиаци- онная темпере- тура во- ды
	N. Lat	W. Long	(°C)	(%)	e) (°C)	f)
21.30	60°43'	178°38'	-14,0	-	-1,5	-
21.45	60 46	178 32	-14,3	-	-1,5	-
22.00	60 48	178 28	-14,3	-	-1,5	-1,4
22.15	60 49	178 25	-14,6	-	-1,5	-
22.30	60 50	178 25	-15,1	-	-1,5	-
22.45	60 50	178 25	-15,1	-	-1,5	-
23.00	60 50	178 20	-14,5	-	-1,5	-1,6
23.15	60 51	178 20	-15,2	-	-1,5	-
23.30	60 51	178 20	-15,2	-	-1,5	-1,6
23.45	60 51	178 20	-15,4	-	-1,5	-1,5
00.00	60 52	178 19	-15,3	85	-1,5	-1,5
00.15	60 52	178 19	-14,5	85	-1,4	-1,6
00.30	60 52	178 19	-14,5	86	-1,3	-1,6
00.45	60 52	178 19	-14,6	85	-1,3	-1,8
01.00	60 52	178 19	-14,6	86	-1,3	-1,8
01.15	60 52	178 19	-14,3	86	-1,3	-1,7
01.30	60 52	178 19	-14,7	86	-1,3	-1,7
01.45	60 52	178 19	-14,3	83	-1,3	-1,8
02.00	60 52	178 19	-14,5	86	-1,3	-1,8
02.15	60 52	178 19	-14,3	86	-1,3	-1,7
			-14,6			

Mean value over flight -1,3 -1,65
 Mean-square deviation S 0,1 0,13
 Dispersion $\hat{\sigma}^2$ 0,01 0,01

Wind $40^{\circ}-60^{\circ}$ = 14-9 m/sec

KEY: a) Time (Greenwich); b) coordinates; c) air temp. (°C);
 d) relative humidity (%); e) water surface temperature (mercury thermometer) (°C); f) radiation temperature of water (°C).

7-8 March

/80

a) Время (гри- вича)	б) Координаты		Темпера- тура воз- духа (°C) c)	Влаж- ность относи- тельная (%) d)	Темпера- тура по- верхности воды по ртутному термометру e)(°C)	Радиа- цион- ная температура воды (°C)f)
	о.ш.	з.д.				
23.00	60°18'	179°20'	-14,1	98	1,0	-
23.15	60 18	179 20	-14,0	97	0,9	-
23.30	60 18	179 20	-13,8	97	0,9	-
23.45	60 18	179 20	-14,1	97	0,9	-
00.00	60 18	179 20	-13,8	97	1,0	-
00.15	60 18	179 20	-14,1	97	1,2	-
00.30	60 17	179 27	-13,5	97	1,5	-
00.45	60 17	179 27	-13,3	96	1,5	-
01.00	60 17	179 27	-14,2	92	1,5	-
01.15	60 17	179 27	-15,0	92	1,5	-
01.30	60 17	179 27	-15,0	92	1,4	-
01.45	60 17	179 28	-14,9	91	1,4	-
02.00	60 16	179 29	-14,7	91	1,4	-
02.15-	60 16	179 32	-15,2	91	1,4	-
02.30	60 16	179 32	-15,2	91	1,4	-
02.45	60 14	179 32	-15,1	91	1,4	-
03.00	60 14	179 32	-15,2	91	1,4	-
			-14,4			

Mean value over flight I,3

Mean-square deviation S 0,23

Dispersion $\hat{\sigma}^2$ 0,05Wind $40^\circ = 22-18$ m/sec

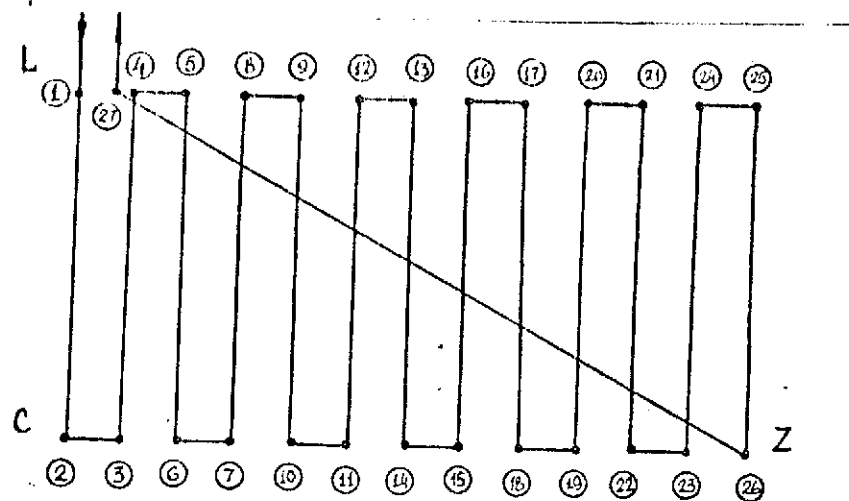
(IR radiometer did not operate - icing, storm)

KEY: a) Time (Greenwich); b) coordinates; c) air temp. (°C);
 d) relative humidity (%); e) water surface temperature (mercury thermometer) (°C); f) radiation temperature of water (°C).

APPENDIX IV. 1

/81

FLIGHT PLANS, TIME- AND COORDINATE-TABLES

/82

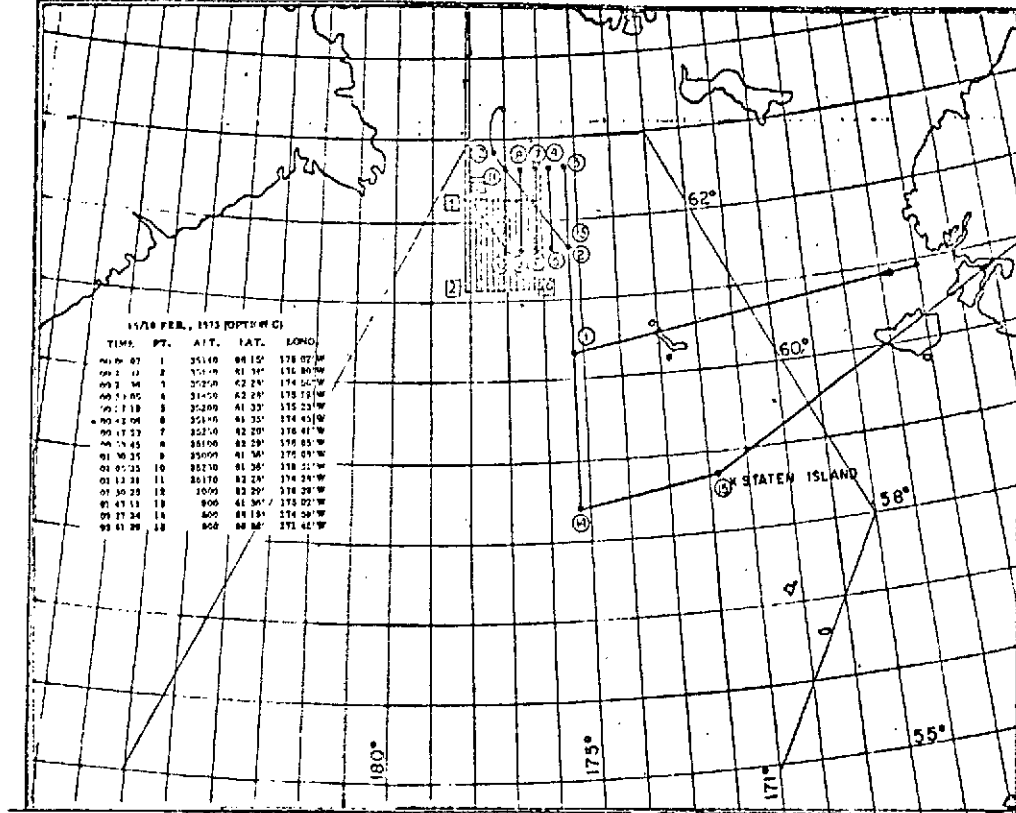
Option "C"

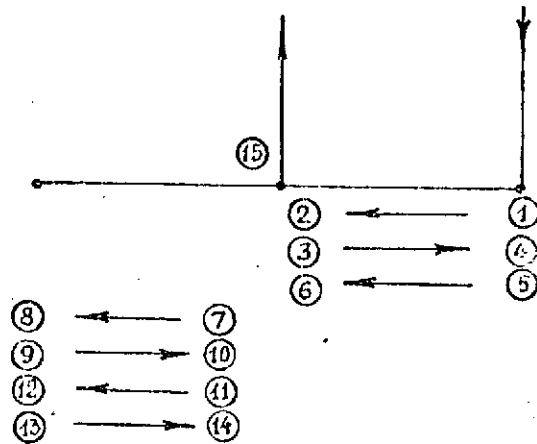
15 February

Point	Time	Point	Time	Point	Time
I	22 18	10	23 33	19	0 35
2	22 33	11	23 35	20	0 47
3	22 35	12	23 46	21	0 49
4	22 48	13	23 50	22	I 01
5	22 51	14	0 04	23	I 08
6	23 02	15	0 06	24	I 17
7	23 05	16	0 18	25	I 19
8	23 I7	17	0 20	26	I 32
9	23 21	18	0 33	27	2.29

Coordinates:

- $60^{\circ}00'$ $178^{\circ}00'$
- $62^{\circ}20'$ $178^{\circ}10'$
- $61^{\circ}23'$ $176^{\circ}15'$



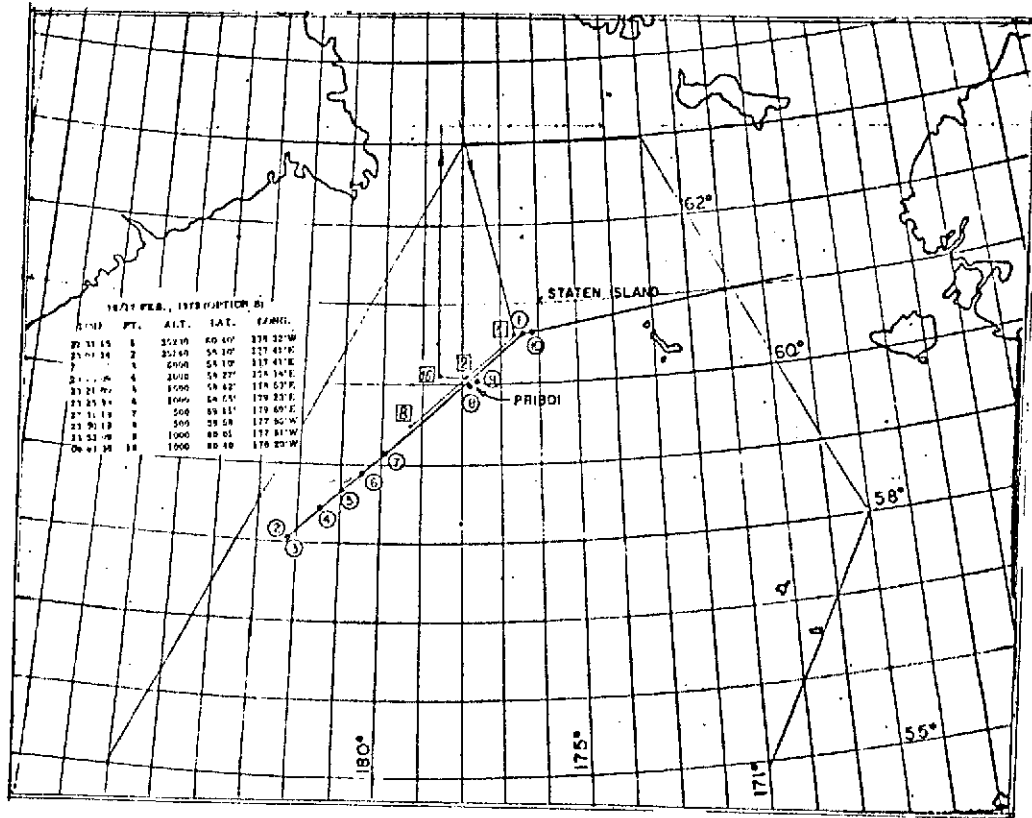


Option "B"

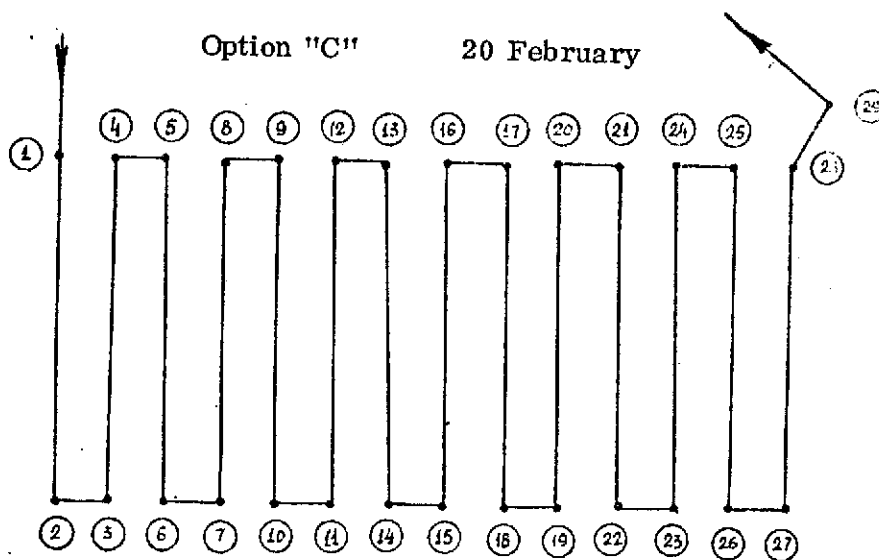
16 February

Point	Time	Point	Time
I	22 14	9	23 27
2	22 32	10	23 38
3	22 33	11	23 38
4	22 51	12	23 53
5	22 52	13	23 53
6	23 10	14	0 05
7	23 10	15	0 35
8	23 26		

Coordinates: - 60°00' 178°00'
 - 60 45 176 30



/85

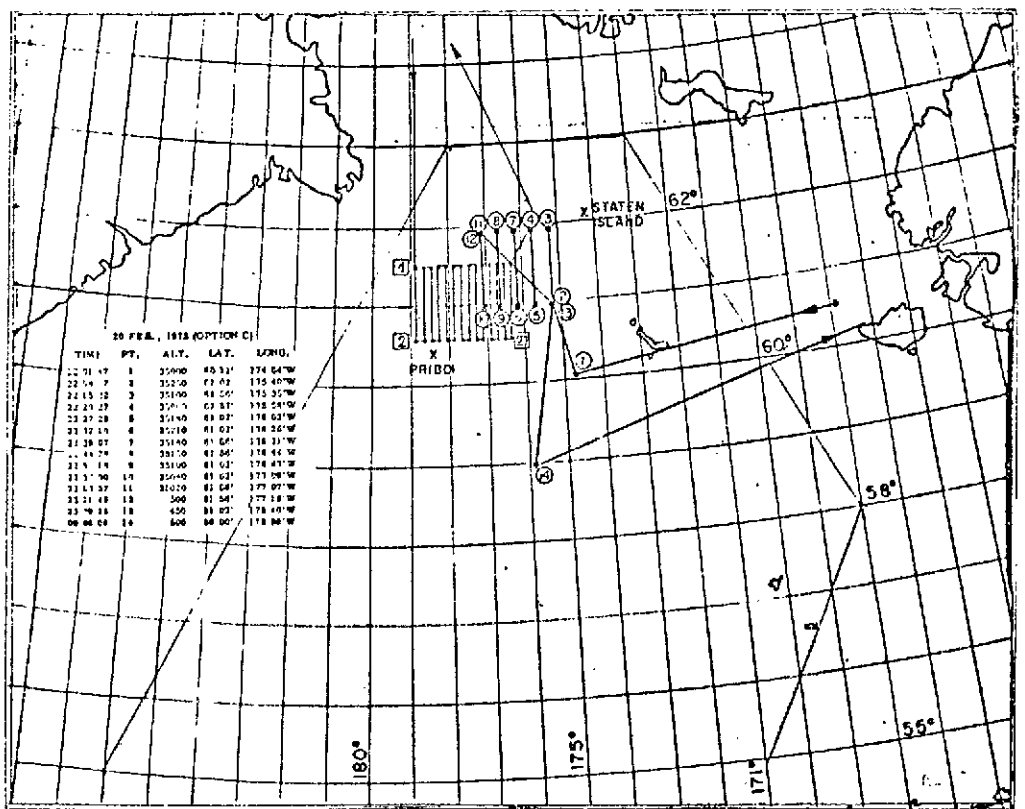


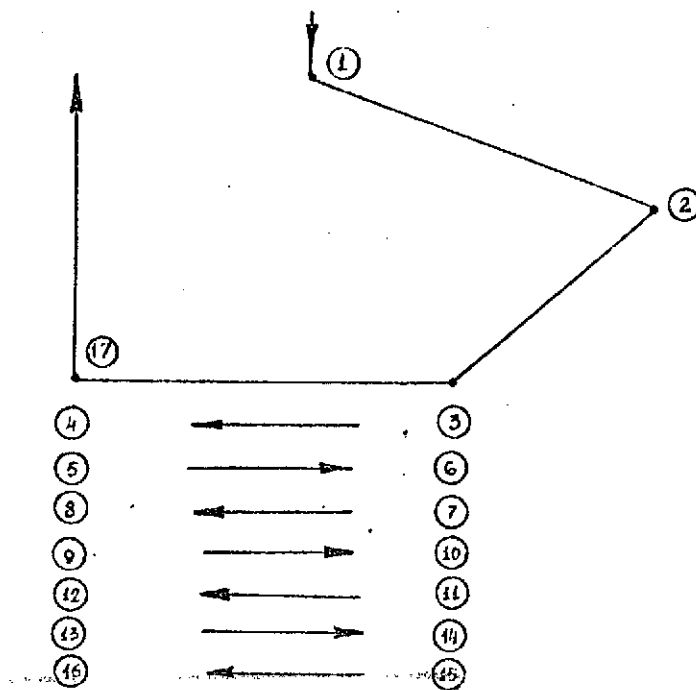
Point	Time	Point	Time	Point	Time
I	22 13	II	23 24	2I	0 35
2	22 27	I2	23 39	22	0 49
3	22 28	I3	23 39	23	0 49
4	22 42	I4	23 53	24	I 02
5	22 42	I5	23 53	25	I 03
6	22 54	I6	0 05	26	I 17
7	22 56	I7	0 05	27	I 18
8	23 09	I8	0 20	28	I 32
9	23 10	I9	0 20	29	I 50
10	23 24	20	0 34		

Coordinates:

- 61°21'	178°40'
- 60 30	178 40
- 60°30'	176°55'
- 61 21	176 54

'87





Option "B"

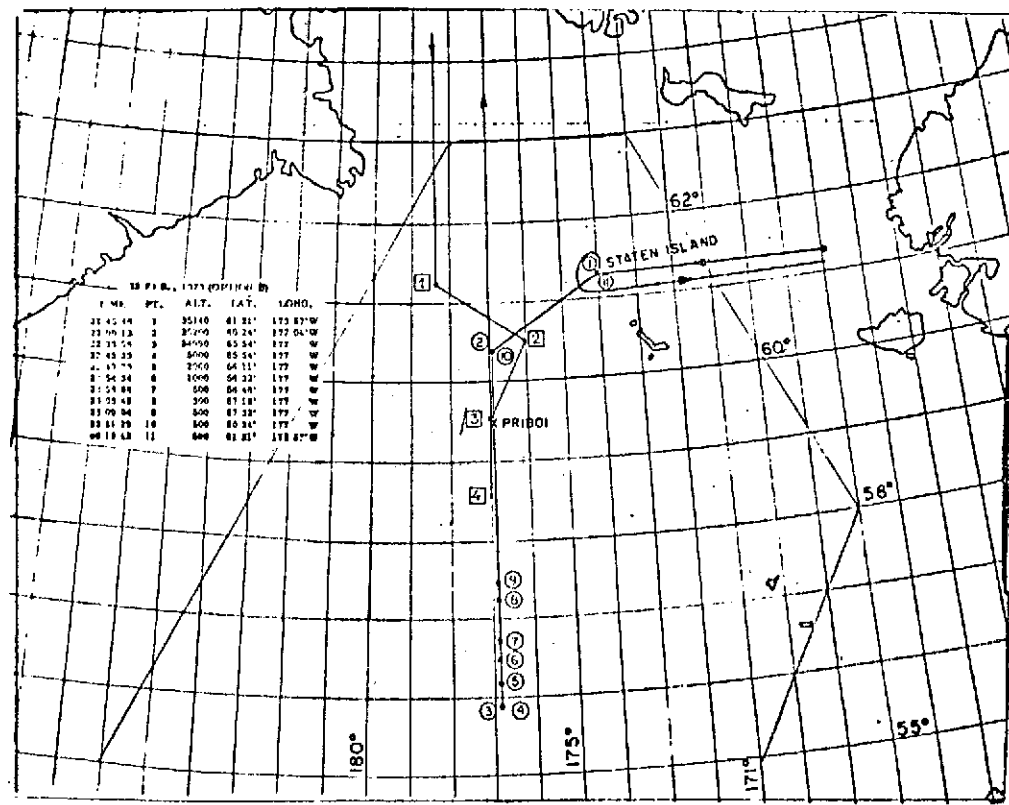
23 February

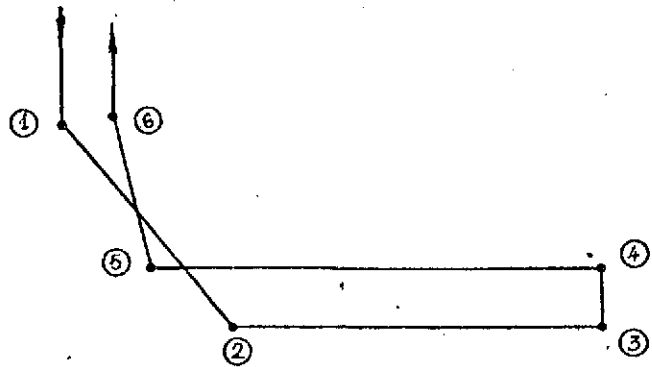
Point	Time	Point	Time
I	22- 22	10	0 II
2	22 44	II	0 II
3	22 58	I2	0 29
4	23 I7	I3	0 30
5	23 I7	I4	0 48
6	23 35	I5	0 48
7	23 35	I6	I 06
8	23 53	I7	I 35
9	23 53		

Coordinates:

- $59^{\circ}30'$ $177^{\circ}00'$
 - 58 40 I $77^{\circ}00'$

/89



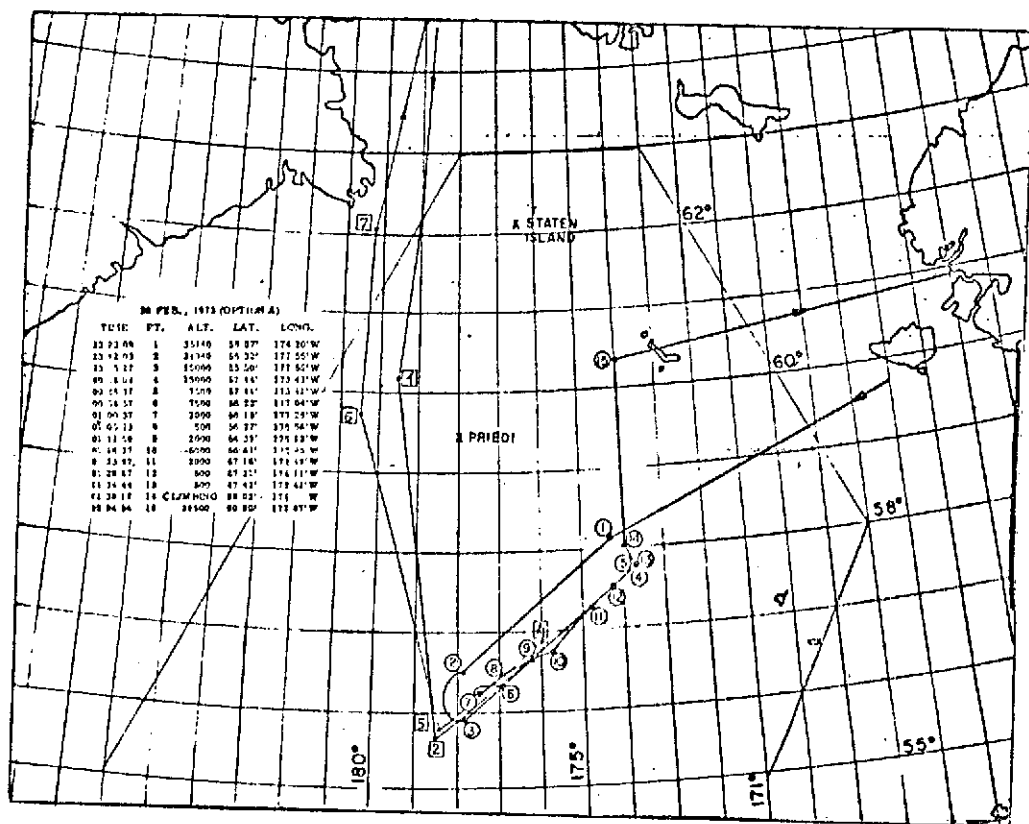


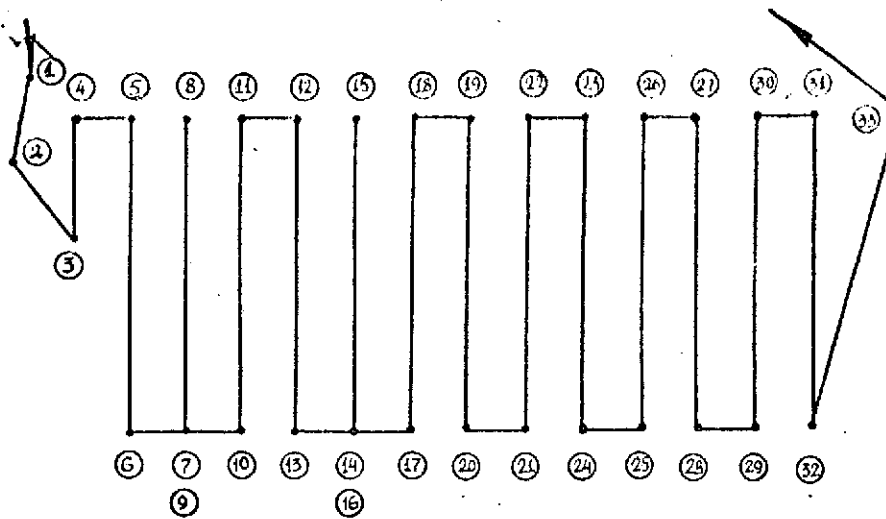
Option "A" 26 February

Point	Time
2	0-35
3	0 47
4	0 53
5	I I2
6	I 35

Coordinates: - $56^{\circ}47'$ $175^{\circ}53'$
 - 55 35 178 75

/91





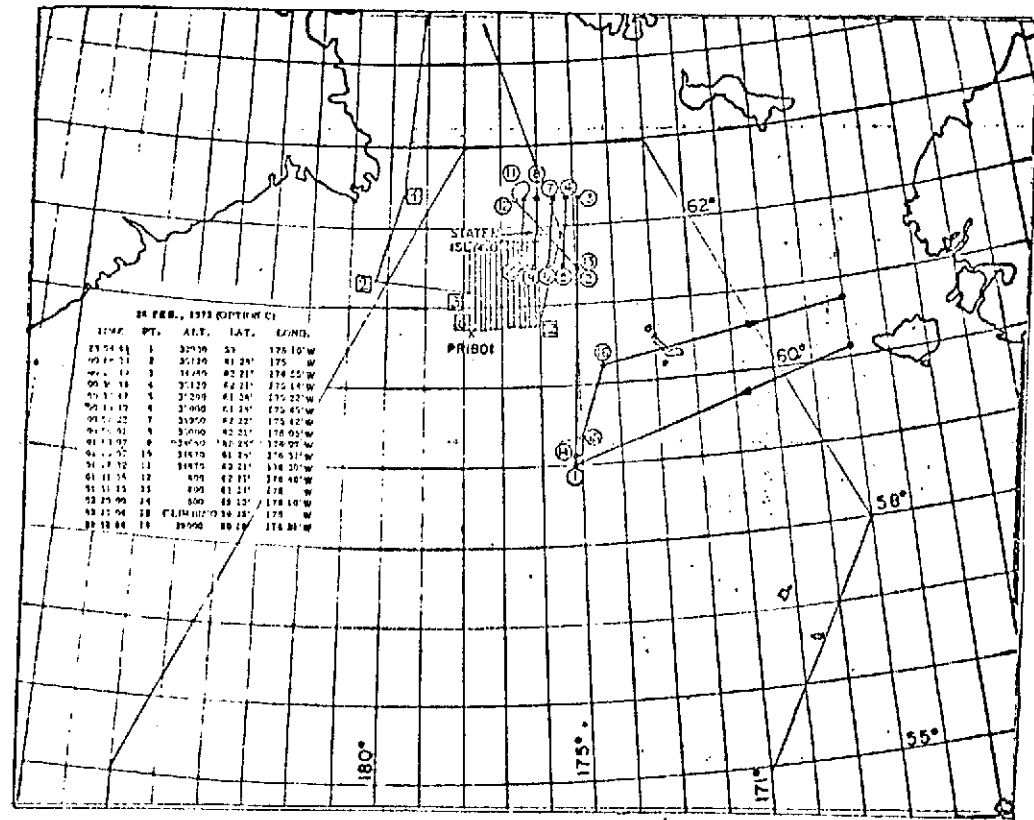
Option "C" 28 February

Point	Time	Point	Time	Point	Time
I	23 45	I2	I 15	23	2 41
2	23 57	I3	I 26	24	2 51
3	0 I2	I4	I 30	25	2 53
4	0 I7	I5	I 42	26	3 07
5	0 I9	I6	I 44	27	3 09
6	0 29	I7	I 56	28	3 I9
7	0 3I	I8	2 I2	29	3 2I
8	0 43	I9	2 I4	30	3 36
9	0 47	20	2 22	3I	3 38
10	I 0I	2I	2 24	32	3 48
II	I 13	22	2 39		

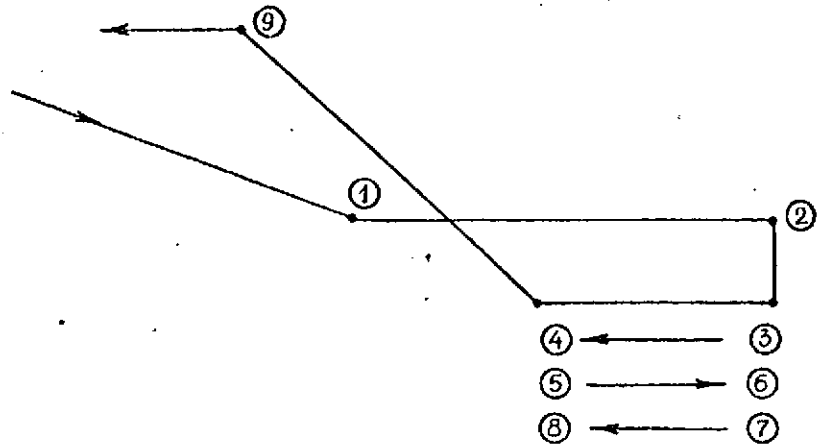
Coordinates:

- $60^{\circ}40'$ $I77^{\circ}40'$
- $61^{\circ}40'$ $I77^{\circ}45'$
- $60^{\circ}40'$ $I76^{\circ}00'$

1/93

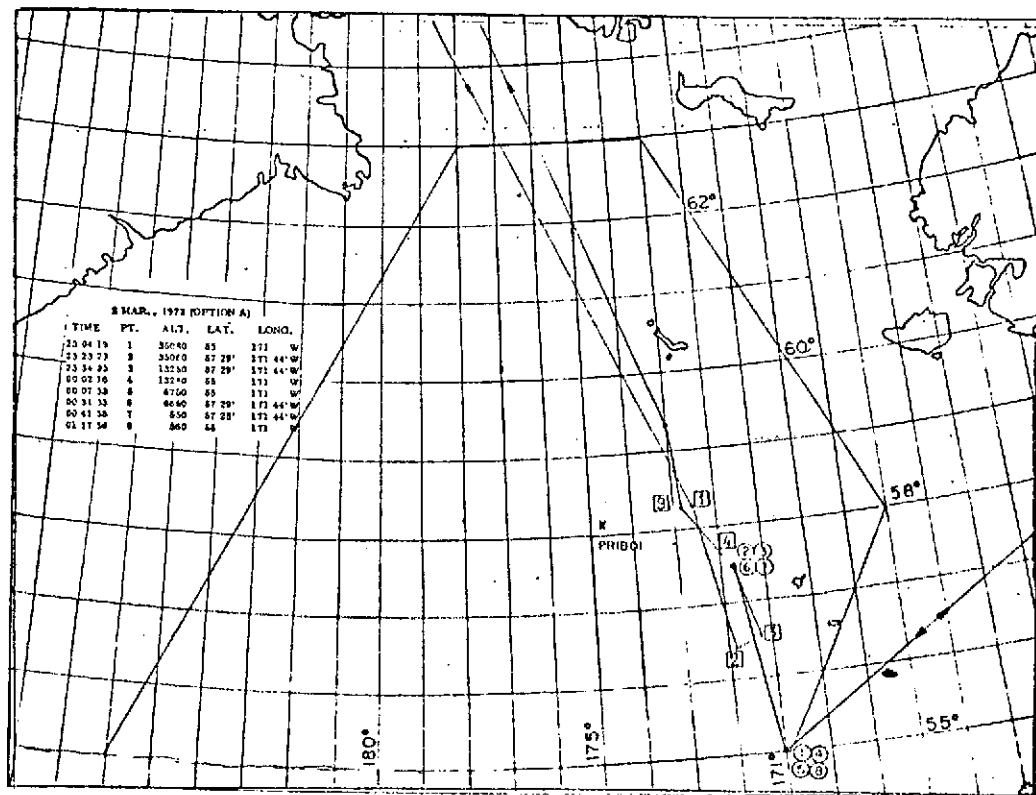


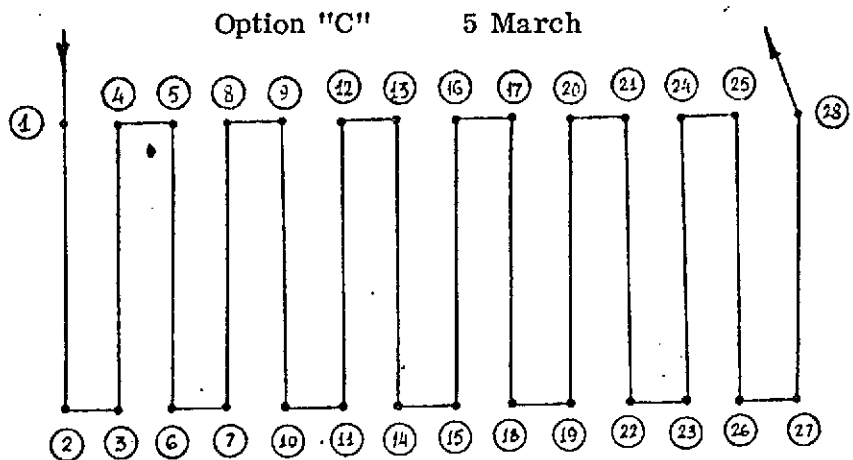
Option "A" 2 March



Point	Time
1	0 29
2	0 59
3	1 00
4	1 22
5	1 23
6	1 47
7	1 47
8	2 16
9	2 20

Coordinates: - $57^{\circ}25'$ $171^{\circ}40'$
 - 56 30 $171^{\circ}25'$



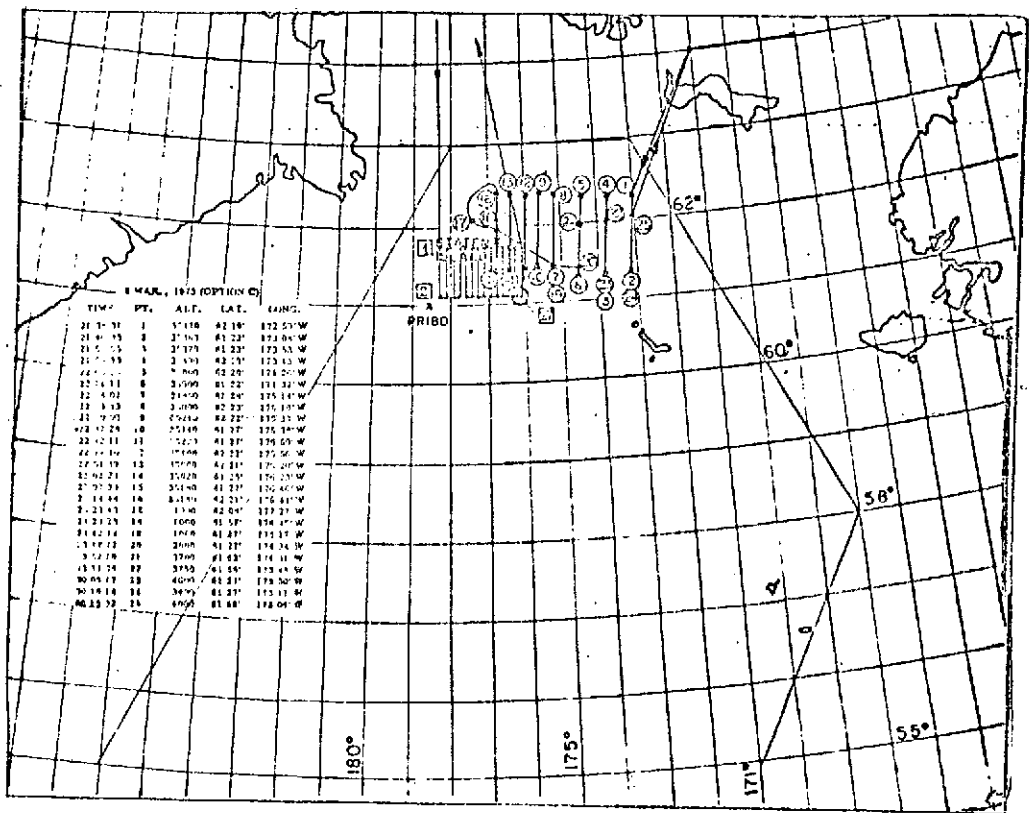


Point	Time	Point	Time	Point	Time
I	22 29	II	23 49	20	I 07
2	22 44	I2	0 01	21	I 09
3	22 44	I3	0 04	22	I 25
4	22 58	I4	0 20	23	I 26
5	22 58	I5	0 22	24	I 40
6	23 15	I6	0 35	25	I 40
7	23 16	I7	0 36	26	I 54
8	23 28	I8	0 52	27	I 56
9	23 30	I9	0 53	28	2 08
10	23 47				

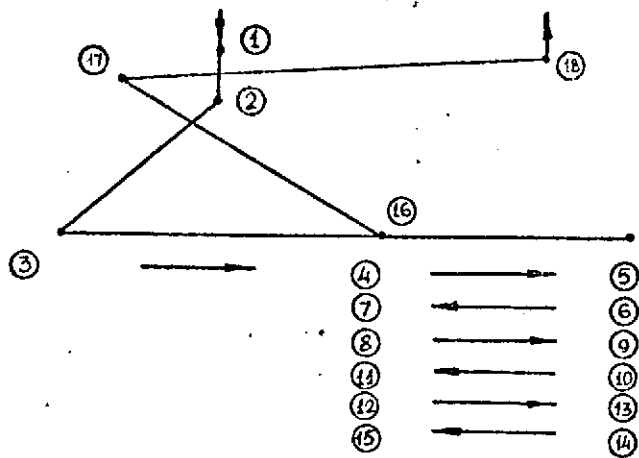
Coordinates:

- $61^{\circ}53'$ $178^{\circ}20'$
- 60 52 178 20
- 60 52 176 35
- 61 53 176 31

/97



198

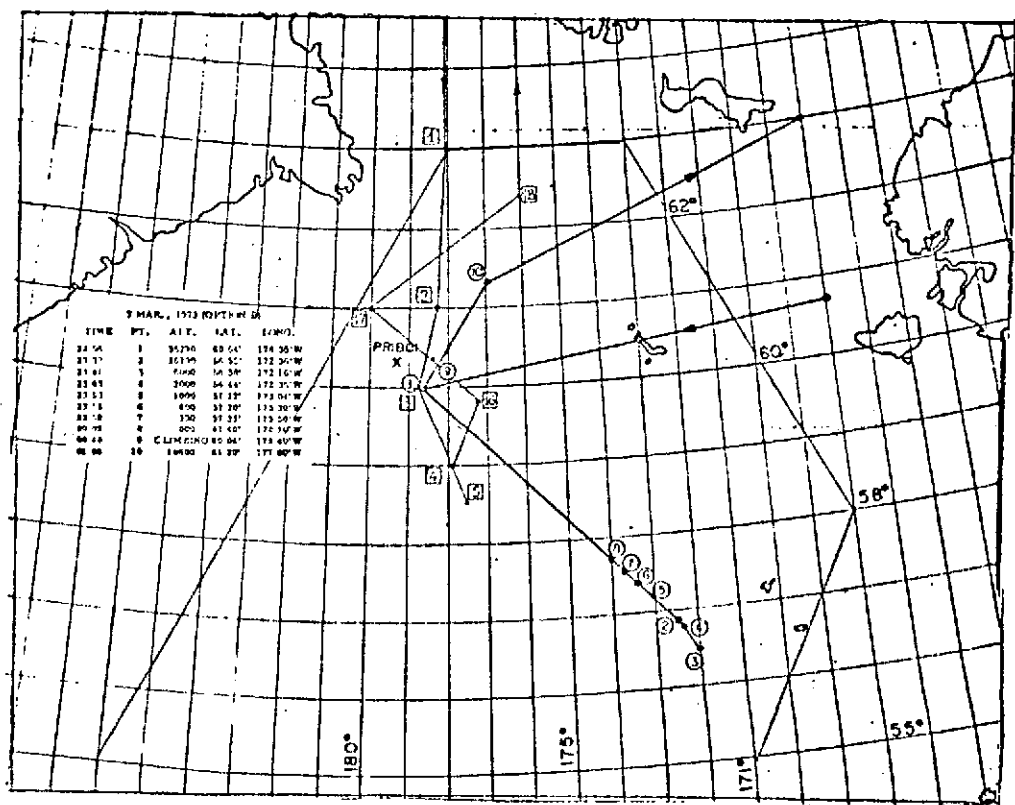


Option "B" 7 March 1973

Point	Time	Point	Time
2	23 41	10	I 23
3	0 08	11	I 40
4	0 27	12	I 40
5	0 44	13	I 56
6	0 45	14	I 57
7	I 02	15	2 II
8	I 03	16	2 39
9	I 23	17	2 50

Coordinates: $-60^{\circ}00'$ $178^{\circ}40'$
 $-59^{\circ}00'$ $177^{\circ}55'$

/99



APPENDIX IV.3

/100

TABLES OF DATA FROM AIRCRAFT SOUNDING OF THE ATMOSPHERE

Time I	H	P	t	Td	Visual observations
	2	3	4	5	6
17 February 1973					
01 34	3.73	627	-33.0	-	Below 8 Sc. Sea visible through gap
01 49	3.73	627	-32.3	-45.9	Below 7 Sc. Sea and ice translucent
01 52	3.73	627	-32.6	-44.3	Below 7 Sc. Sea and ice translucent
02 08	3.73	627	-33.6	-42.1	Below 8 Sc.
02 22	3.73	627	-33.3	-44.9	Below 9 Sc.
02 25	3.73	627	-33.3	-43.8	Below 9 Sc.
02 39	3.73	628	-32.8	-47.7	Below 8 Sc.
02 42	3.71	629	-33.2	-	Below 9 Sc.
02 55	3.72	628	-33.1	-43.4	Below 9 Sc.
02 58	3.72	629	-32.9	-42.6	Below 9 Sc.
03.II	3.72	629	-32.8	-44.6	Below 8 Sc.
21 February 1973					
01 14	8.66	339	-57.6		Toward Ci, below 8 Sc, Cu (two layers)
01 26	8.69	338	-56.9		Toward Ci, below 9 Sc, Cu (two layers)
01 28	8.69	338	-56.9		Ci on horizon, below 9 Sc, Cu (two layers)
01 40	8.66	339	-57.3		
01 42	8.67	338	-57.7		
01 54	8.68	338	-57.0		
01 56	8.69	337	-56.7		

I	2	3	4	5	6
02 08	8.66	339	-57,9		
02 10	8.67	338	-57,6		
02 21	8.68	338	-57,1		
02 23	8.69	337	-56,6		
02 36	8.62	340	-58,9		
02 37	8.60	341	-59,2		
02 50	8.66	339	-57,8		Below 10 Cs, translucent Sc, Cu.
02 52	8.66	339	-56,9		Below 10 Cs, translucent Cu.
03 03	8.58	342	-59,3		Below 10 Cs, ice, water translucent
03 05	8.58	342	-59,3		Below 10 Cs, ice, water translucent
03 17	8.63	340	-57,5		Below 10 Ci, Cs, Sc, ice, water translucent
03 19	8.64	339	-57,5		Below 10 Ci, Cs, Sc, ice, water translucent
03 31	8.57	343	-59,3		Below 10 Cs, Sc, ice, water translucent
03 38	8.61	341	-59,3		Below 10 Ci, translucent Sc, ice, open water spaces
03 46	8.65	339	-58,2		Below 10 Cs, translucent Sc
03 51	8.57	339	-57,6		Below 10 Cs, translucent Sc, sea
04 02	8.60	341	-59,4		Below 9 As, Ci
04 06	8.60	341	-59,4		Below 10 As, Ci translucent Sc
04 18	8.64	340	-58.5		Below 10 Ci, Cs translucent Sc, sea
04 20	8.65	339	-58.1		Below 10 Cs, Ci translucent Sc, sea
04 31	8.60	342	-59.7		Below 10 As, Ci

1	2	3	4	5	6
27 February 1973					
03 35	4.50	575	-27,4	Above 1 Ci toward Ac, below 6 Sc, Cu cong	
03 40	4.07	610	-24,I	Above 4 Ci, toward Ac, below 6 Cu cong	
03 45	4.07	610	-24,0	Above 5-6 Ci, below 4 Cu cong, Cu med	
03 47	4.07	610	-23,8	Above 3 Ci, below 4 Cu med, Cu cong, Cu fr	
03 50	2.74	730	-15,6	Above 3 Ci, below 4 Cu med, Cu cong	
03 52	1.58	848	~ 7,2	Upper level Cu fr	
				Lower level ~0.90	
03 54	0.65	955	~ 0,4	Above 7-8 Cu med, Cu cong	
04 00	0.65	955	- 1,4	Above 5 Ci, Cu	
3 March 1973					
03 27	8 36	352	-46,I	Clear above. Below 10 Cs, end of field Cs, beyond As	
03 37	8 36	352	-46,3	Clear Above. Below 10 As, Ac (multi-layered)	

I	2	3	4	5	6
03 53	8.34	353	-46,8		Clear above. Below 10 Ac, As (Multi-layered)
03 55	6.92	421	-34,8		Below 10 Ac, As (multi-layered)
03 57	5.45	506	-24,0		Below 10 As, Ac thin layer Ac.
03 59	3.97	609	-16,9		Below 10 As
04 00	3.60	638	-13,5		Above 1 Ac, below 10 As
04 08	4.02	605	-18,2		Clear above. Below 10 As - near upper level
04 13	4.72	555	-21,9		Entered As from the side
04 15	5.45	506	-23,7		Upper edge As
04 18	5.46	505	-24,4		Above 6 Ci, below 10 As. Entered As from the side
04 22	5.46	505	-24,4		In As. (Left As from the side. Entered As
04 32	4.12	593	-18,7		Clear above. Upper level As
04 42	3.50	646	-14,8		Upper level Ns.
04 46	1.97	781	-7,1		Upper level Ns.
04 49	0.58	931	-3,7		Lower edge FrNb snow
05 01	0 50	940	-6,7		Above 10 FrNb, snow
05 12	0 47	943	-11,7		Lower edge FrNb, snow

	1	2	3	4	5	6
6 March 1973						
01 28	8.82	332	-52,9		Below 3 Cu, Ci on horizon	
01 41	8.84	33I	-5I,8		Above 2 Ci. Below 4 Cu	
01 43	8.84	33I	-5I,8		Above 2 Ci. Below 3-4	
01 55	8.81	332	-52,7		Above 1-2 Ci. Below 2-3 Cu.	
01 58	8.84	33I	-5I,8		Above 1-2 Ci. Below 4 Cu	
02 15	8.83	332	-5I,5		Above 1 Ci. Below 6 Cu	
02 25	8.84	33I	-5I,7		Clear	
02 30	8.85	33I	-5I,3		Clear	
02 43	8.85	33I	-5I,3		Above 2 Ci, below 2 Cu	
02 48	8.85	33I	-5I,0		Above 1 Ci, below 2 Cu	
02 59	8.82	332	-5I,5		Clear	
03 04	8.84	33I	-5I,7		Clear	
03 17	8.84	33I	-5I,7		Ci on horizon. Below 2 Cu; Ci	
03 22	8.84	33I	-5I,7		Ci on horizon. Below 2 Cu	
03 33	8.82	332	-52,4		Clear	
03 37	8.84	33I	-5I,7		Clear	
03 50	8.83	332	-5I,8		Above 1 Ci, below 2 Cu	
03 55	8.85	33I	-5I,5		Above 1 Ci, below 2 Cu	
04 05	8.80	333	-52,7		Clear	
04 09	8.84	33I	-5I,8		Clear. 15 min entered Ci from side; 17 min left Ci from side	
04 22	8.85	33I	-50,6		Above 1 Ci, below 2 Cu	
04 27	8.82	332	-5I,6		Above 1 Ci, below 2 Cu, 35 min entered Ci	
04 37	8.79	333	-52,6		Clear	
04 41	8.81	333	-52,2		Ci along course	
04 55	8.84	33I	-5I,6		Clear	
04 59	8.84	33I	-5I,7		Clear	
05 10	8.81	333	-52,7		Clear	

1	2	3	4	5	6
8 March 1973					
03 07	3.97	609	-I7,6		Above 4 Ci, below 9 Ac, Sc (multi-layered)
03 24	3.97	609	-I6,7		Above 6 Ci, below 9 As, Ac
03 24	3.97	609	-I6,7		Above 6 Ci, below 9 As, Ac
03 39	3.96	610	-I6,9		Above 8 Ac, below 9 Sc, As
03 42	3.96	610	-I6,9		Above 9 As, Ac. Below 10 As, Sc.
03 56	3.98	609	-I5,9		Above 6 Ci fil, below 9 Sc op.
03 59	4.00	607	-Ib,6		Above 8 Ci fil, below 9 Sc, Ac.
04 15	3.96	610	-I7,4		Above 7 Ci, below 10 As.
04 18	3.97	609	-I7,6		Above 7 Ci, below 10 As.
04 32	4.00	607	-I5,8		Above 6 Ci, below 9 Sc.
04 35	3.98	609	-I5,8		Above 6 Ci, below 9 Sc.
04 51	3.98	609	-I6,I		Above 9 Ci, below 10 Ac, Sc
04 54	3.97	609	-I6,0		Above 9 Ci, below 10 Ac, Sc.
05 09	3.97	609	-I6,5		Above 10 Ci, below 10 As, Sc.
05 10	3.96	610	-I6,9		Above 10 Ci, below 10 As, Sc.
05 14	3.98	609	-I7,0		Above 9 Ci, below 10 As, Sc.
05 19	3.98	609	-I7,3		Above 9 Ci, below 10 As, Sc.
05 36	3.74	627	-I7,5		Above 9 Ci, below 10 As.
05 40	5.46	505	-23,I		Above 9 Ci, below 10 As, Sc.
05 45	6.94	420	-33,7		Above 9 Ci, below 10 As, Ac, Sc.
05 48	7.6I	386	-39,5		Lower boundary Ci
05 55	8.37	35I	-47,8		Above 6 Ci, below 10 Ci, Ac, As, Sc, From side left Ci.

I	2	3	4	5	6
06 10	8.32	353	-49,6		Above 3 Ci, below 9 Ac, Sc-strata
06 19	8 78	334	-53,5		Toward Ci, below 5-6 Cu, Sc.
06 30	8 80	333	-53,2		Ci on the horizon
06 40	8 80	333	-53,2		Ci on the horizon
06 43	8 80	333	-53,2		Ci on the horizon
I7 00	8 67	338	-55,8		Clear
07 15	8 67	338	-55,5		Clear

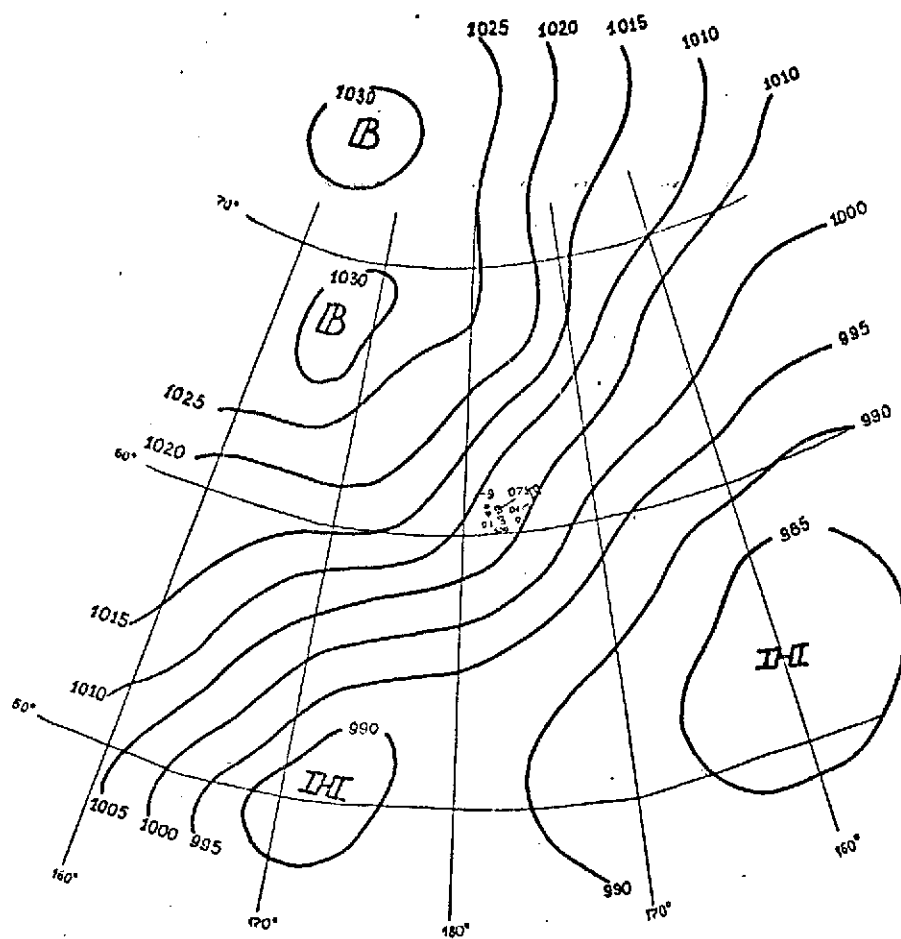


Figure 2.1. Surface synoptic chart, 00 GMT, 16 Feb. 1973.

/109

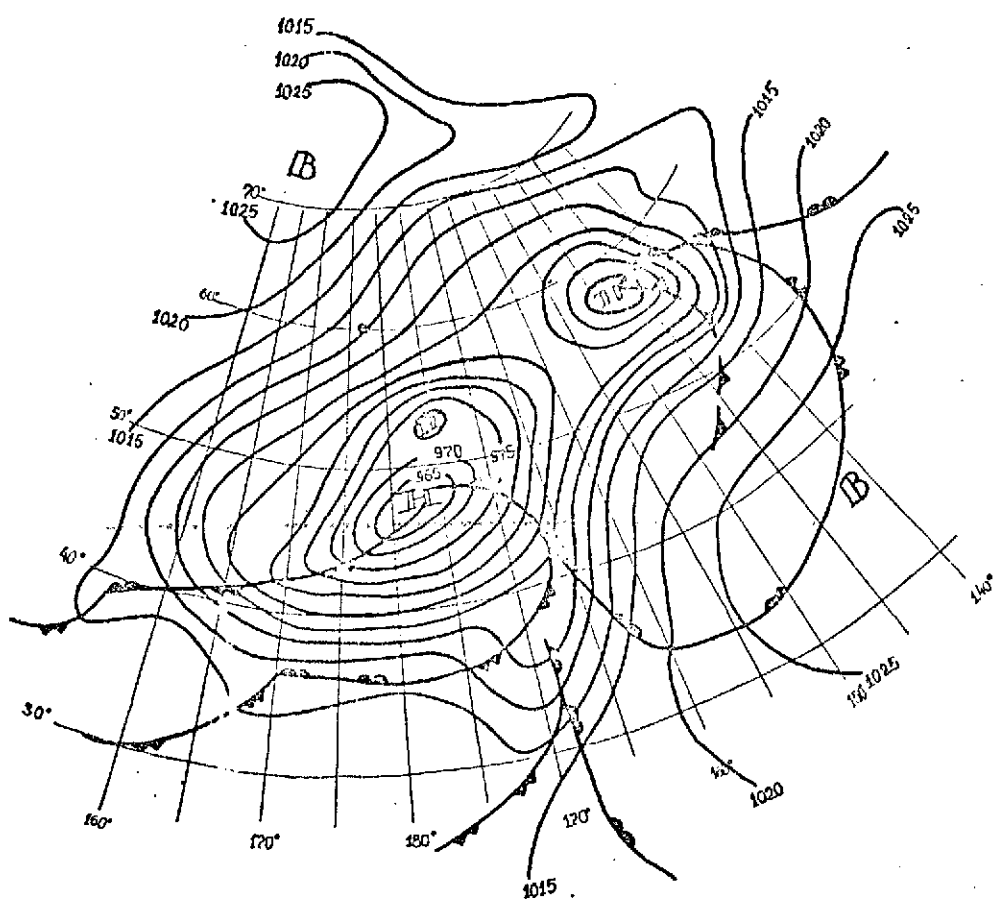


Figure 2.2 Surface synoptic chart, 00 GMT, 17 Feb. 1973.

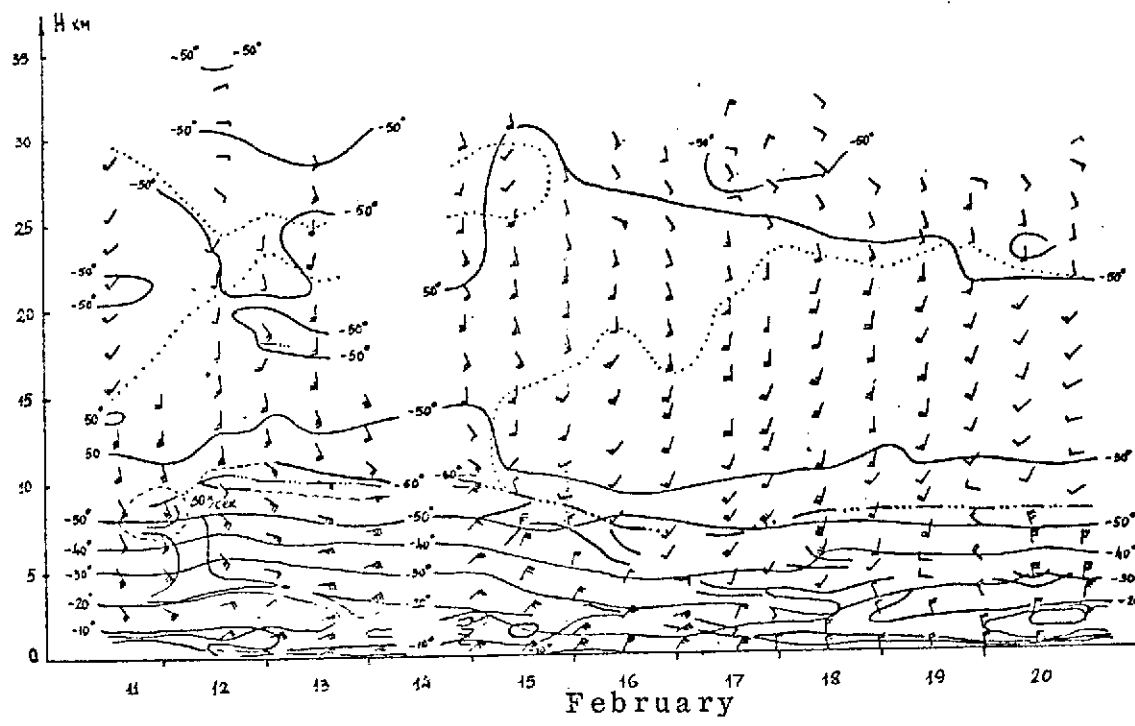


Figure 2.3. Temporal cross-section of the atmosphere above the Bering Sea, 11-20 Feb. 1973.

Legend: — isotherms, -... tropopause, == frontal zone boundaries,
---- isotachs, velopause.

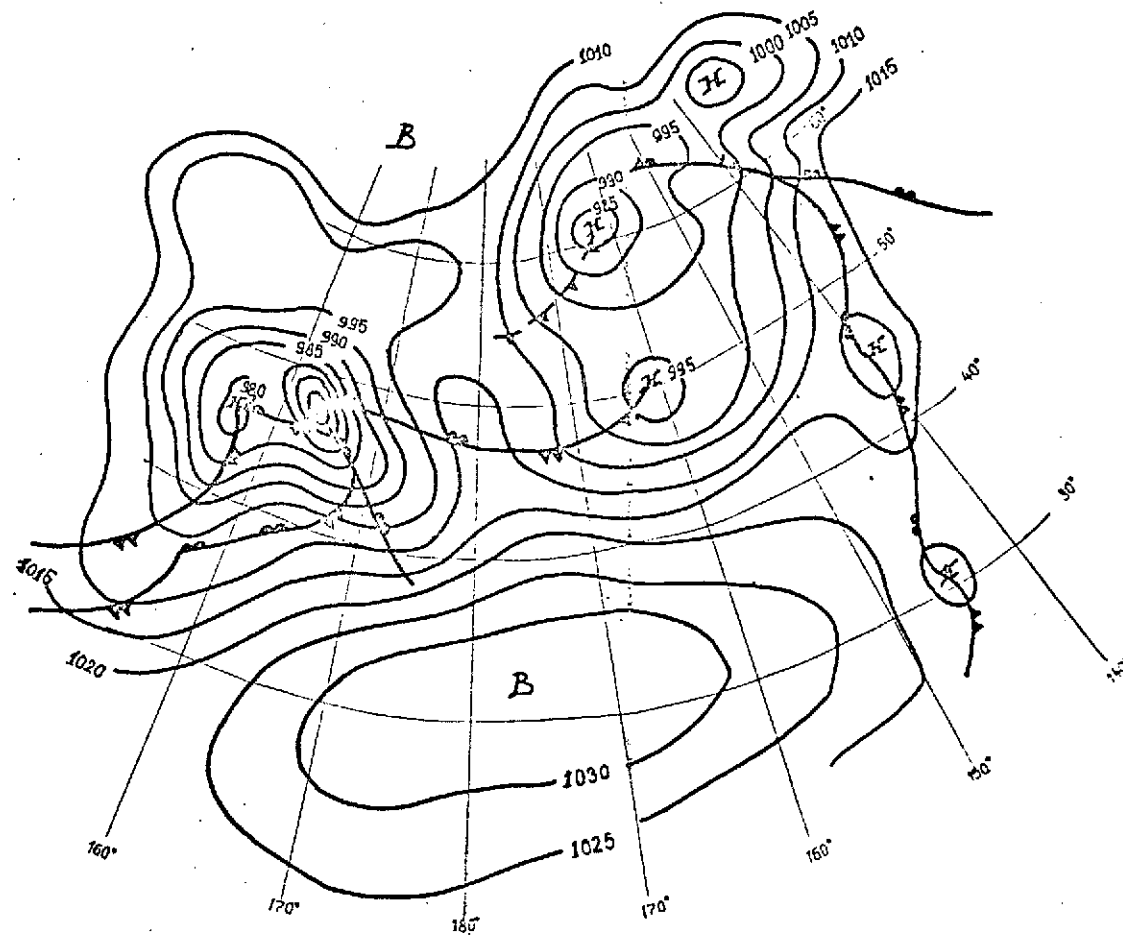


Figure 2.4. Surface synoptic chart 0000 GMT, 21 February 1973.

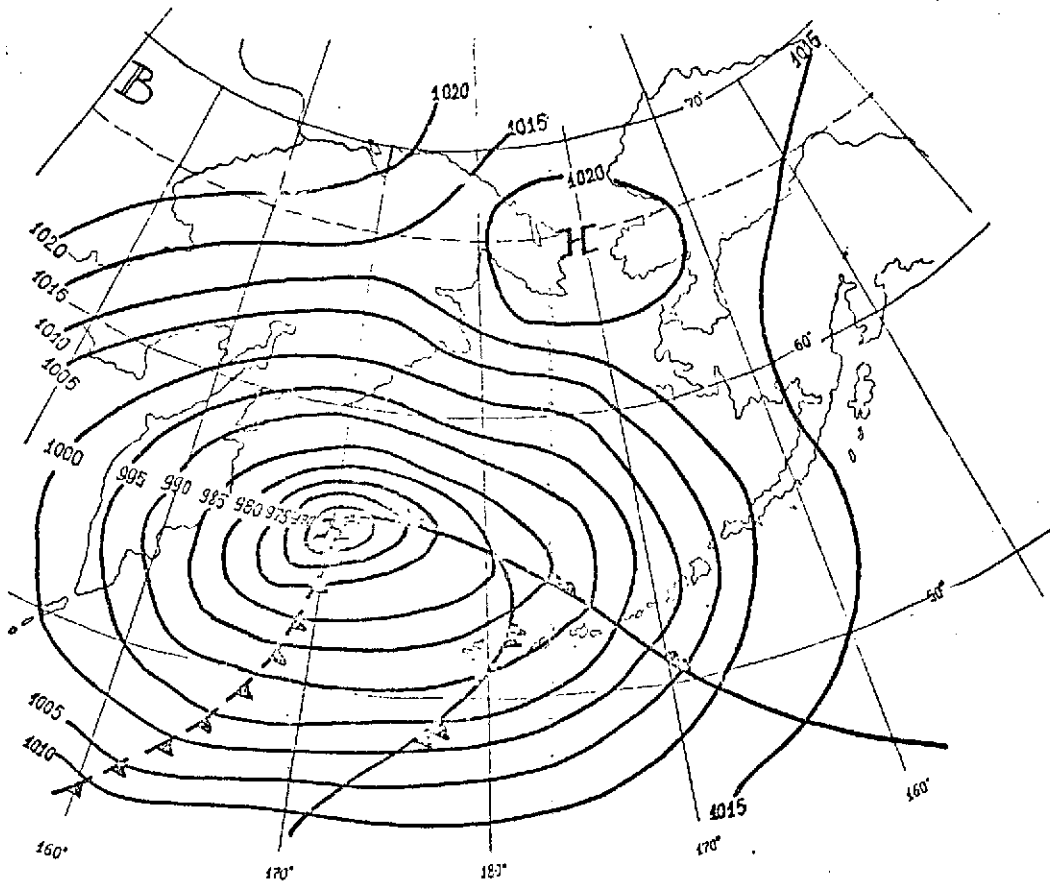


Figure 2.5. Surface synoptic chart, 0000 GMT, 22 February 1973.

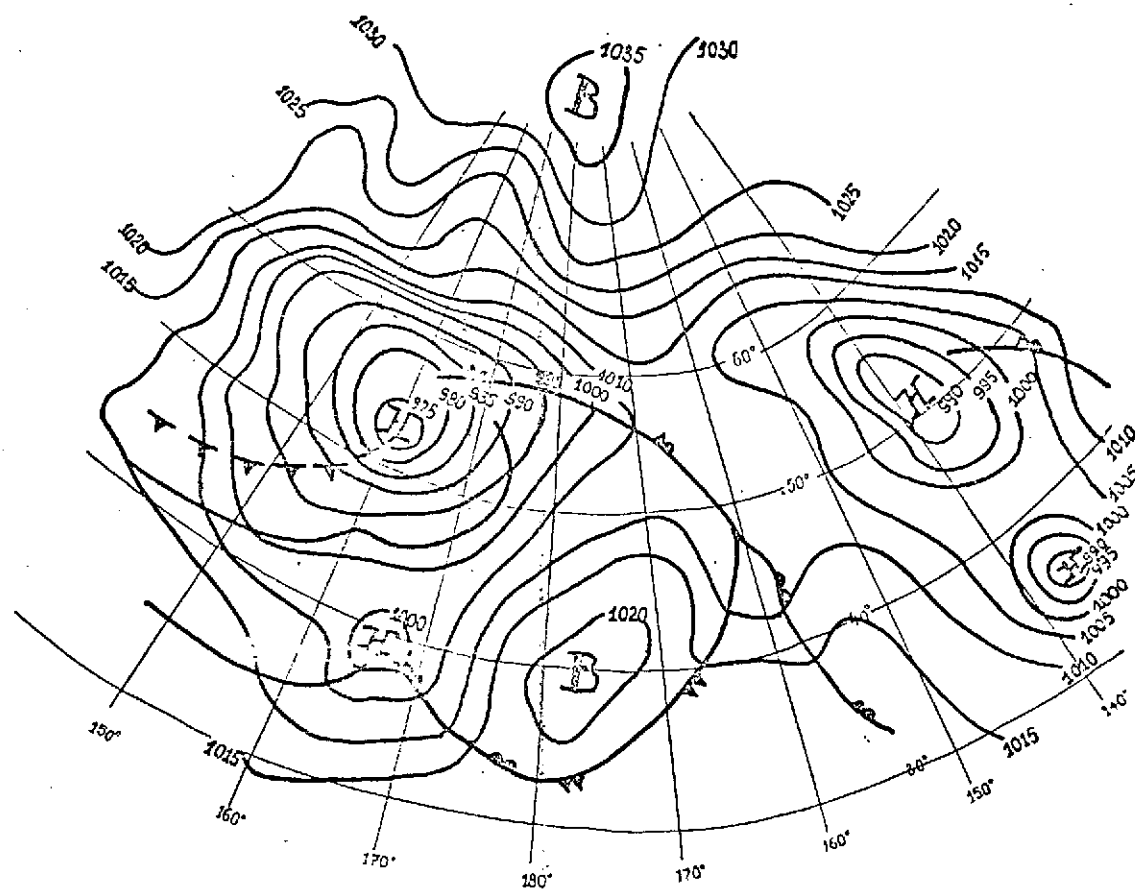


Figure 2.6. Surface synoptic chart 00 GMT, 27 February, 1973.

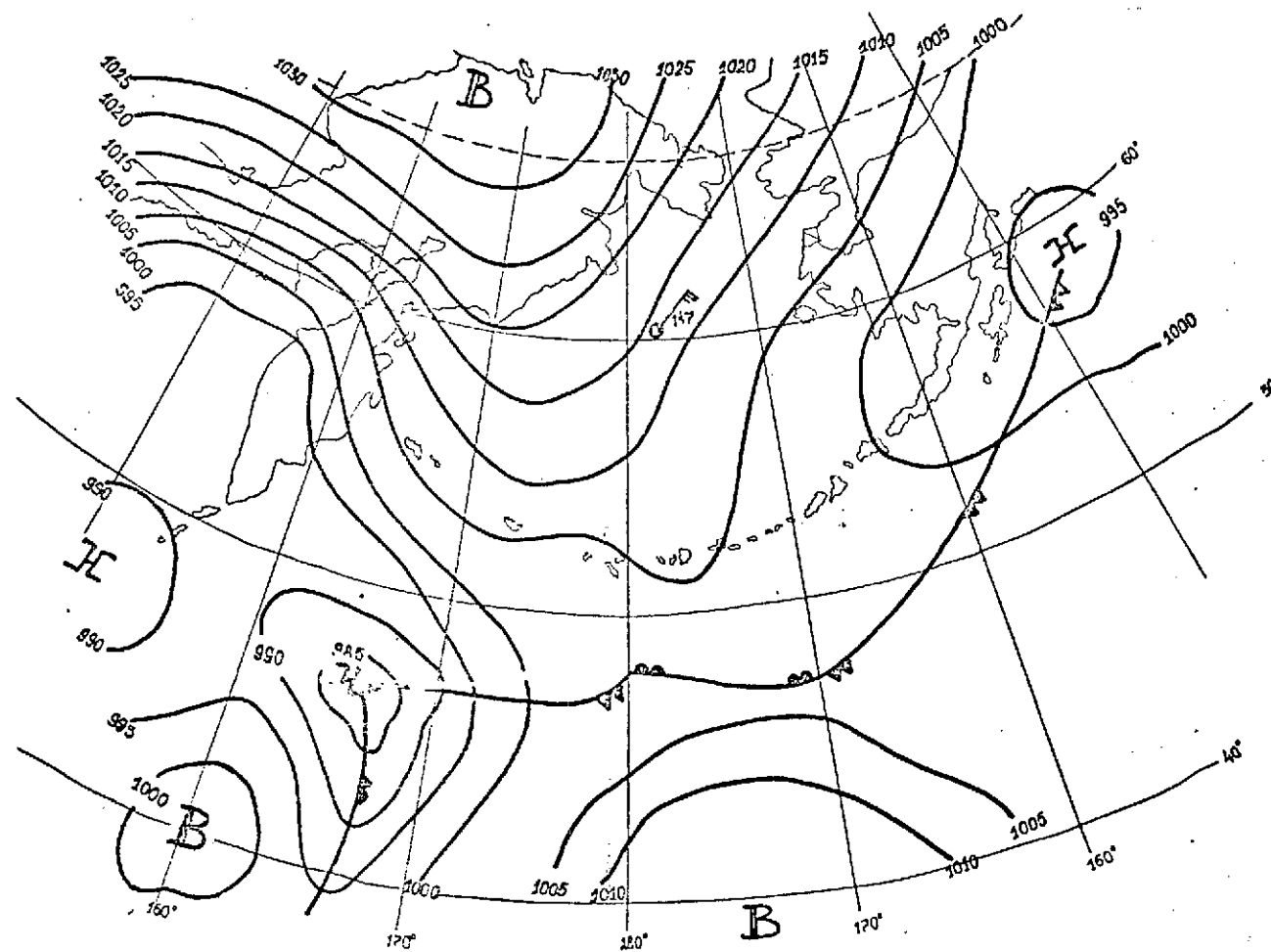


Figure 2.7. Surface synoptic chart for 00 GMT, 1 March 1973.

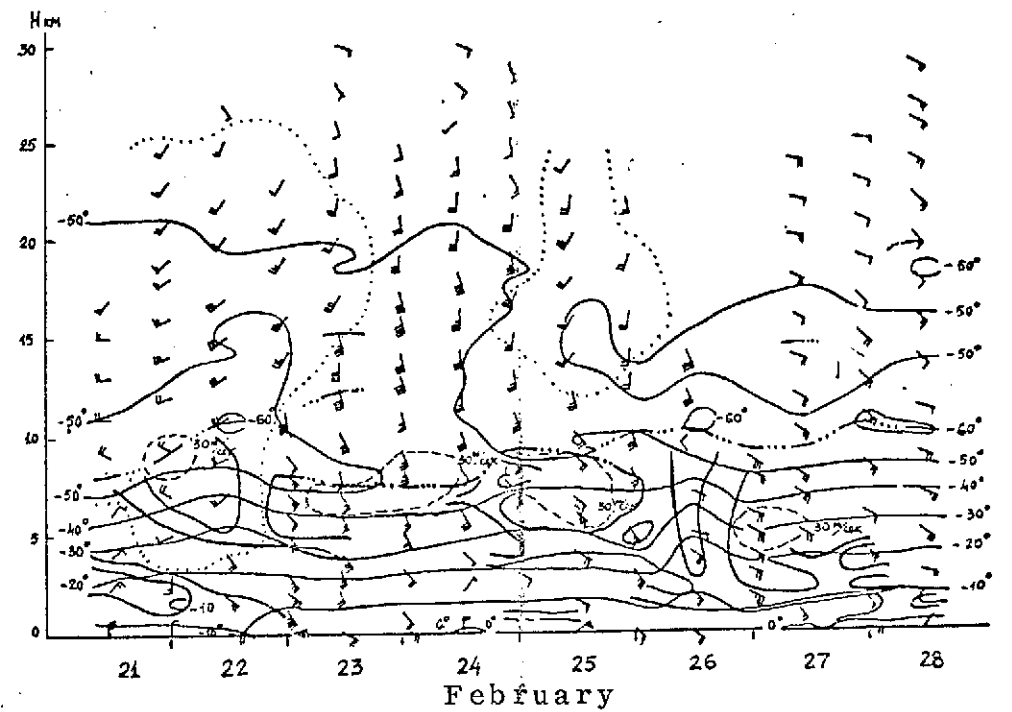


Figure 2.8. Temporal cross-section at the atmosphere above the Bering Sea, 11-20 February 1973.

Legend:

- isotherms —... tropopause
- frontal zone boundaries, ---- isotachs
- velopouse.

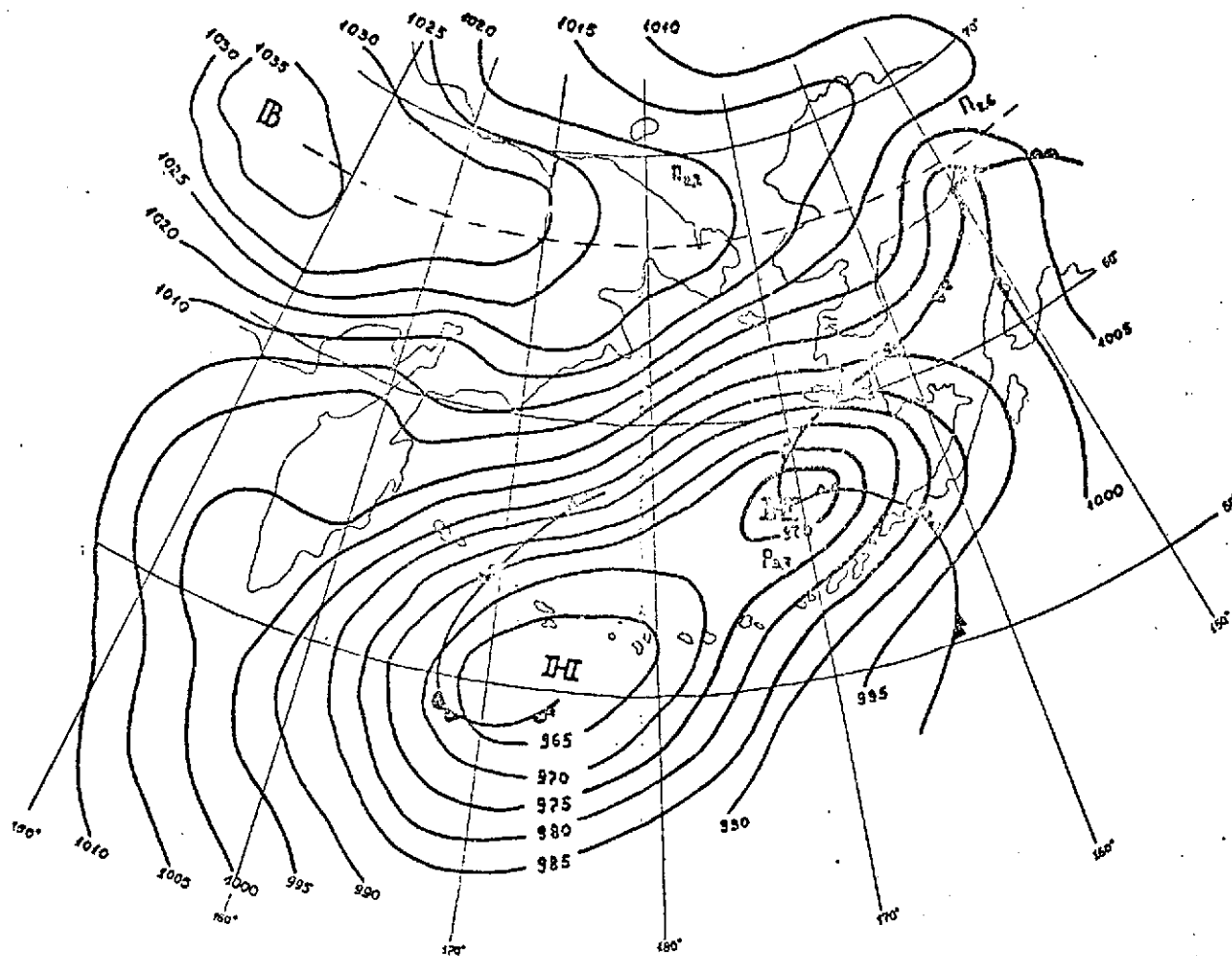


Figure 2.9. Surface synoptic chart, 0000 GMT, 8 March, 1973.

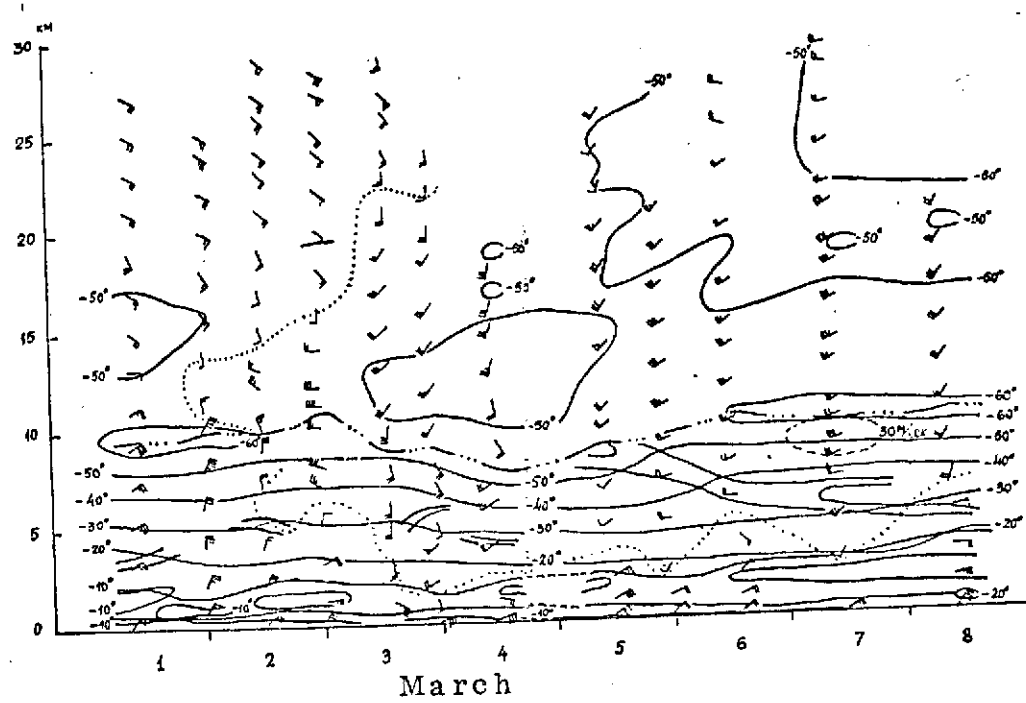


Figure 2.10. Temporal cross-section of the atmosphere above the Bering Sea, 11-20 February 1973.

Legend: — isotherms, -... tropopause
 — frontal zone boundaries, ---- isotachs,
 velopause.

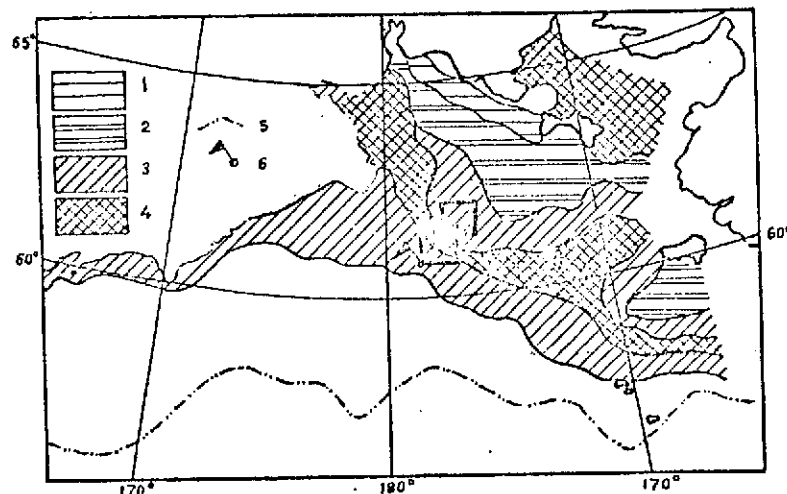


Figure 2.11. Diagram of ice conditions in the operational area of the "Bering" expedition on March 1973.

Legend: 1 - gray ice; 2 - gray-white ice; 3 - preponderance of white ice; 4 - white ice with inclusion of first-year ice of medium thickness; 5 - average boundary of ice in March; 6 - position of "Priboi" during program "C" option.

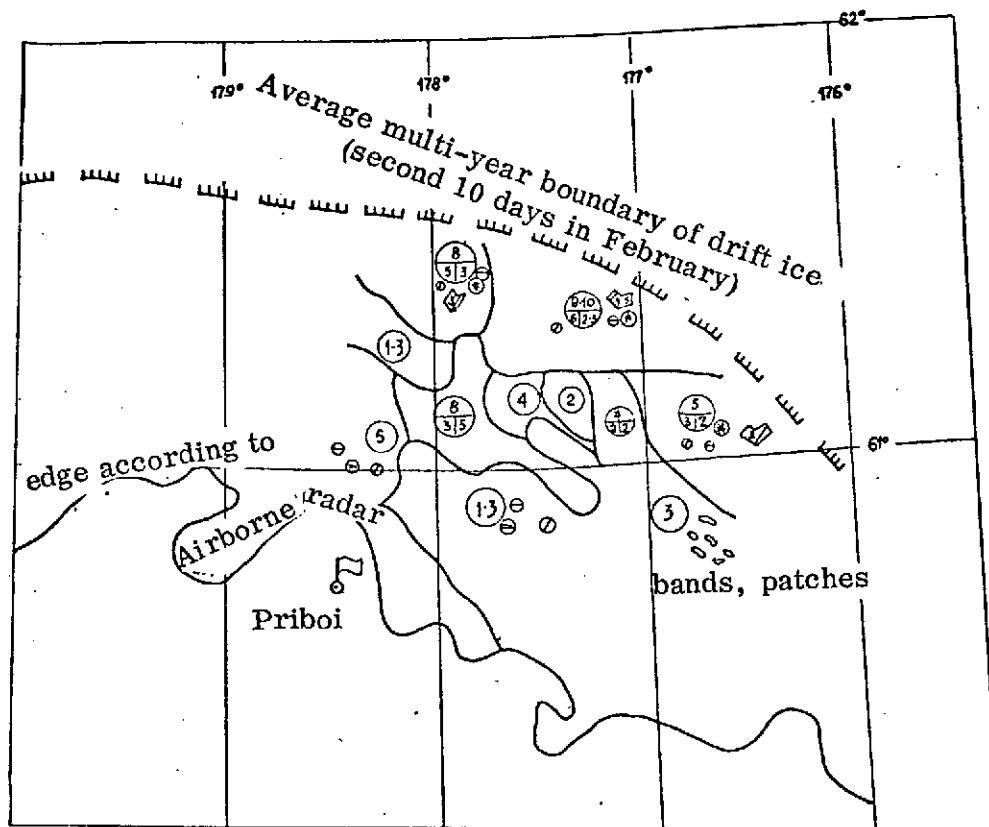


Figure 2.12. Ice situation in the vicinity of the "Priboi" station, 19-20 February, 1973.

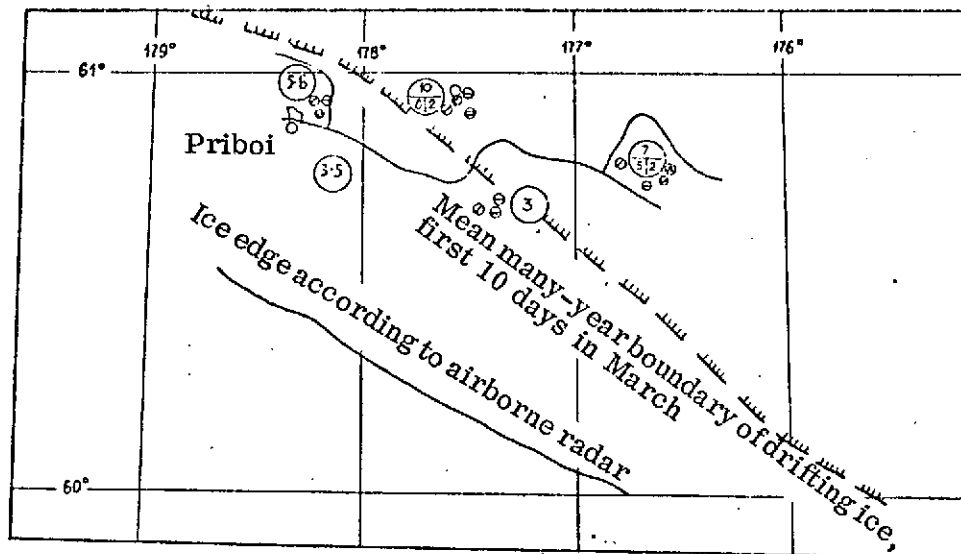


Figure 2.13. Ice situation in the vicinity of the "Priboi" station, 5-6 March 1973.

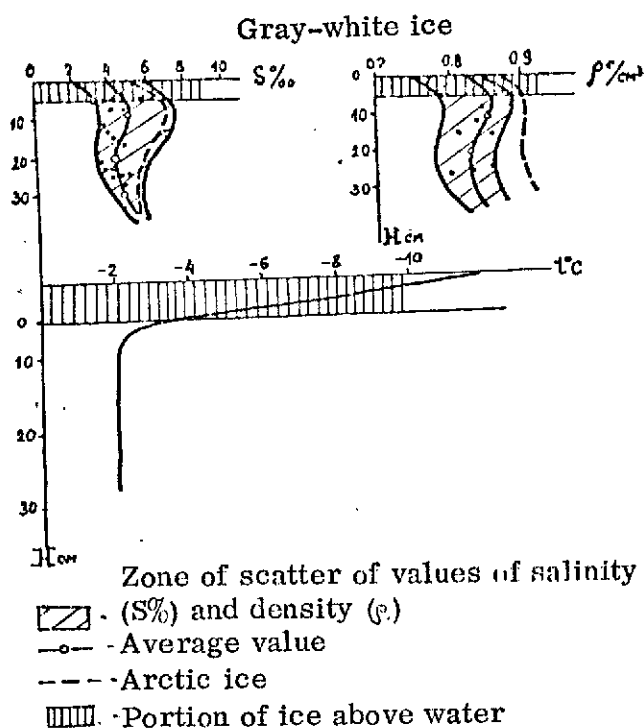


Figure 2.14. Vertical distribution of temperature ($t^{\circ}\text{C}$), density (ρ) and salinity (S) of gray-white ice.

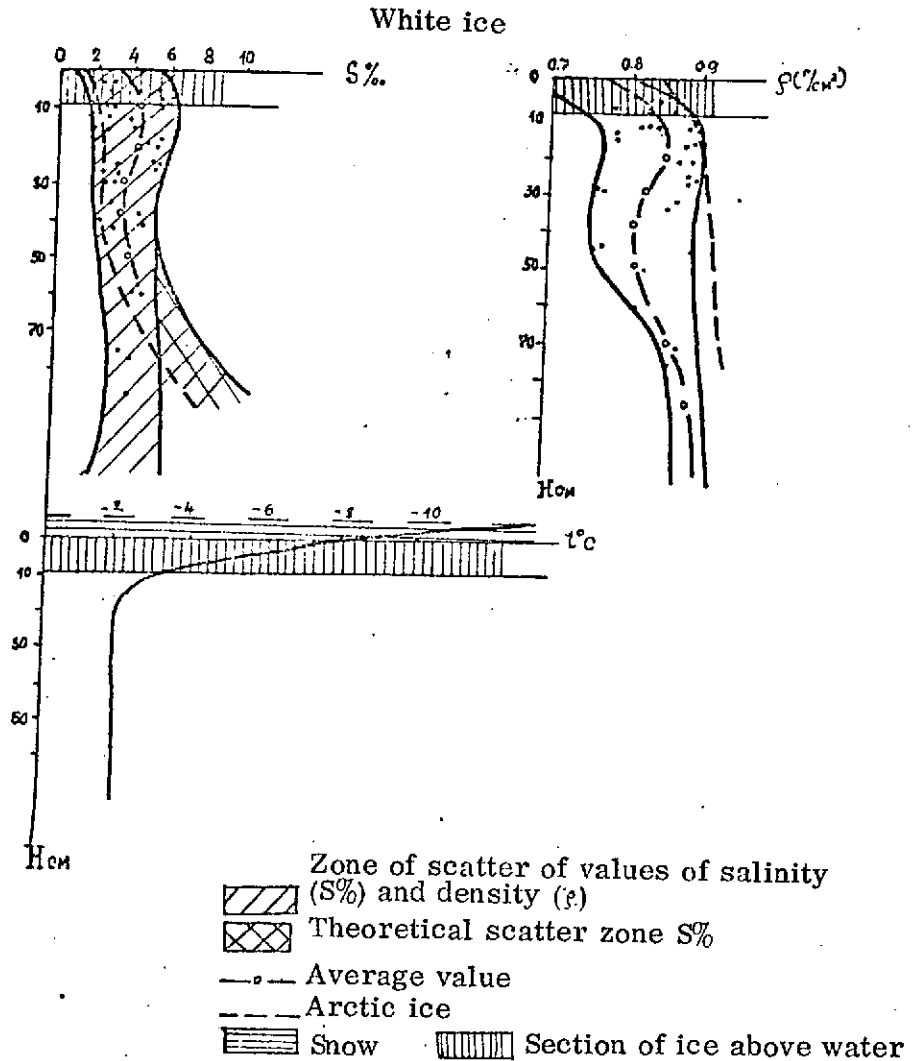


Figure 2.15. Vertical distribution of temperature ($t^{\circ}\text{C}$), density (ρ) and salinity (S') of white ice.

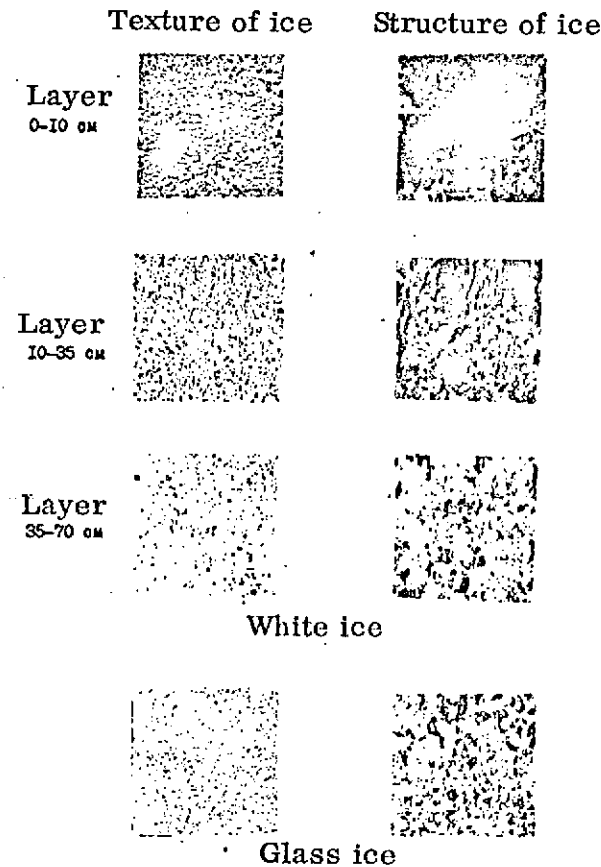
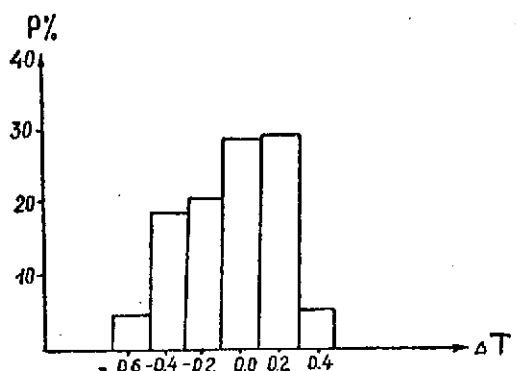


Figure 2.16. Texture and crystalline structure of ice.

<i>№</i>	Age characteristics of ice	Thickness range (cm)
1	10 6/4 Age composition of ice Amount of older ice Amount of younger ice	
2	10 6/4 СВЕТЛЫЙ НИЛАС БЛИЧАТЫЙ (nilas)	3-10
3	10 6/4 СЕРЫЙ ЛЁД (grey ice)	10-15
4	10 6/4 СЕРО-БЕЛЫЙ ЛЁД (grey-white ice)	15-30
5	10 6/4 ТОНКИЙ ОДНОЛЕТНИЙ БЕЛЫЙ ЛЁД (thin first - year ice)	30-70

Table 2. 1. Ice legend.

Figure 3. 1. Histogram of deviations of IR-radiometer readings from mercury thermometer data $\bar{T} = -0.003^{\circ}$.

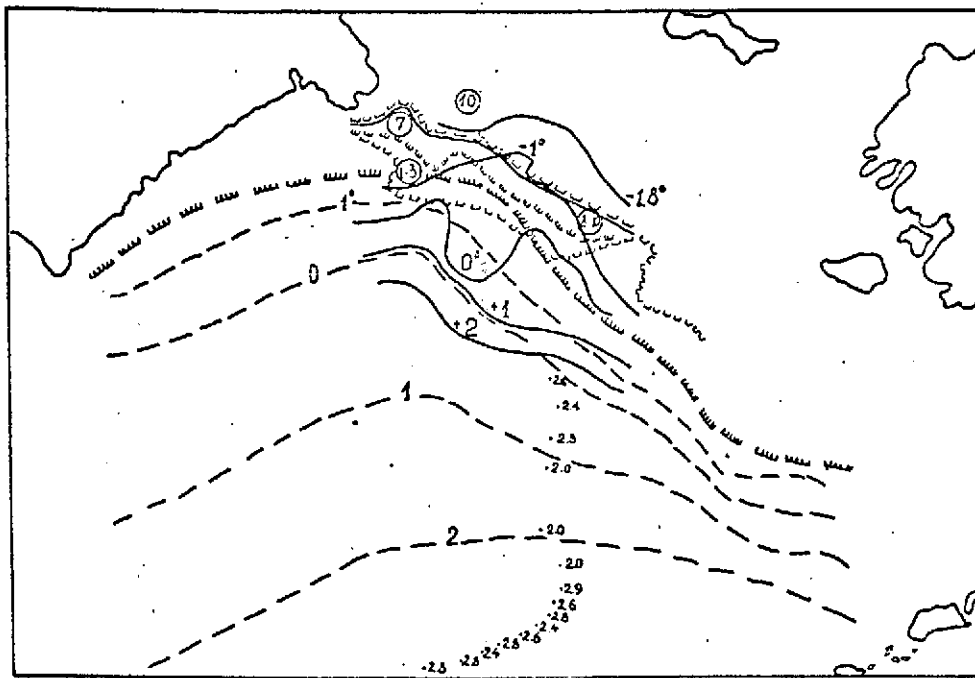


Fig. 3.2. Position of ice edge and isotherms compared with the multi-year data for the period 16-28 February 1973.

— water isotherms, - - - average multi-year water isotherms,
 —, —, — boundaries of ice fields of different salinity, - - - multi-year
 average position of ice edge.

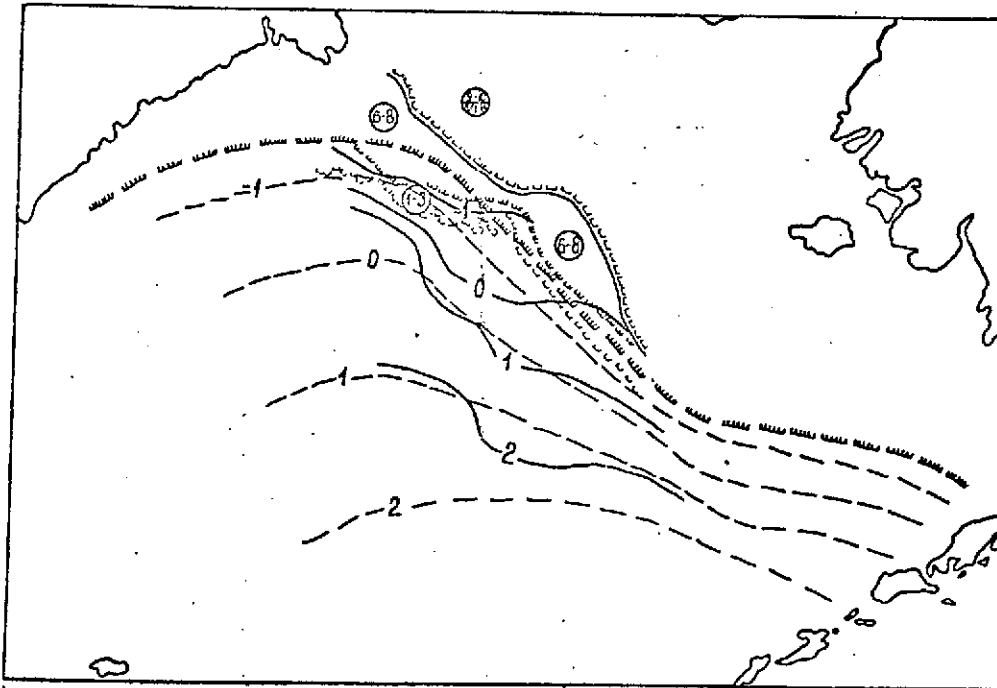


Fig. 3.3 Position of ice edge and isotherms compared with the multi-year data for the period 1-8 March 1973.

— water isotherms, - - - average multi-year water isotherms,
- - - boundaries of ice fields of different salinity, — multi-year
average position of ice edge.

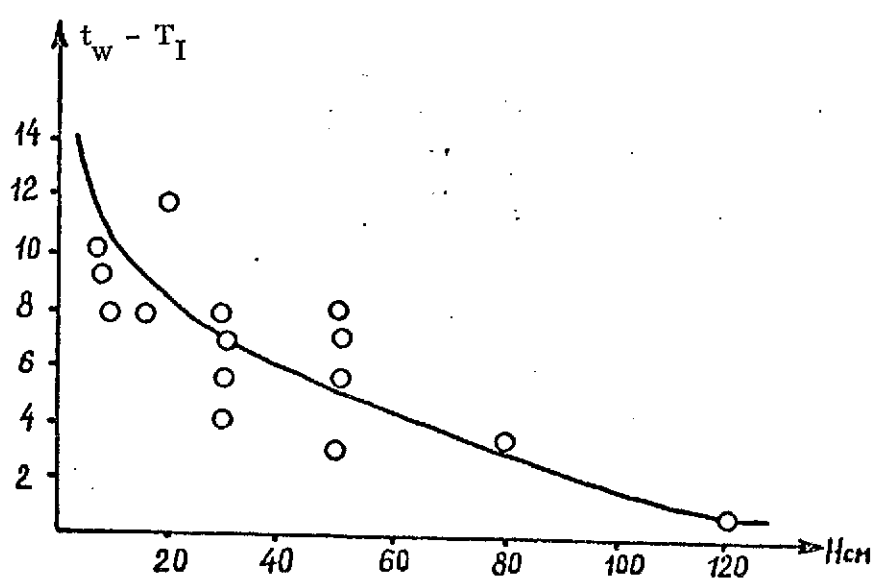


Fig. 3.4. Dependence of water-ice temperature contrast ($T_w - T_I$) on the thickness of the ice.

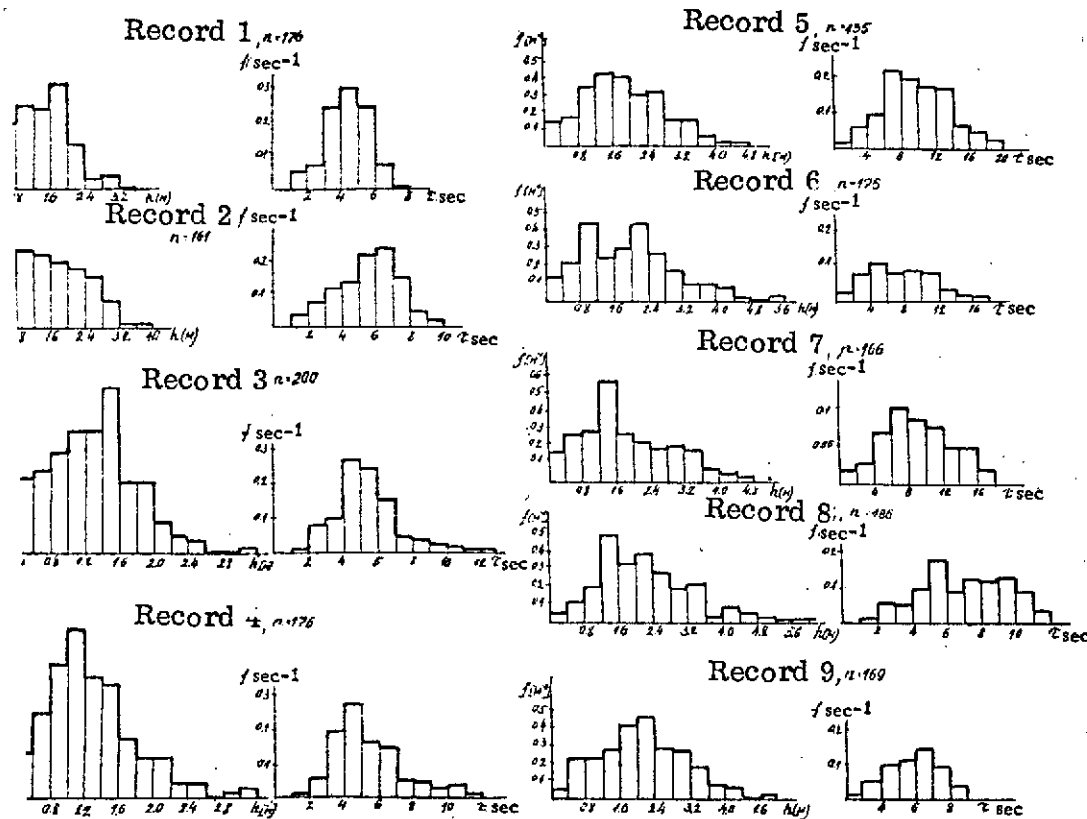


Fig. 3.5. Histograms of wave height (h) and period (T).

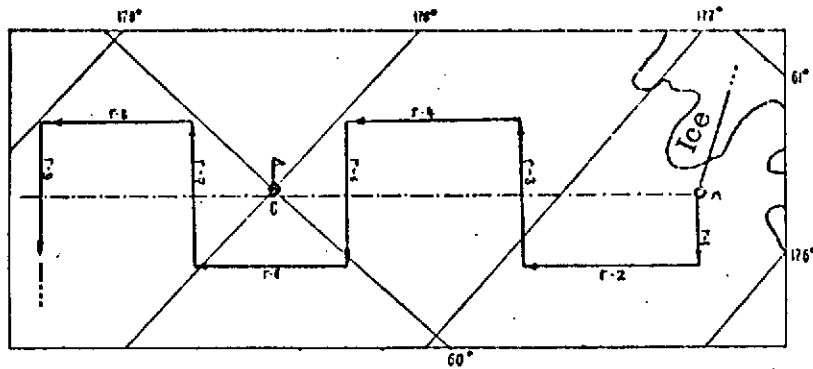


Fig. 3.6. Diagram of radar wave-survey, Program "B" option 16/17 February 1973.

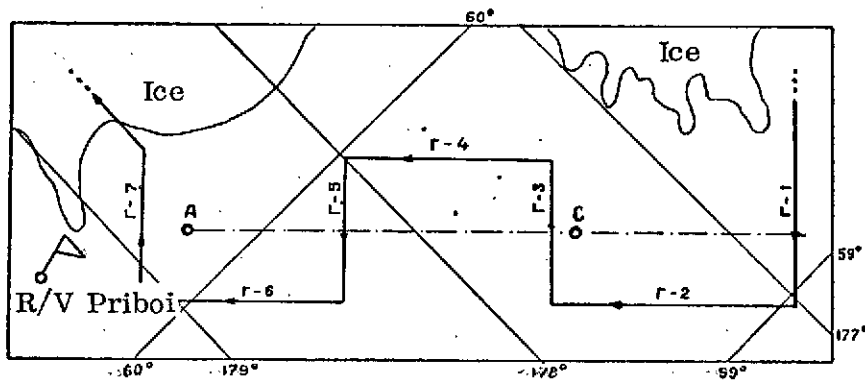


Fig. 3.7. Diagram of radar wave-survey, Program "B" option, 7/8 March 1973.

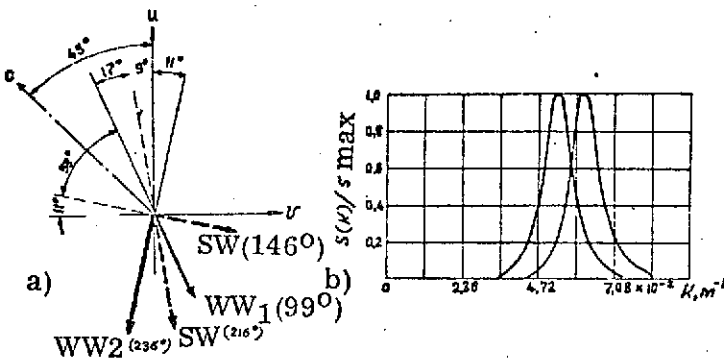


Fig. 3.8. Diagram of the main directions of sea wave systems (a) and sections of the 2 - dimensional spectra of the wave systems WW_1 and WW_2 , (b) for the survey of 7/8 March 1973, tack-2. WW_1 and WW_2 - directions of first and second systems of wind waves; SW - direction of swell; GW - direction of wave groups.

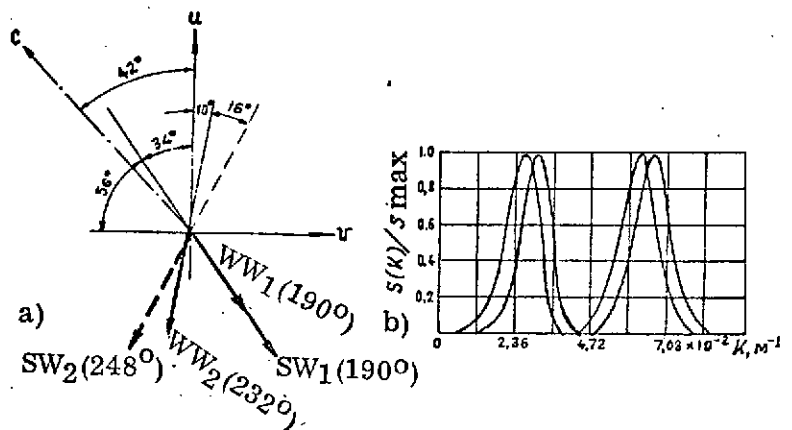


Fig. 3.9. Diagram of the main directions of sea wave systems (a) and sections of the 2-dimensional spectra of the wave systems WW_1 and WW_2 , (b) for the survey of 16/17 February 1973, tack-7. WW_1 and WW_2 - directions of first and second wave systems; SW - direction of wave groups.

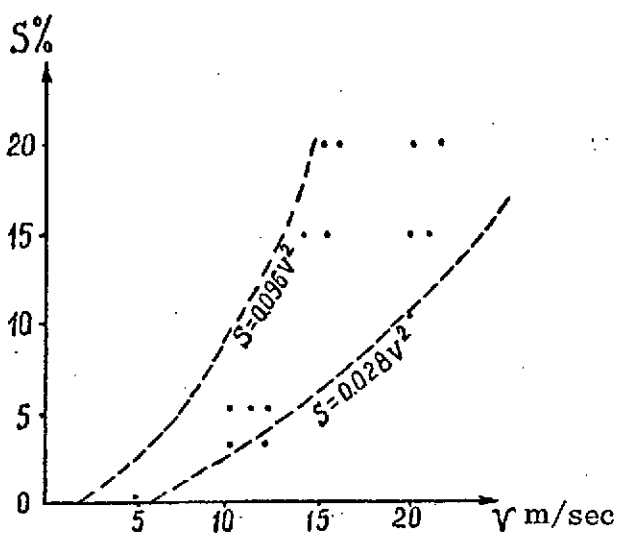


Fig. 3.10. Dependence of area of sea covered by foam on wind velocity.

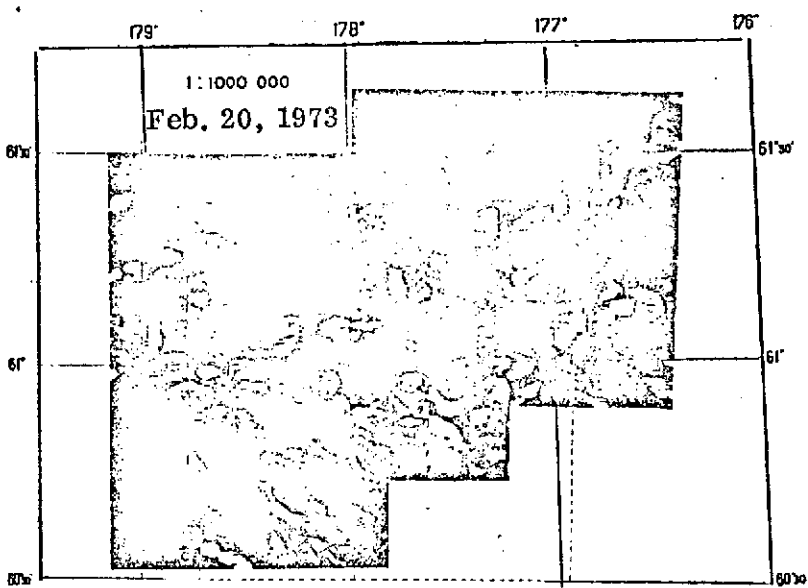


Fig. 4.1. Microwave-survey plot, 20 February 1973.

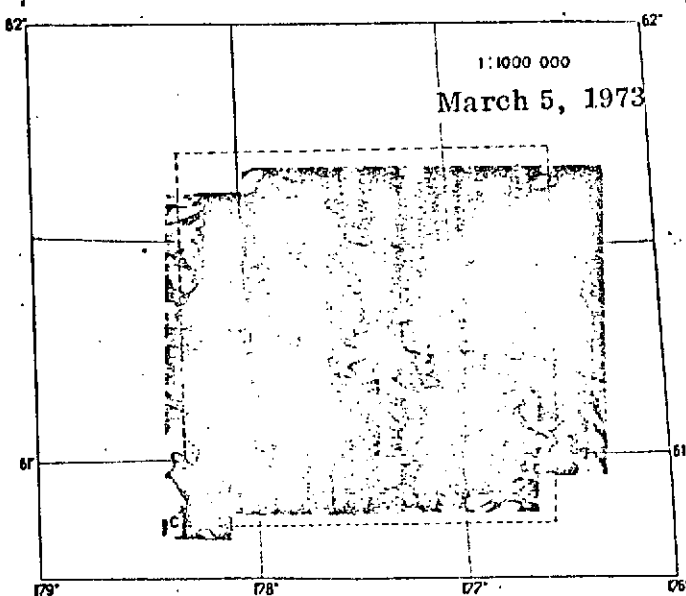


Fig. 4.2. Plot of microwave survey, 5 March 1973.

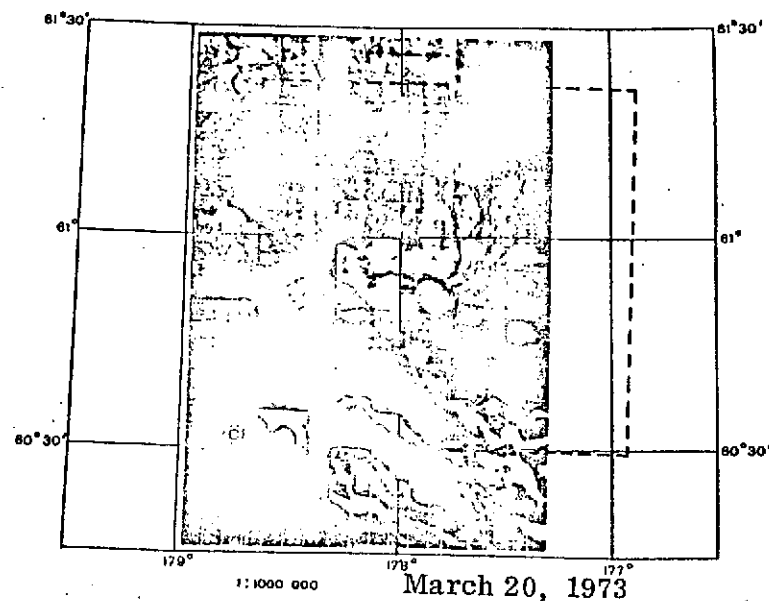


Fig. 4.3. Plot of radar survey, 20 February 1973.

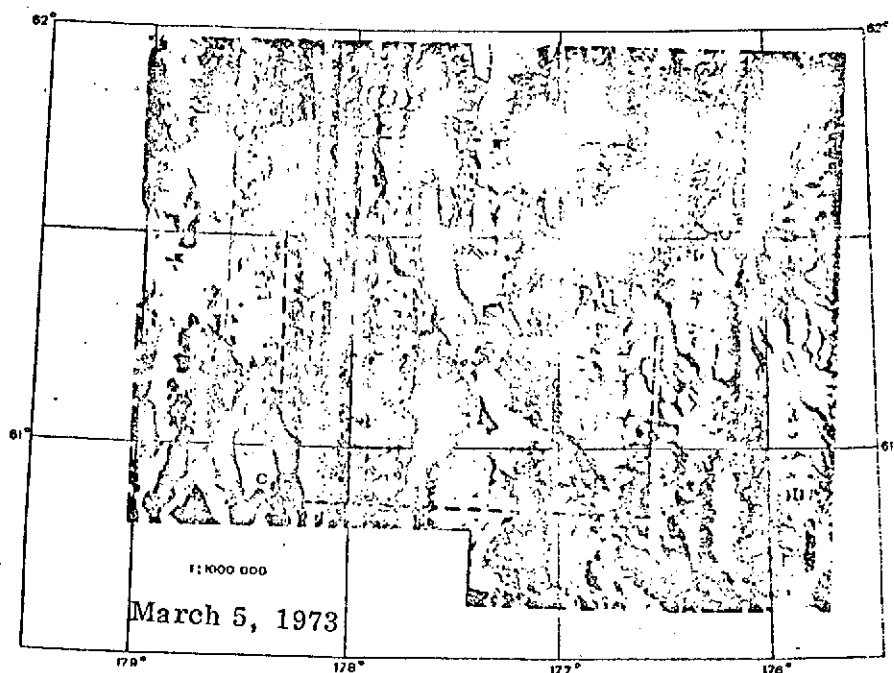


Fig. 4.4. Plot of radar survey, 5 March 1973.

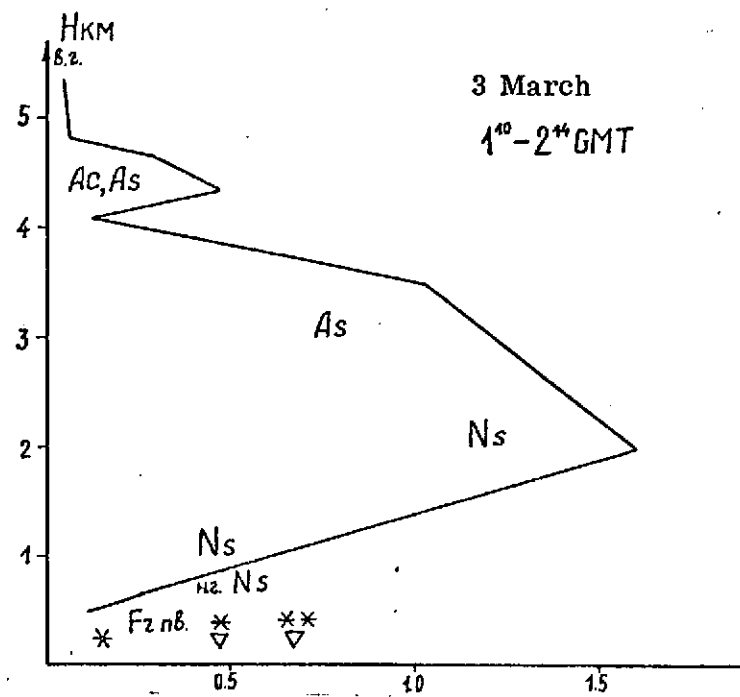


Fig. 4.5. Vertical profile of cloud water content.

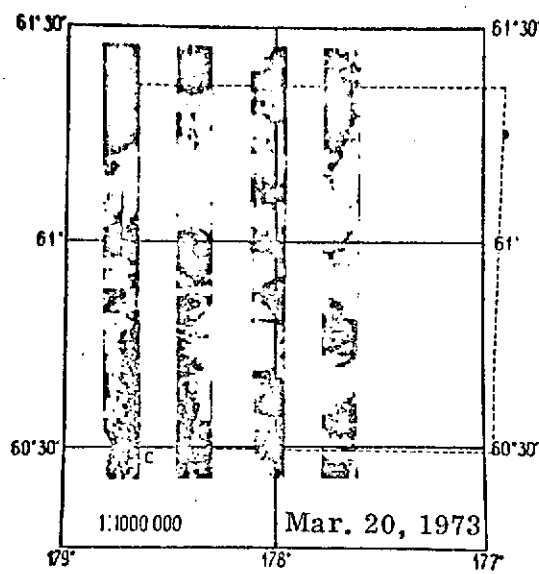


Fig. 4.6. Plot of IR-survey, 20 Feb. 1973.

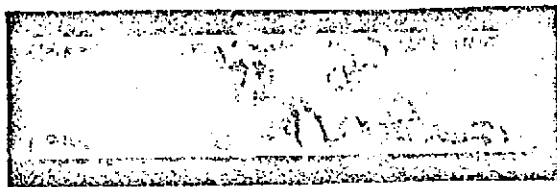


Fig. 4.7. IR-picture of cloud fields in precipitation zones.

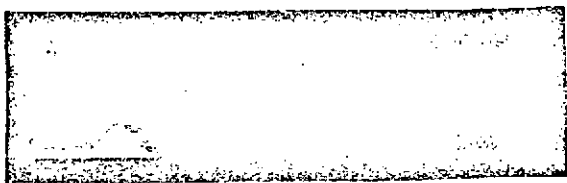


Fig. 4.8. IR-picture of agitated surface.

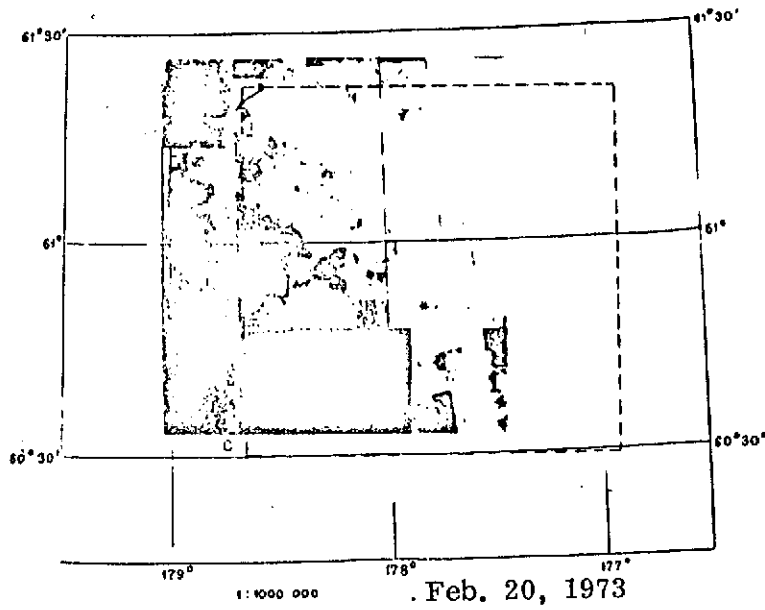


Fig. 4.9. Plot of aerophoto survey, 20 February 1973.

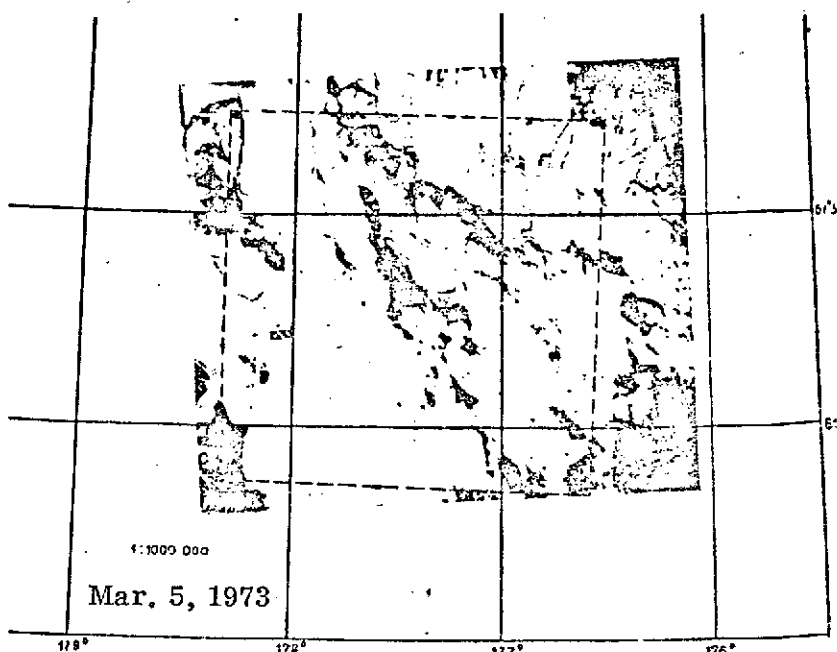


Fig. 4.10. Plot of aerophoto survey, 5 March 1973.

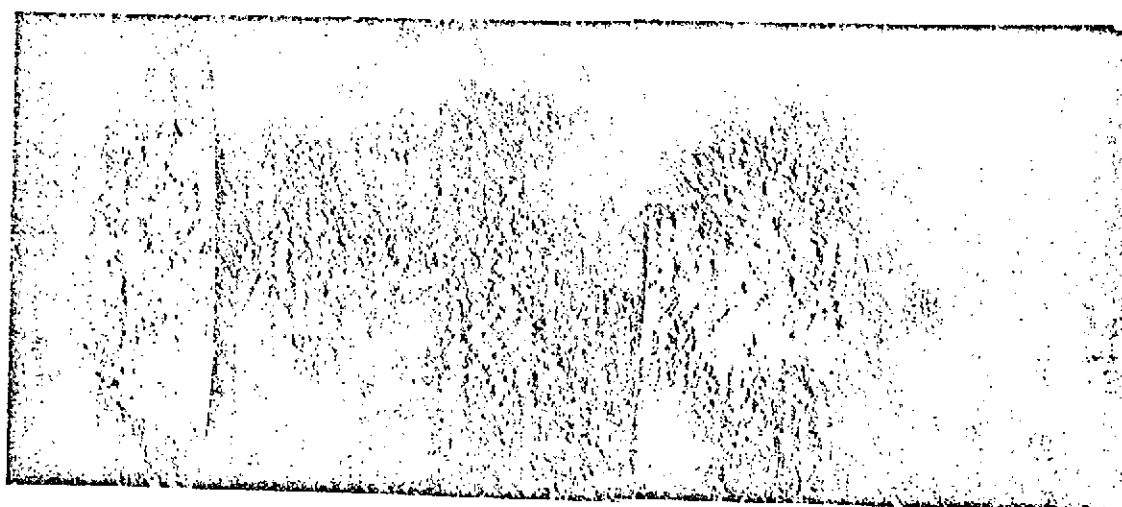


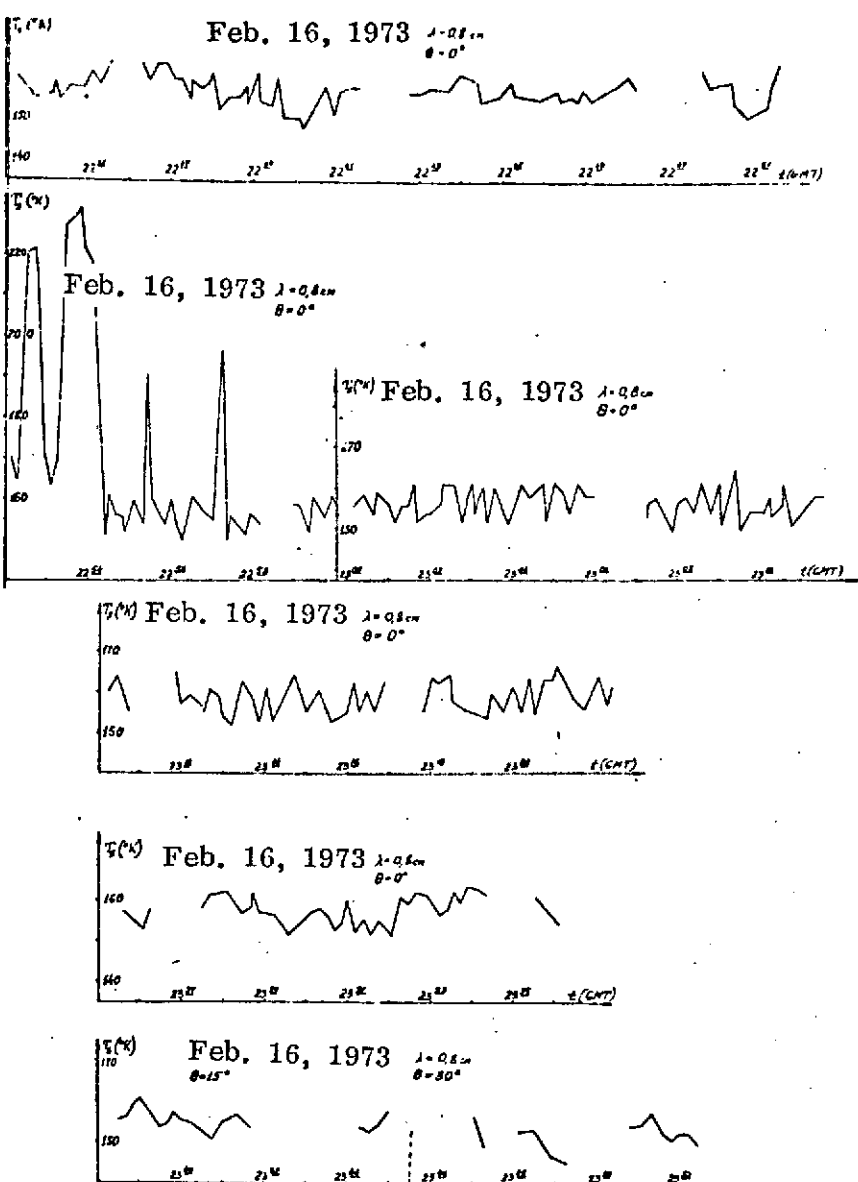
Fig. 4.11. Frame-by-frame aero-photo survey of sea state, 7 March 1973.

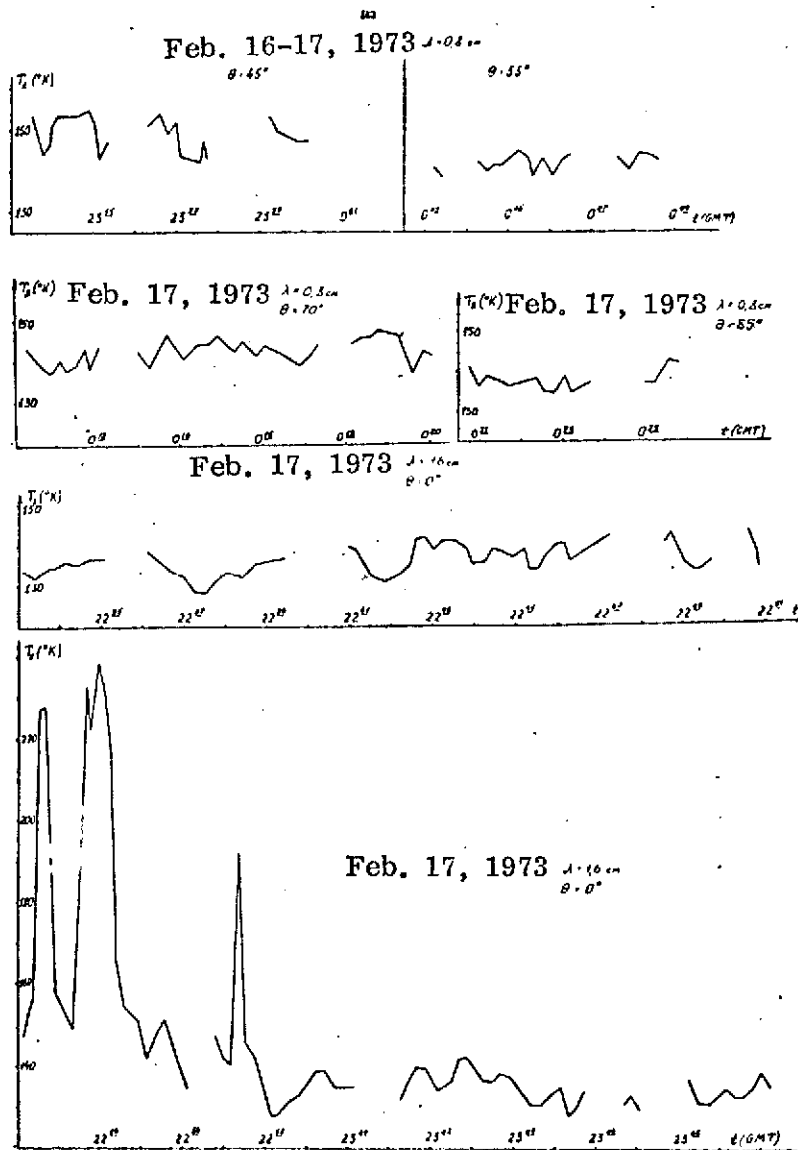
APPENDIX IV.2

/141

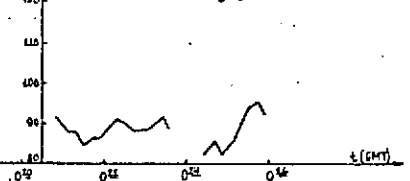
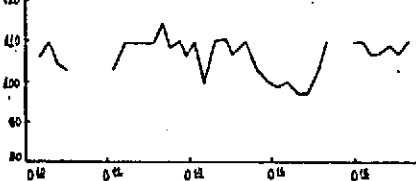
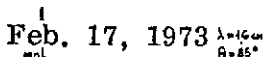
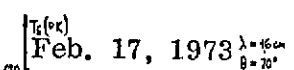
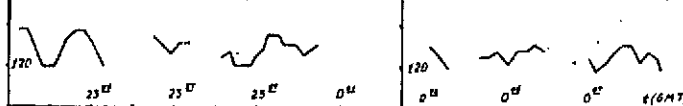
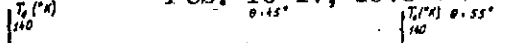
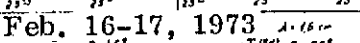
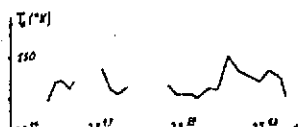
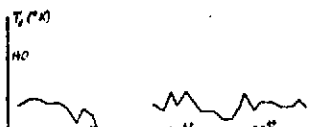
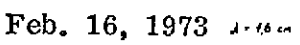
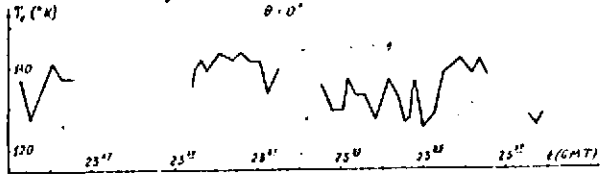
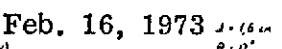
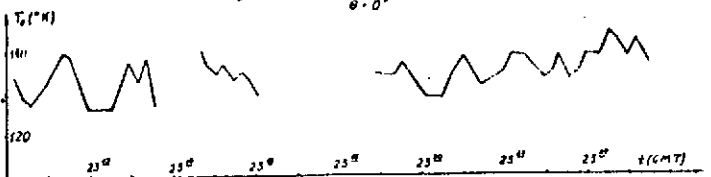
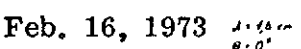
PLOTS OF RADIO BRIGHTNESS TEMPERATURES

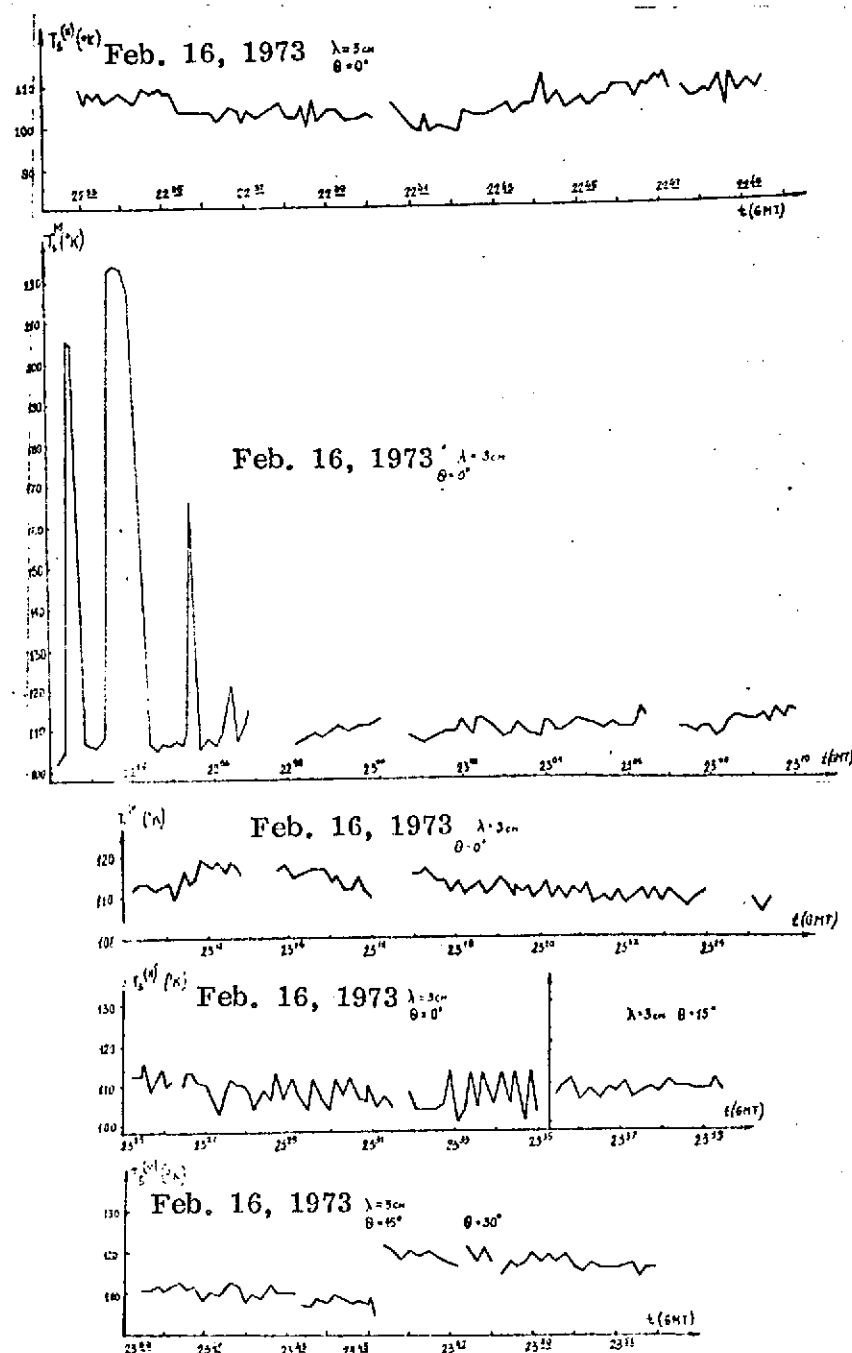
/142

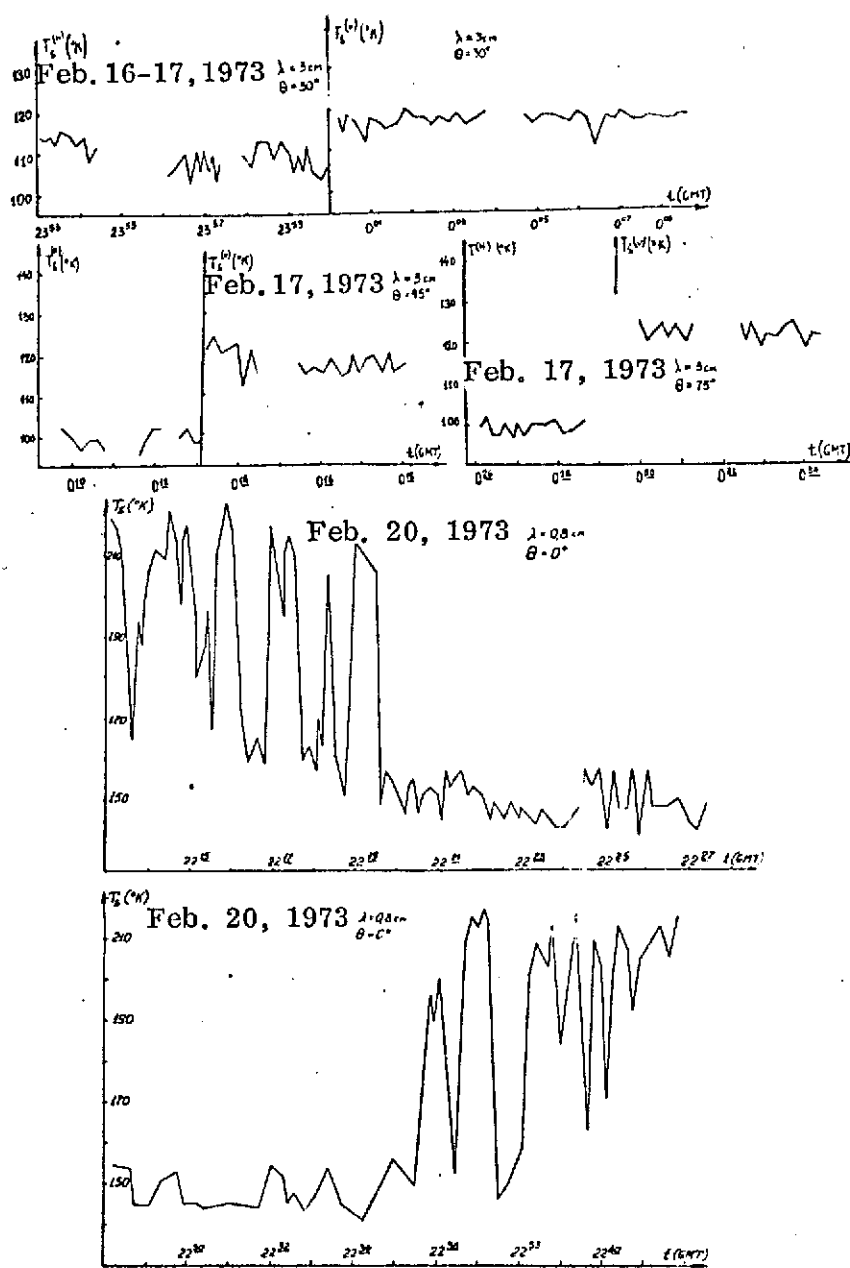


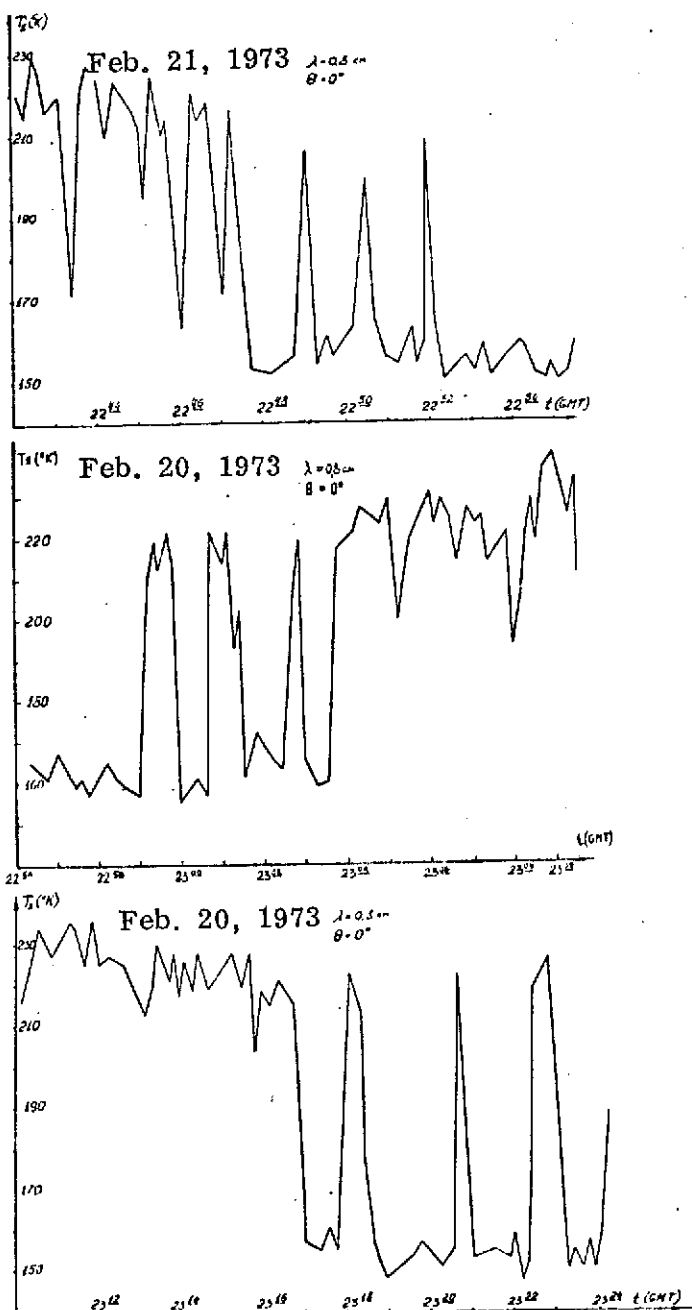


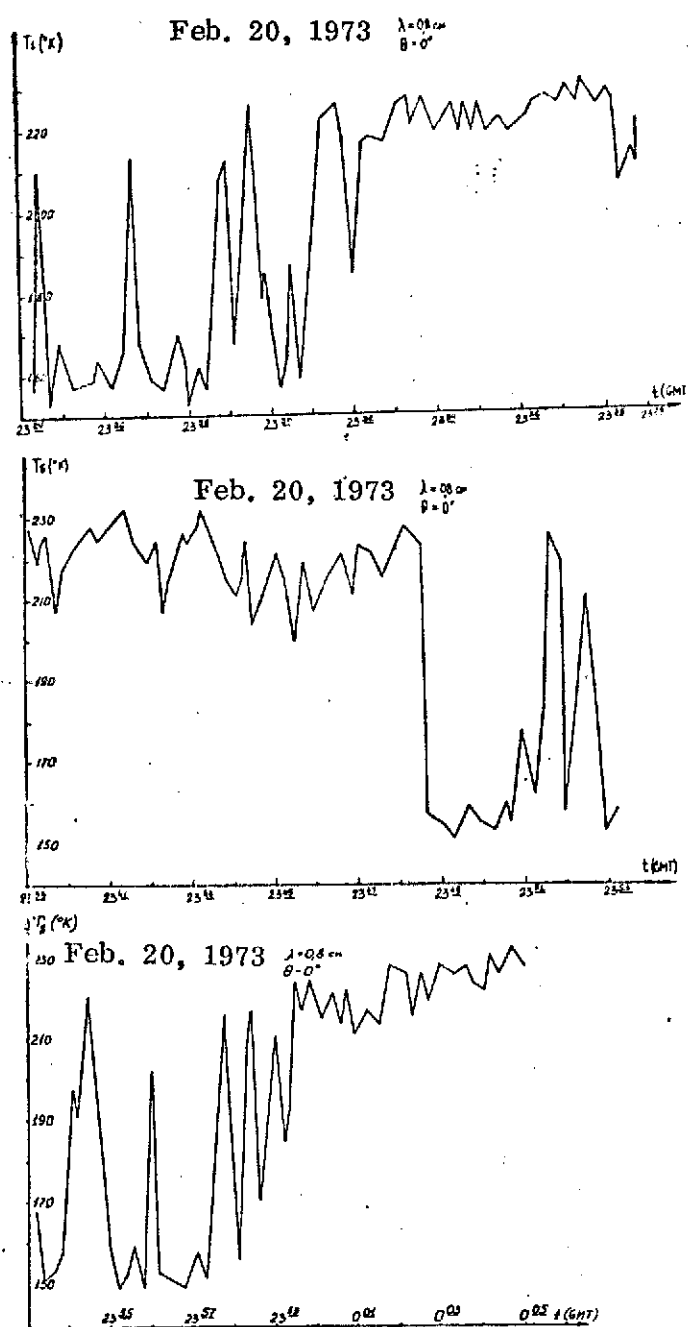
144

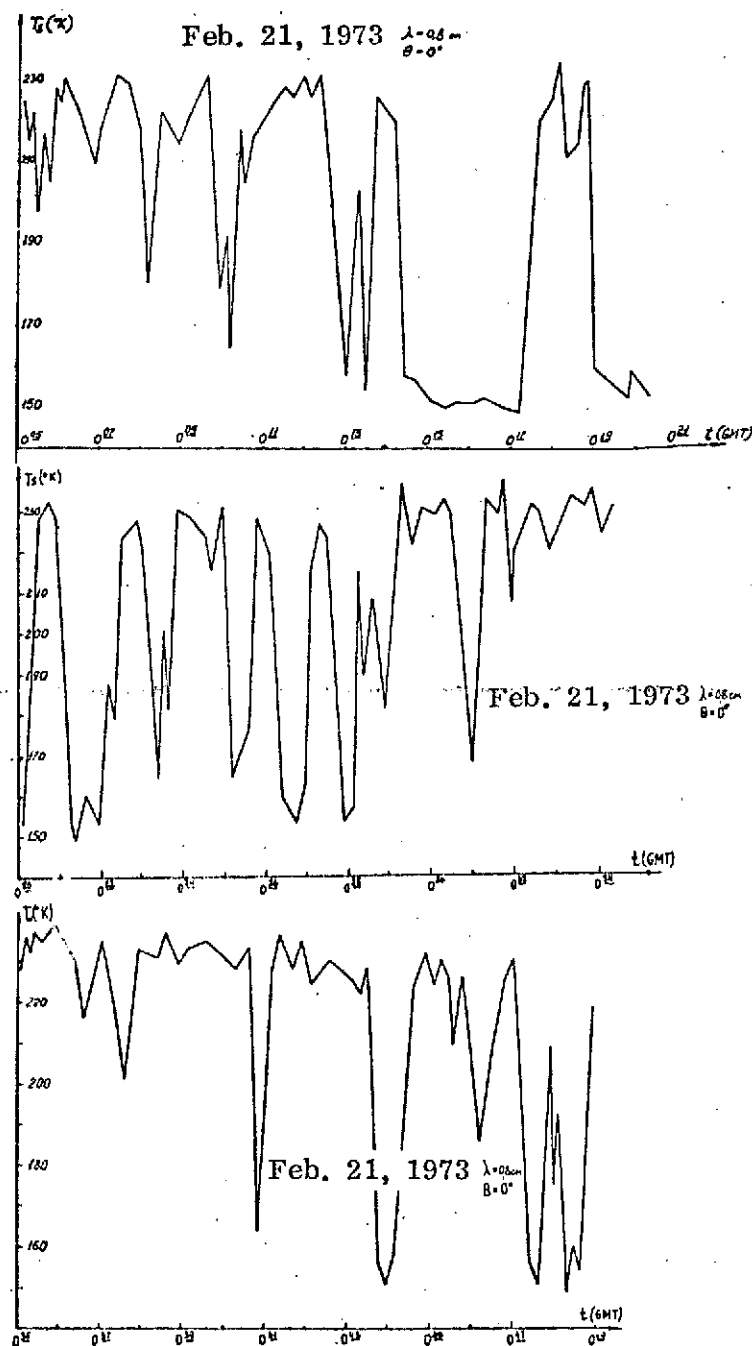


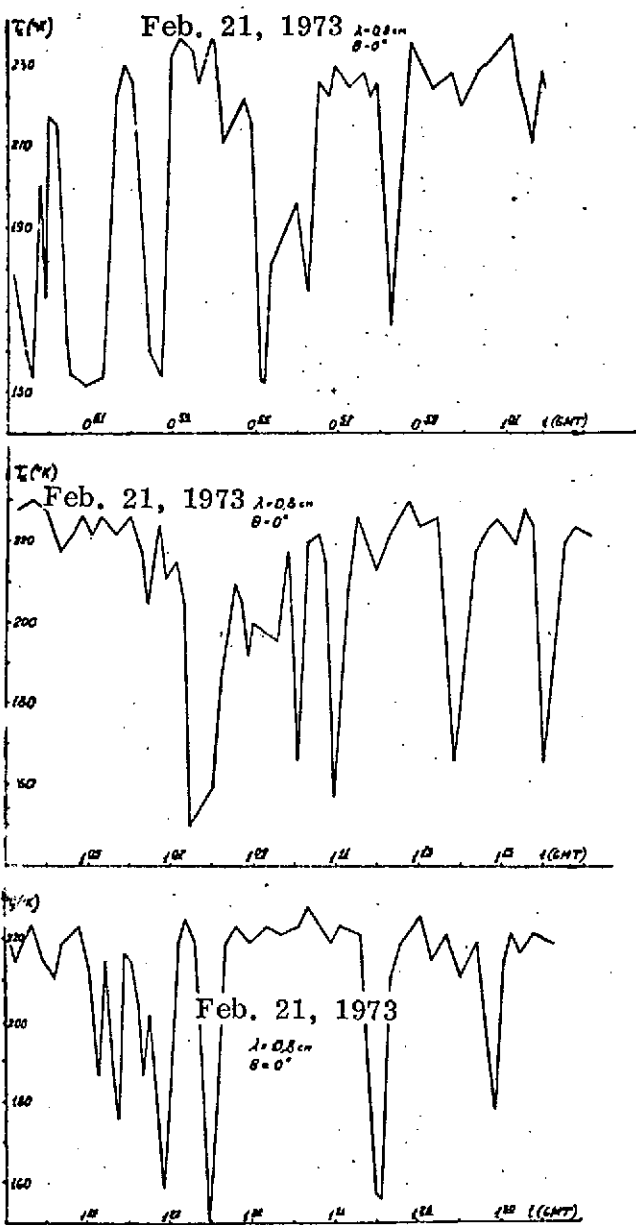


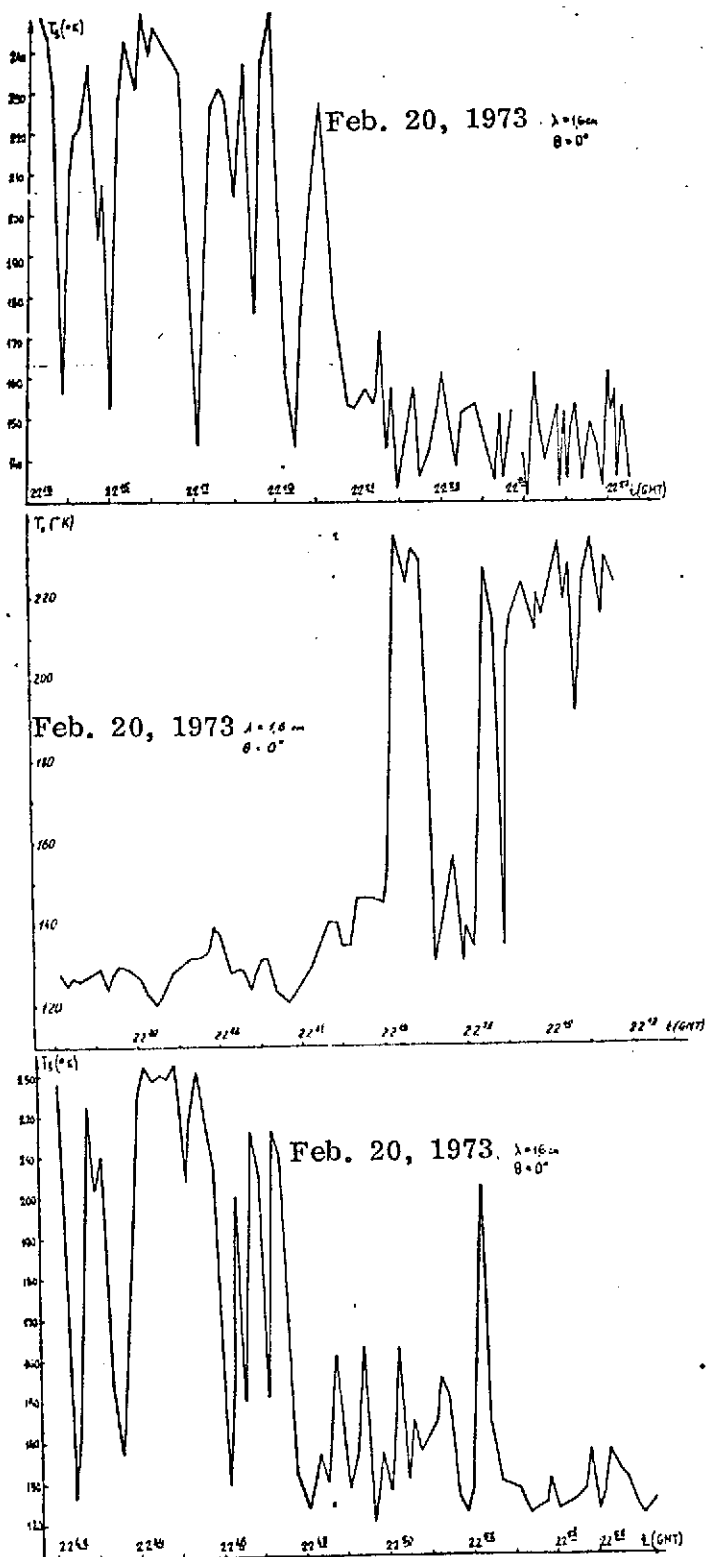




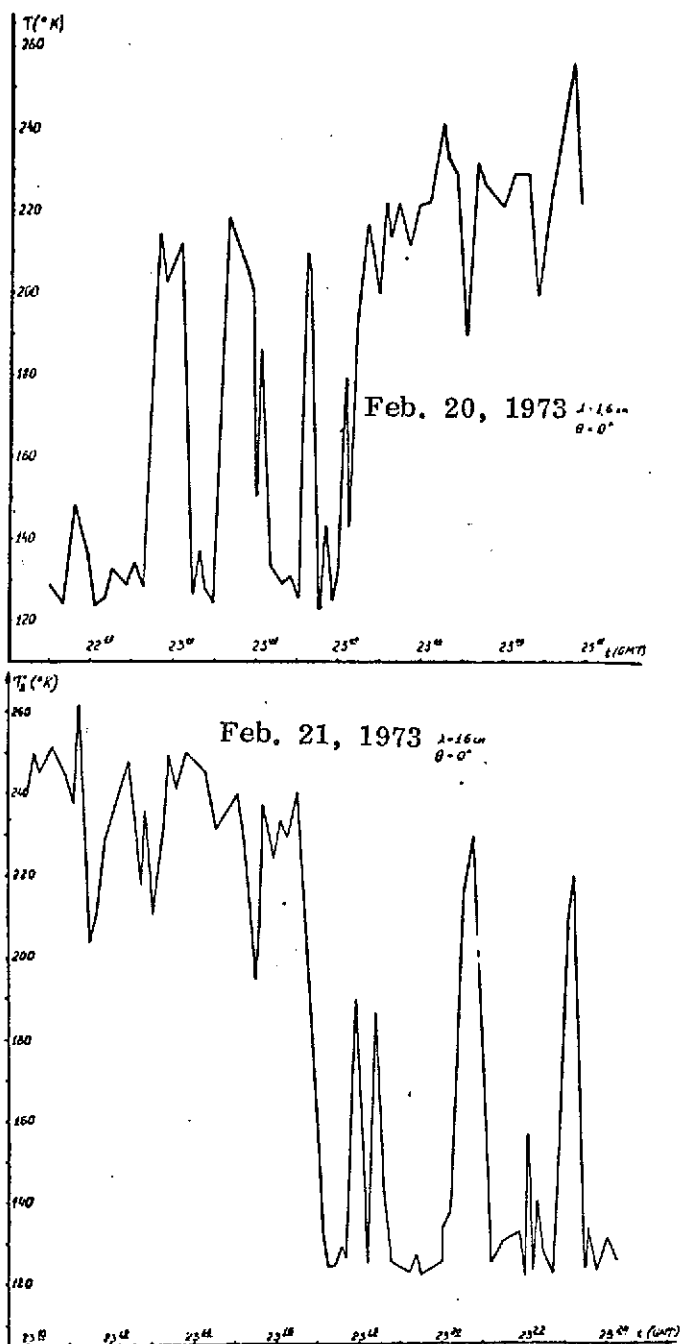


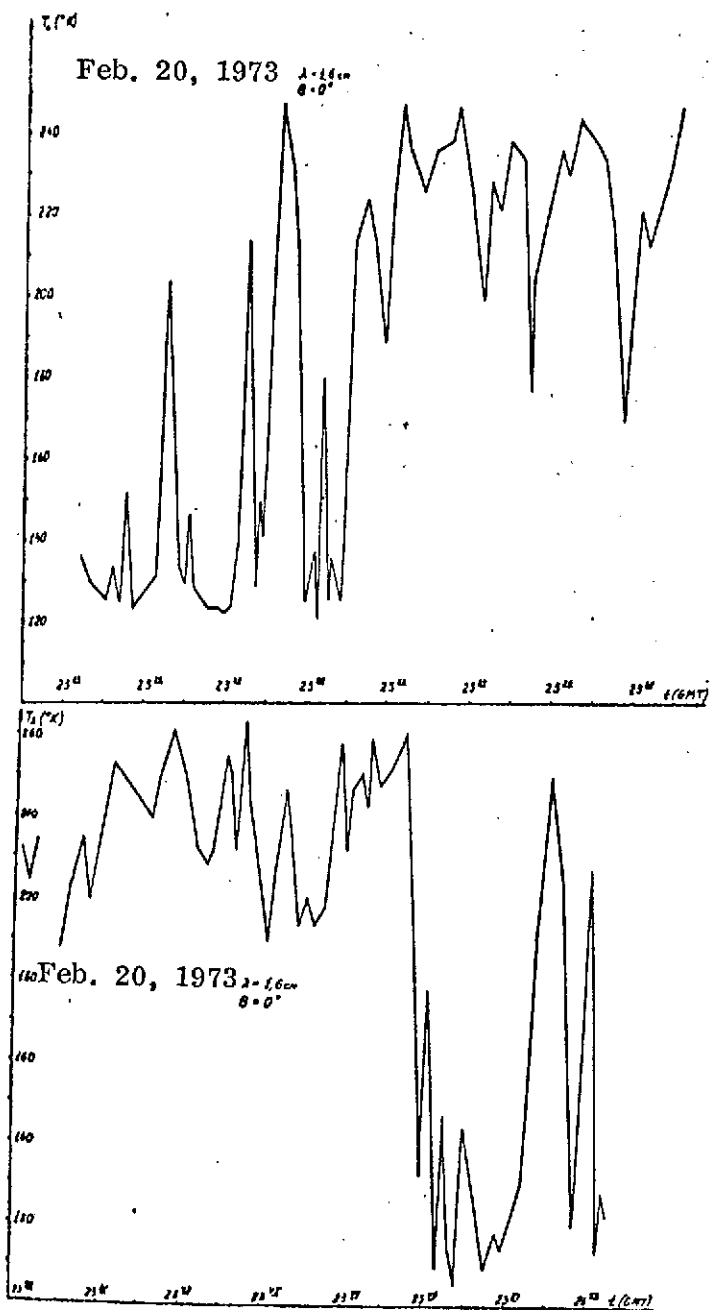


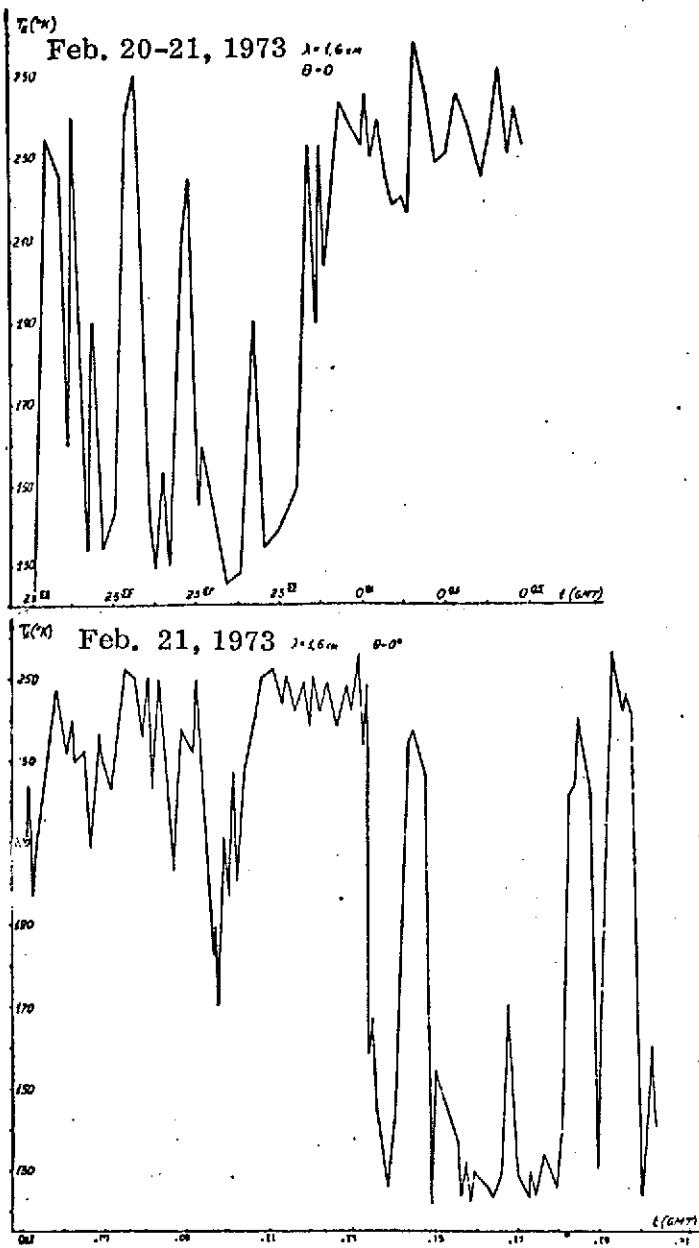


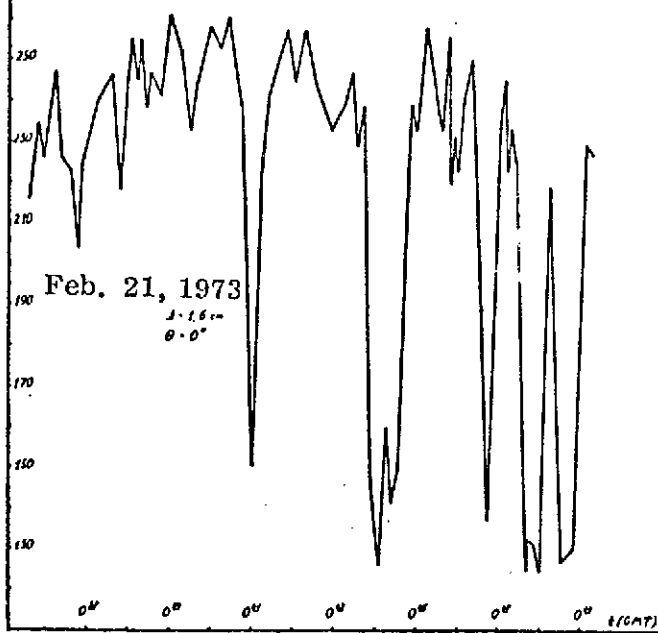
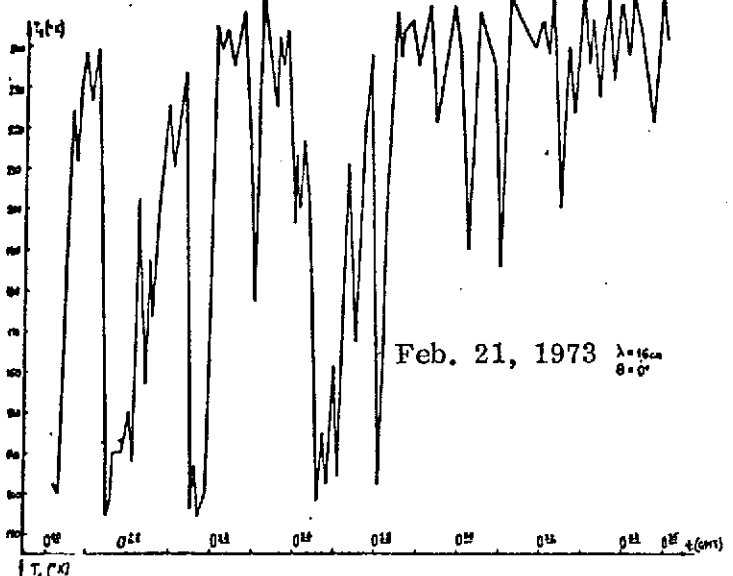


/152

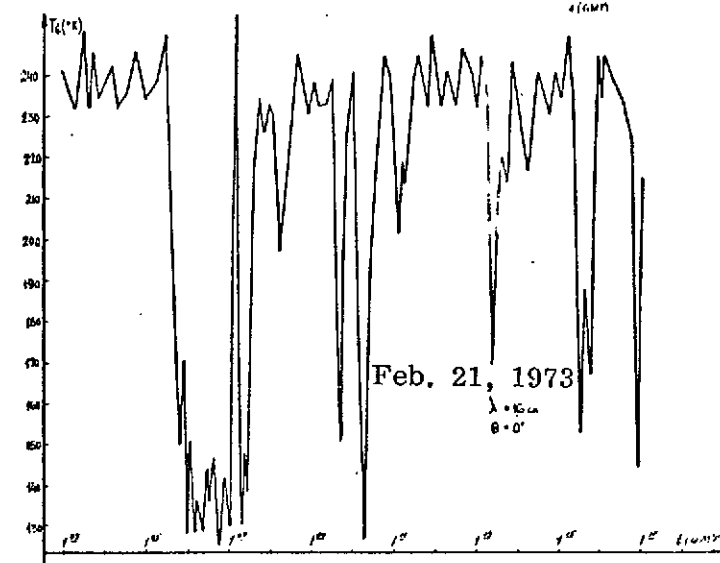
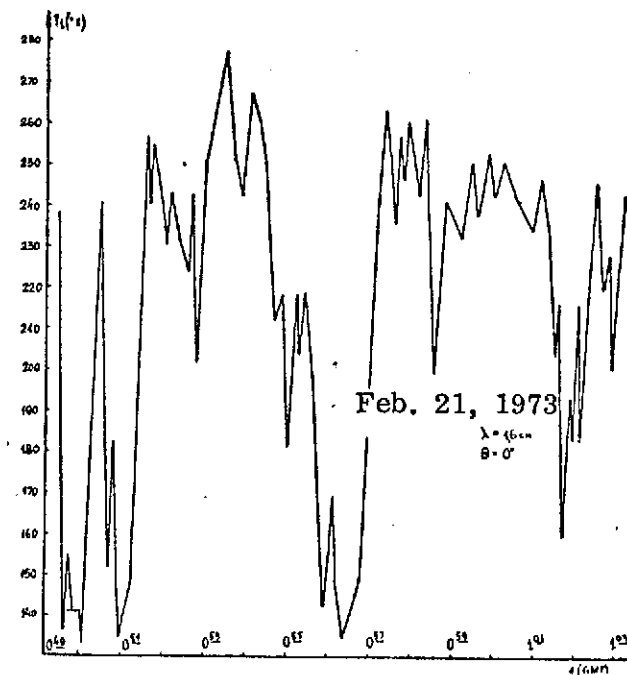


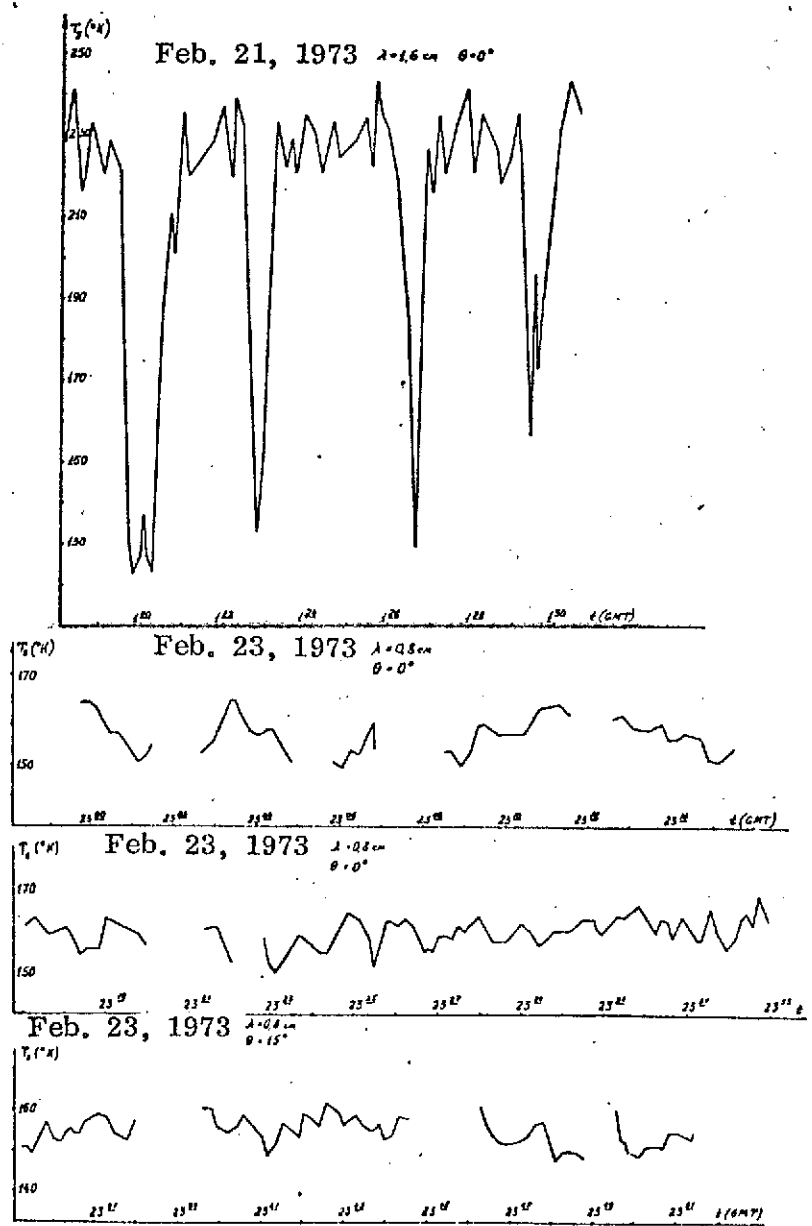


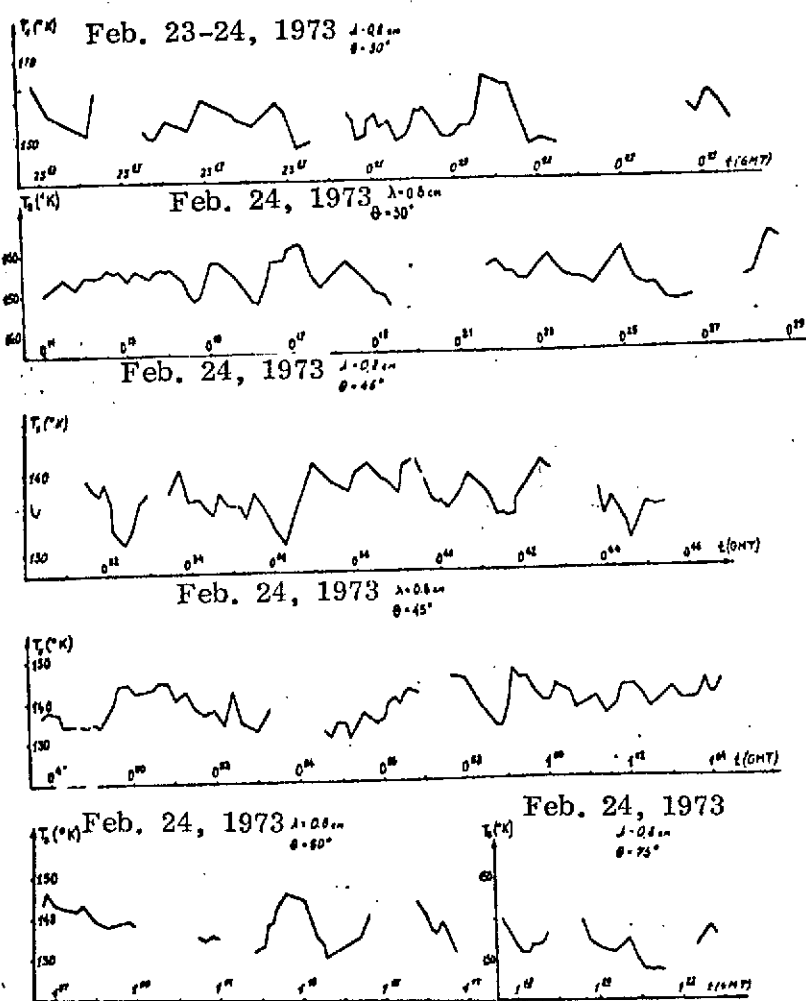


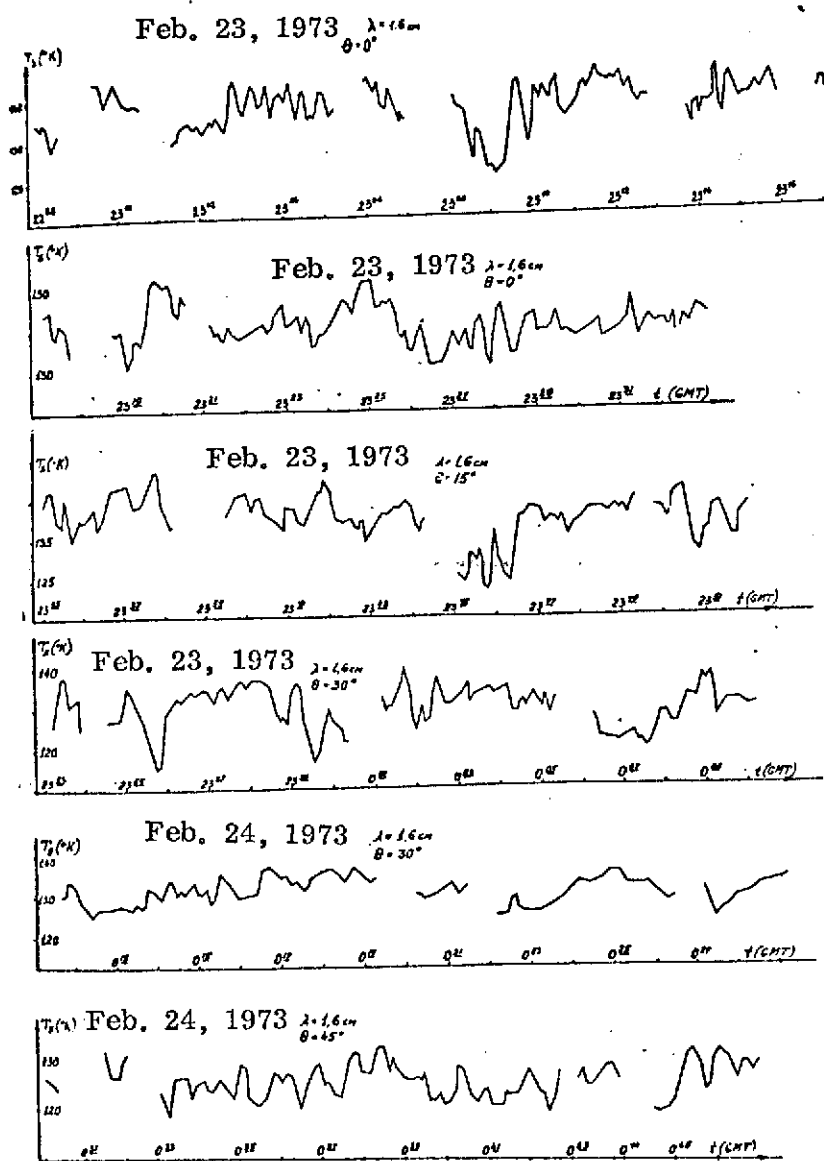


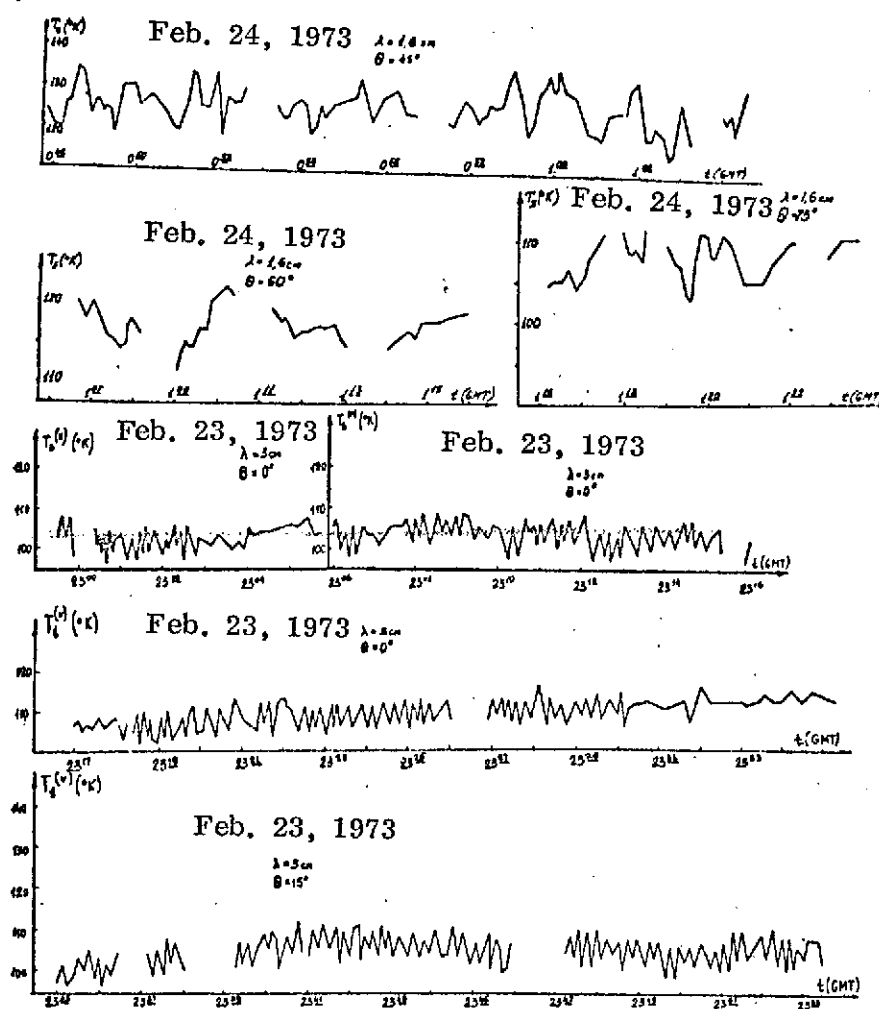
/156

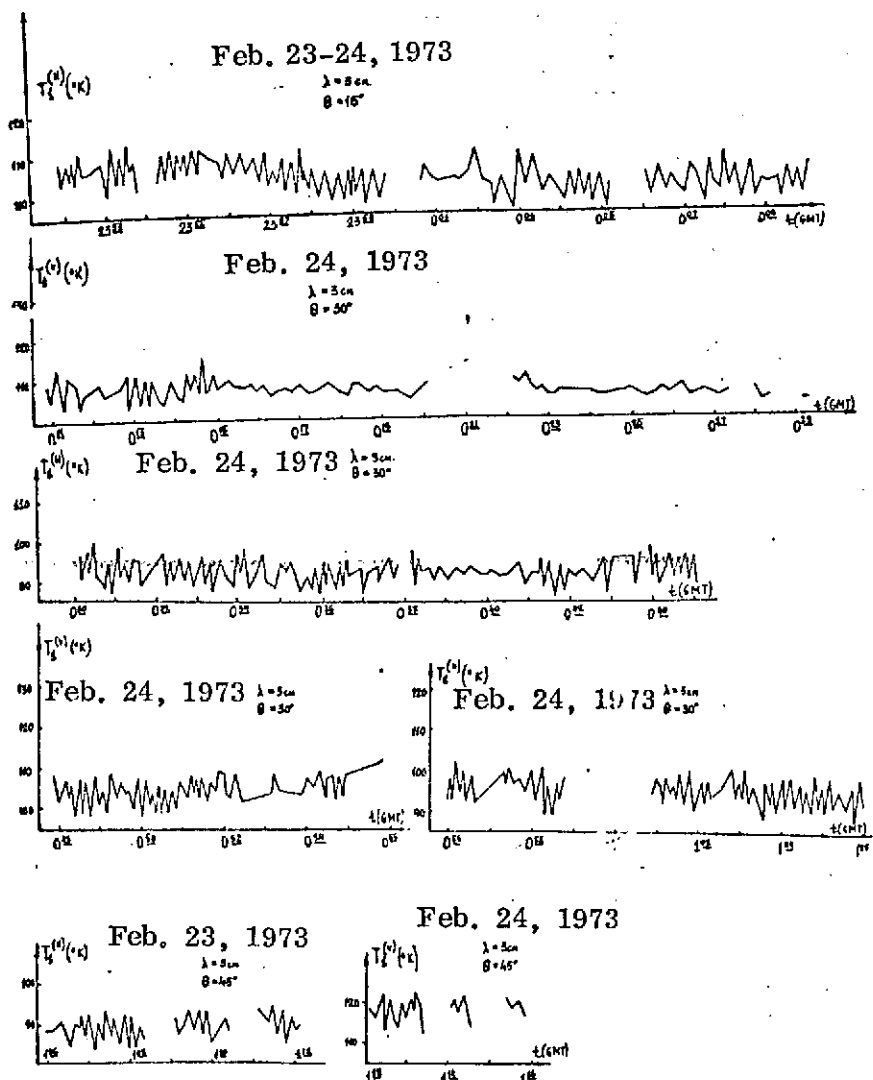




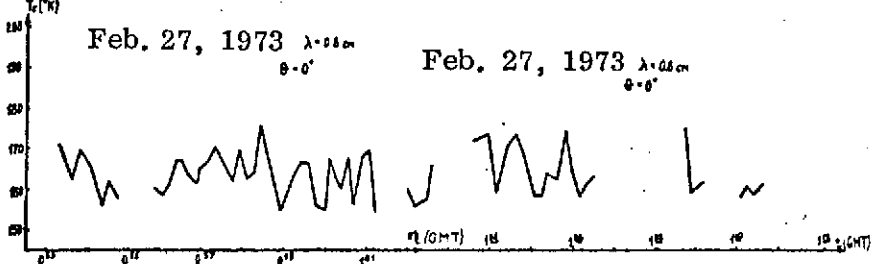
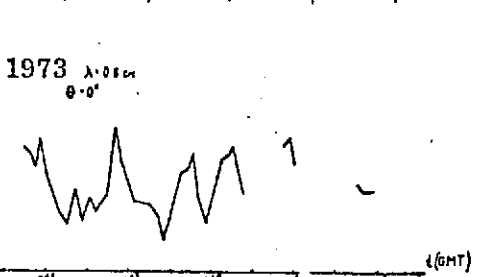
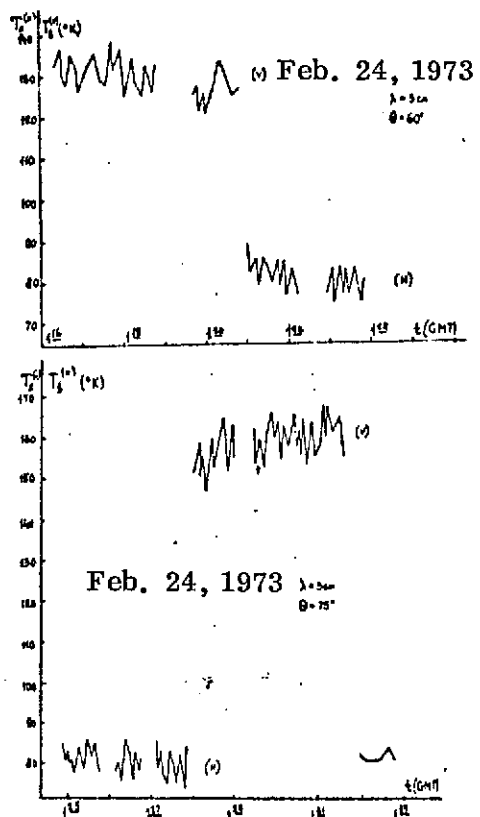


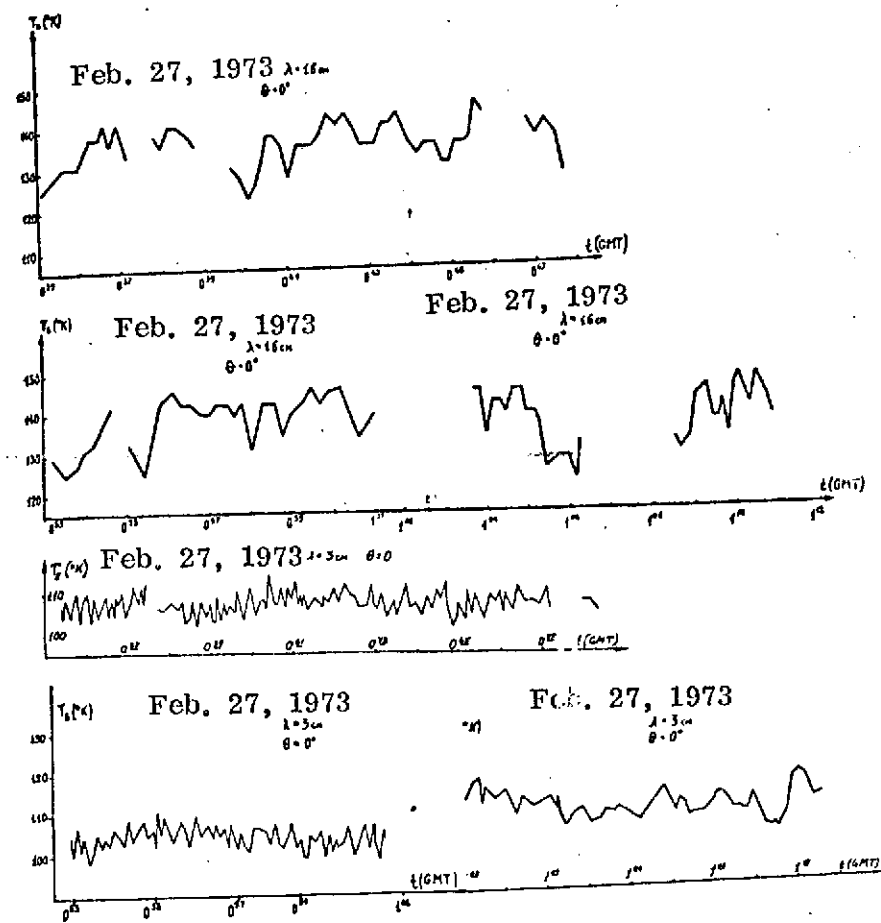


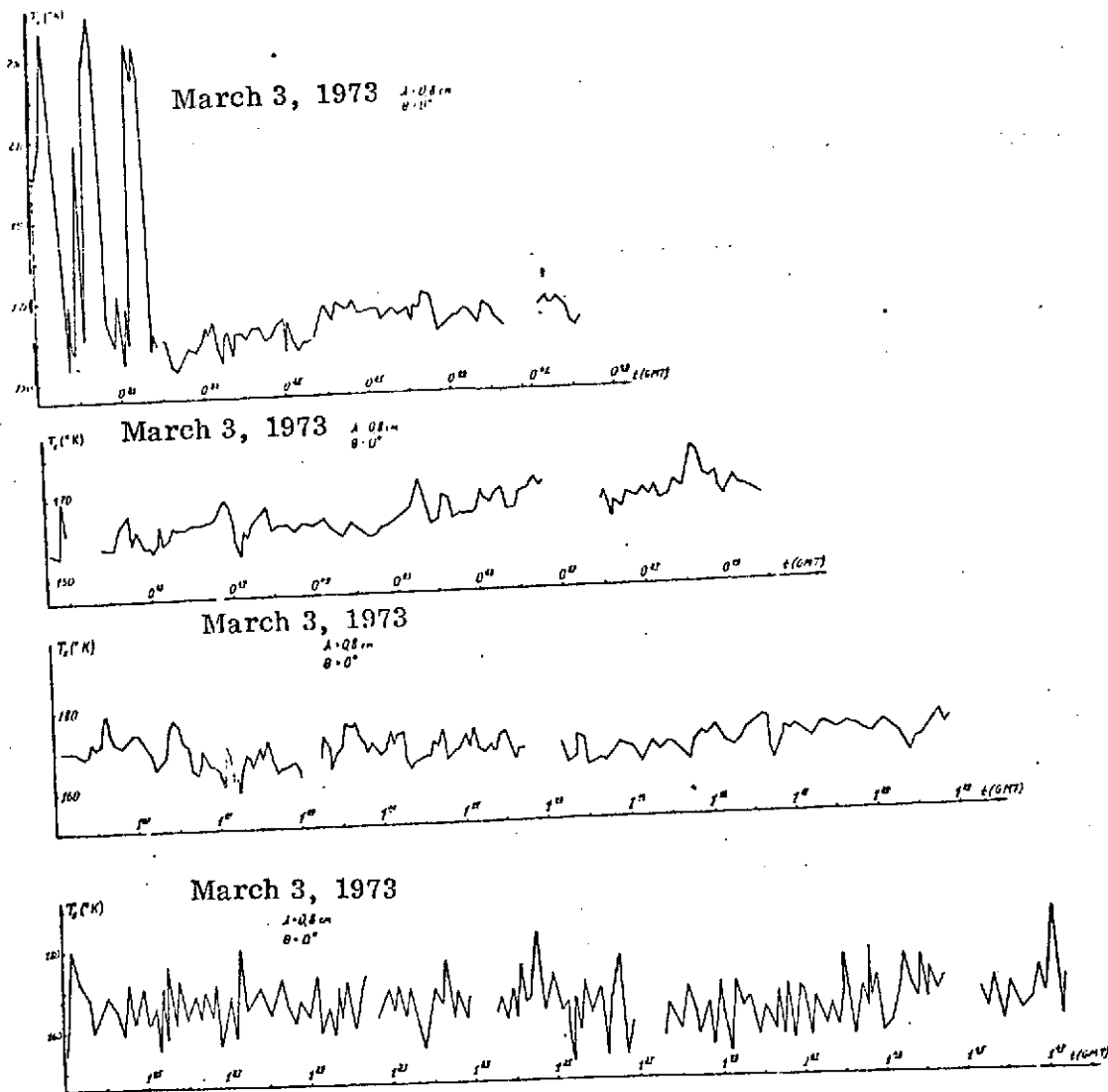




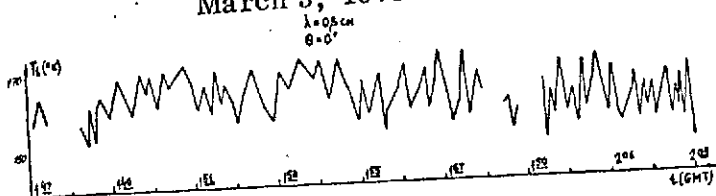
/162



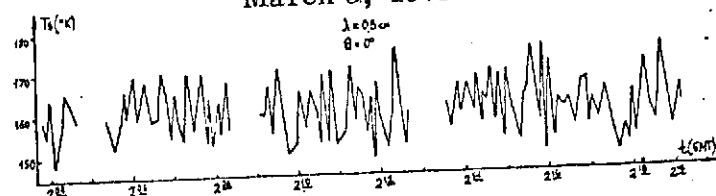




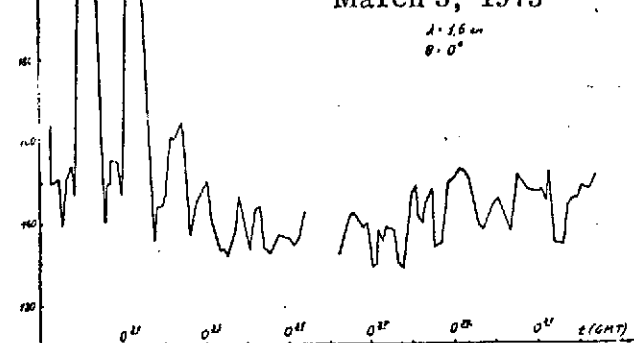
March 3, 1973

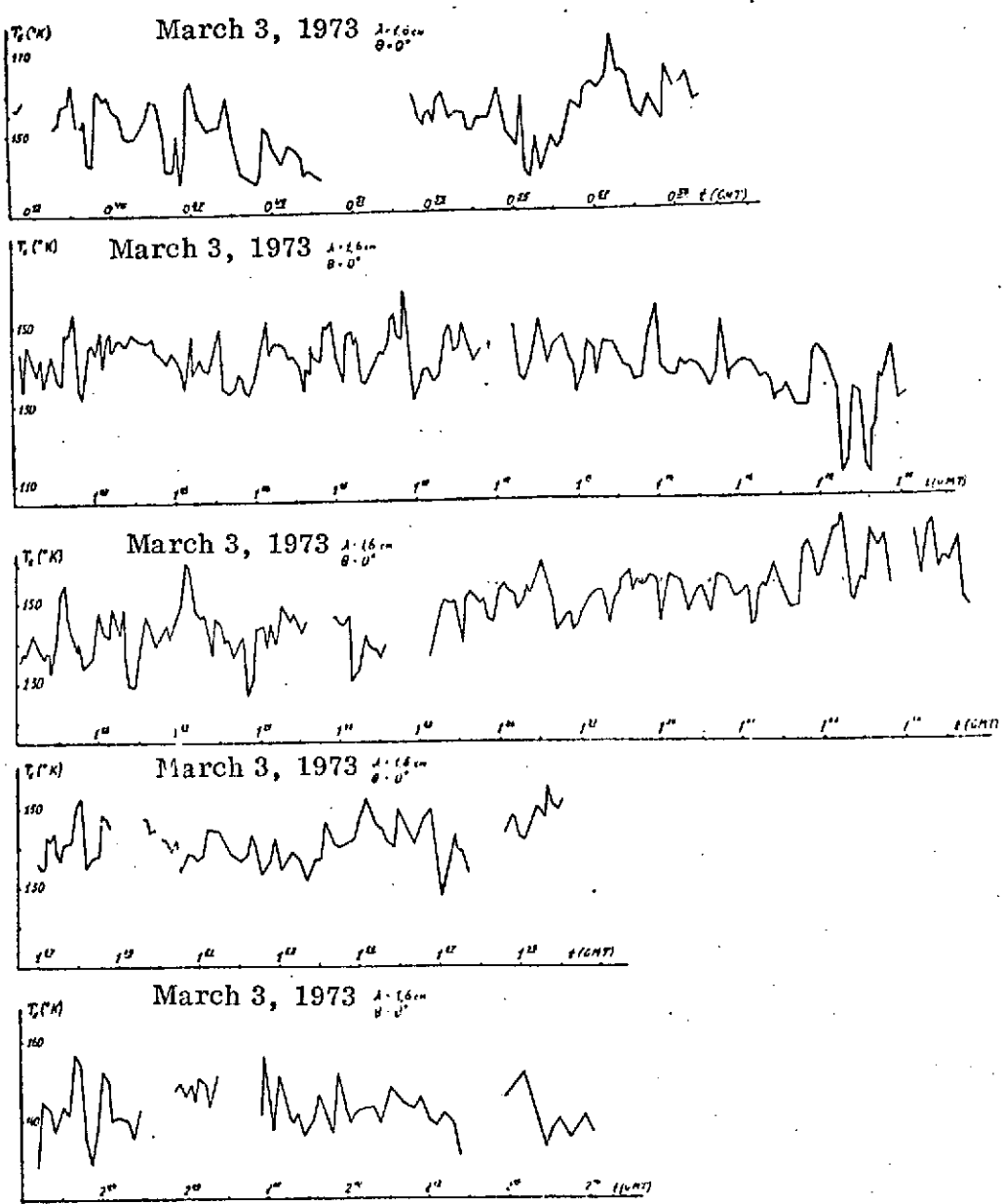


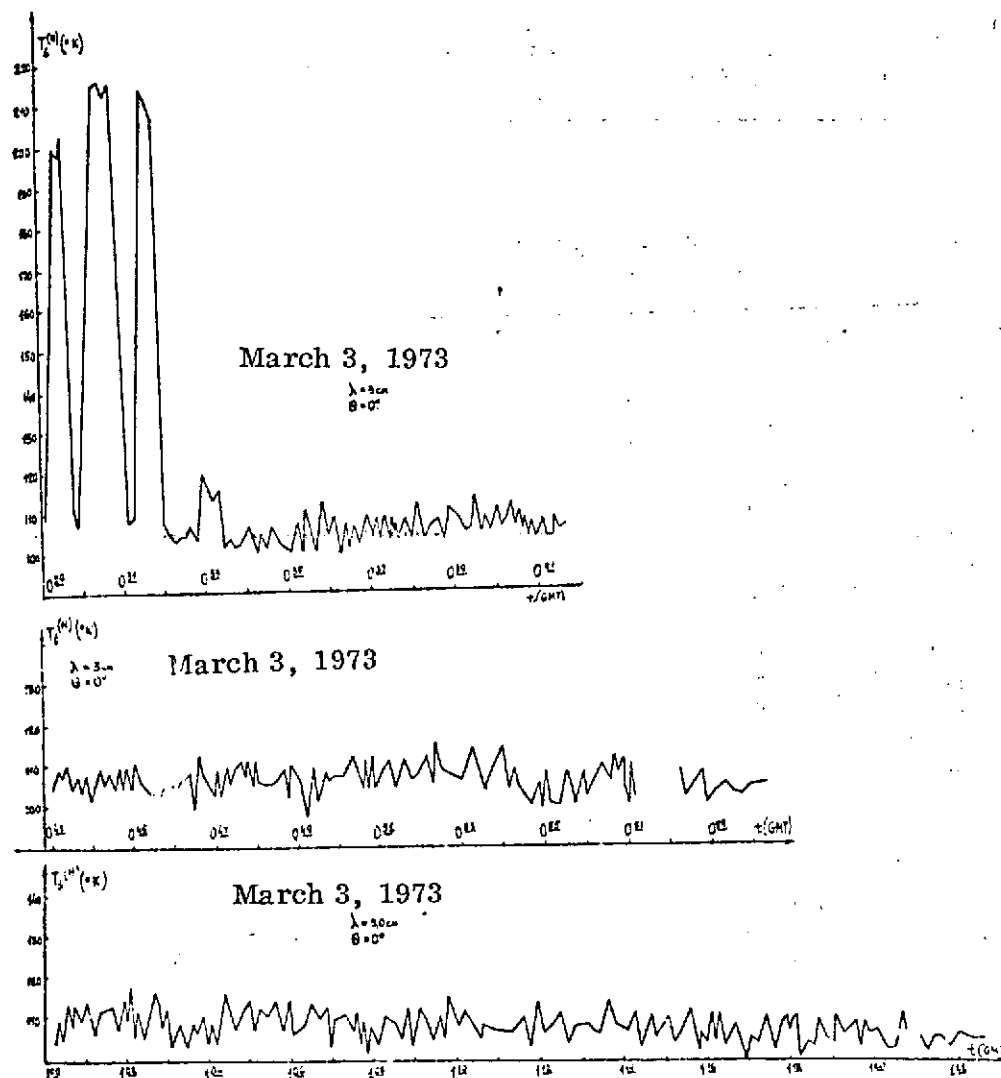
March 3, 1973

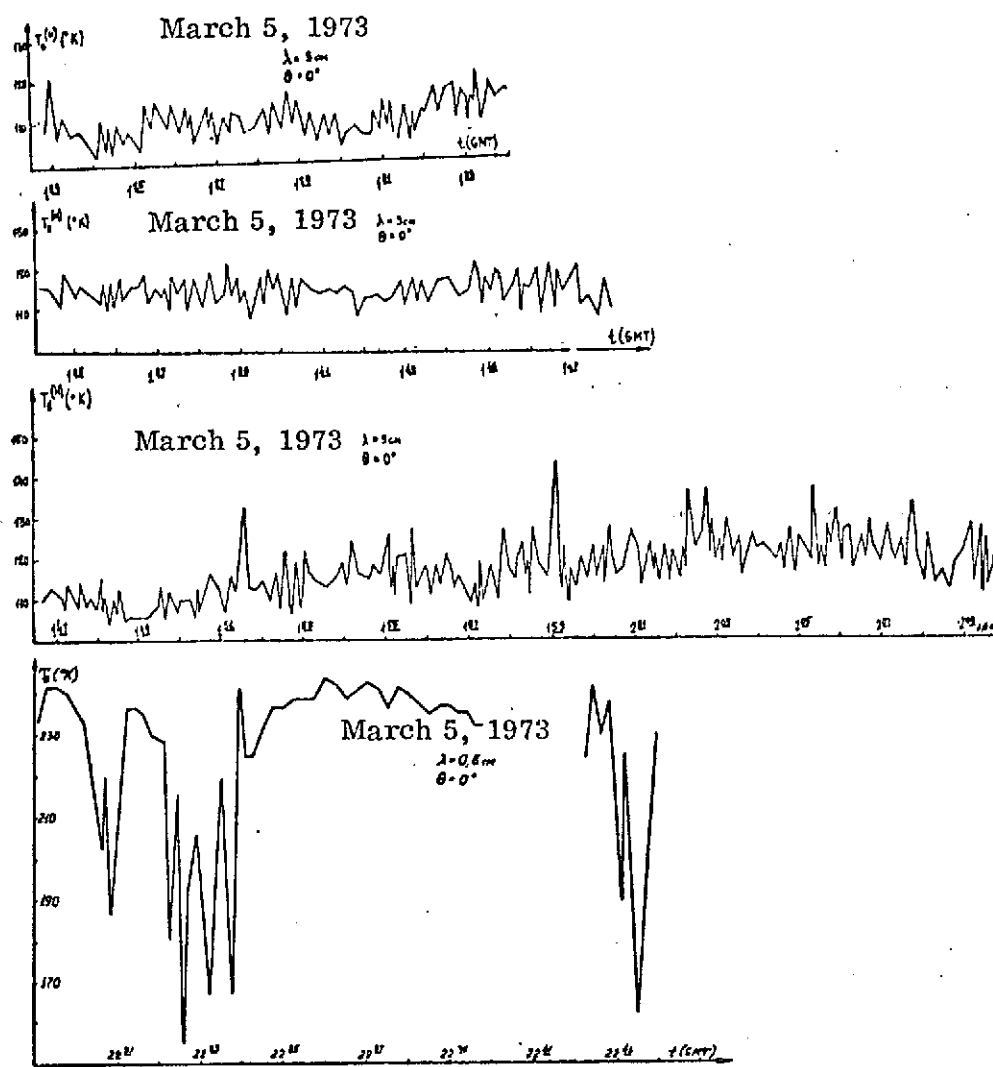


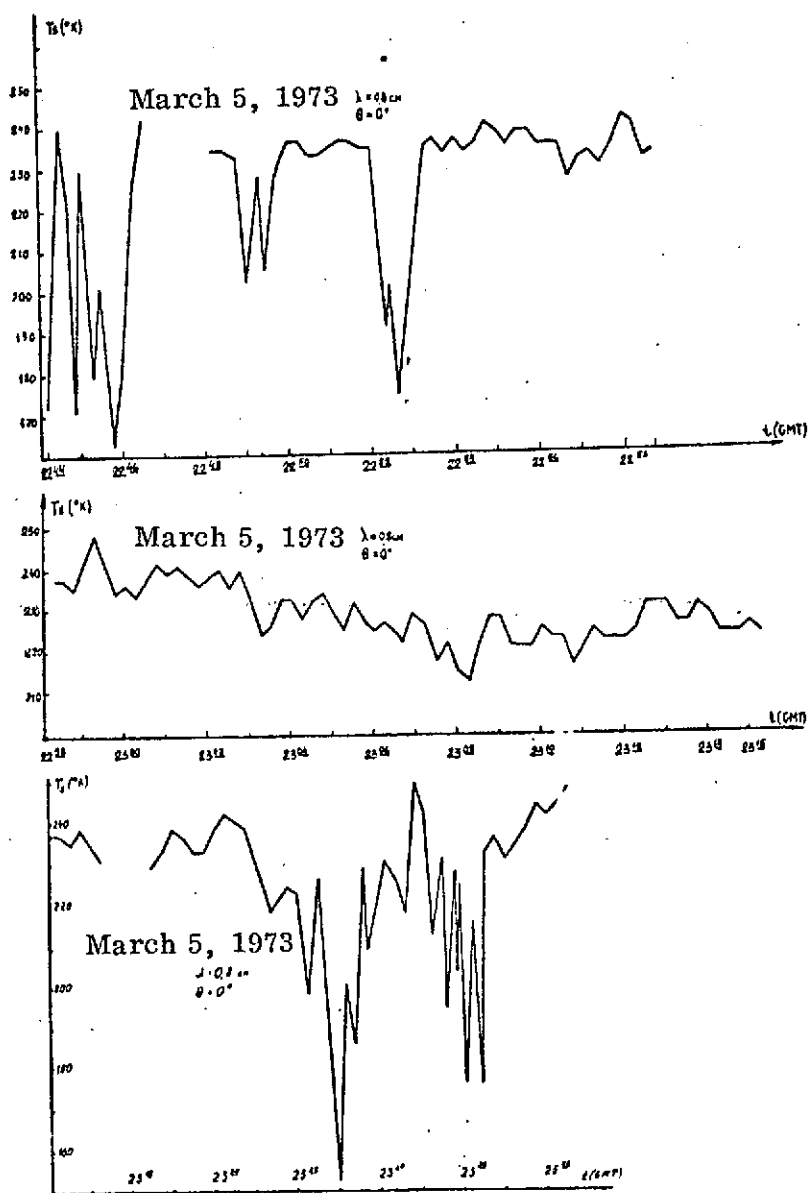
March 3, 1973







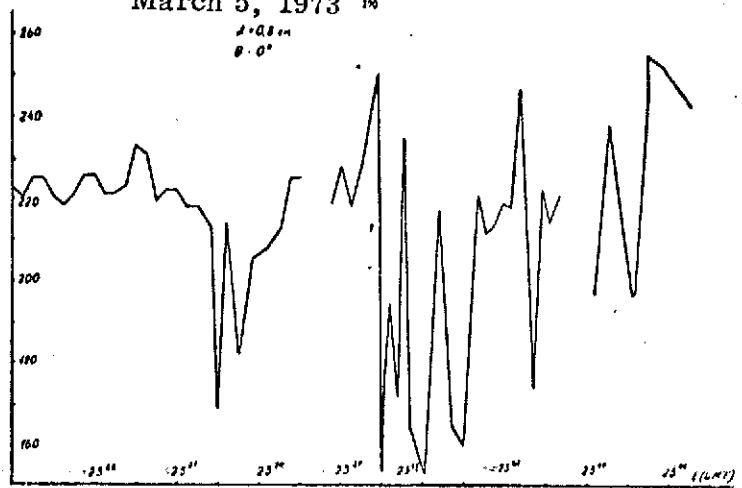




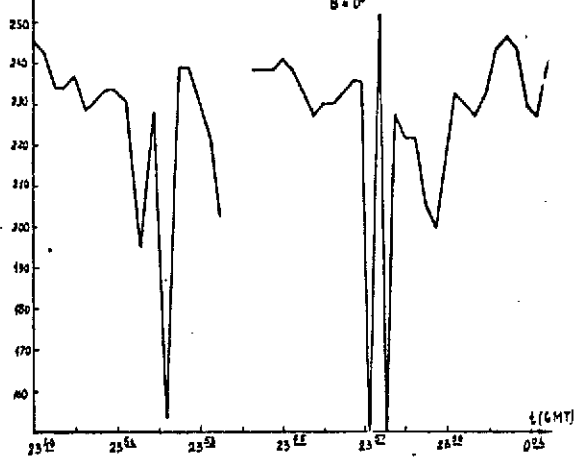
/170

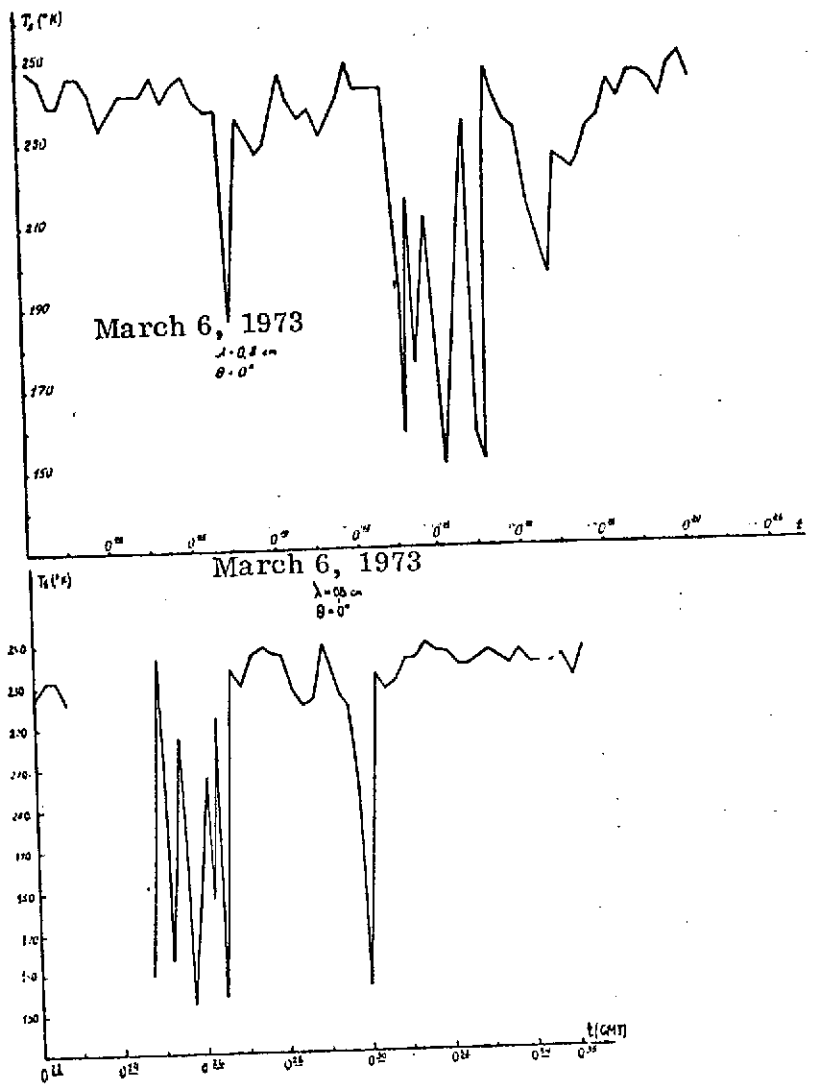
March 5, 1973

$\lambda = 0.8 \text{ cm}$
 $\theta = 0^\circ$

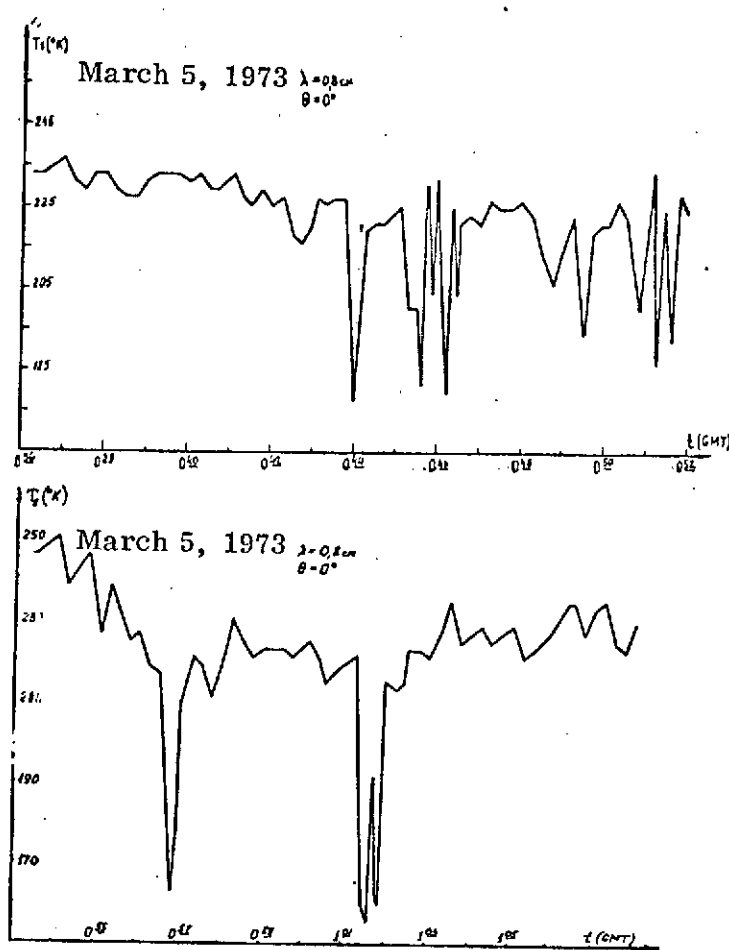


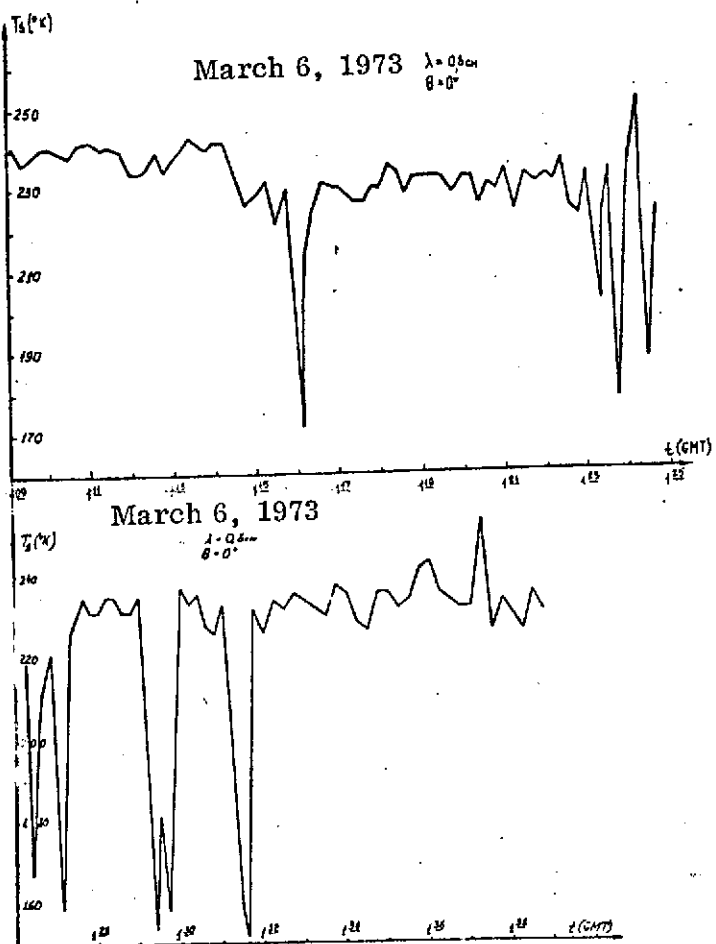
$T_d (\text{sec})$ March 5-6, 1973 $\lambda = 0.8 \text{ cm}$
 $\theta = 0^\circ$



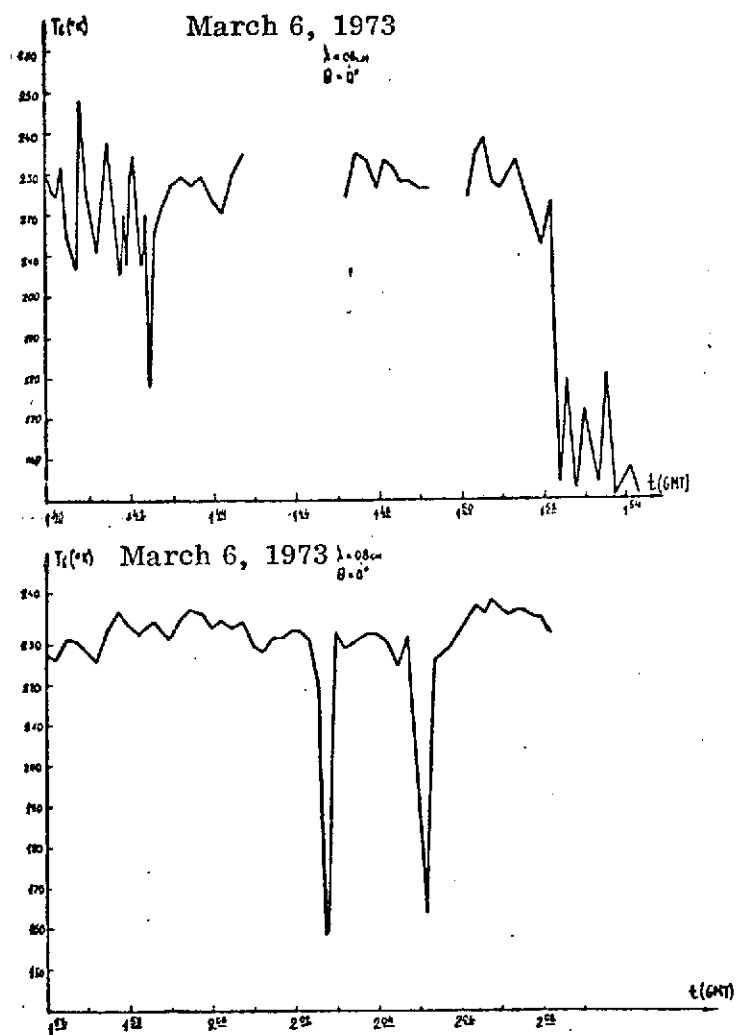


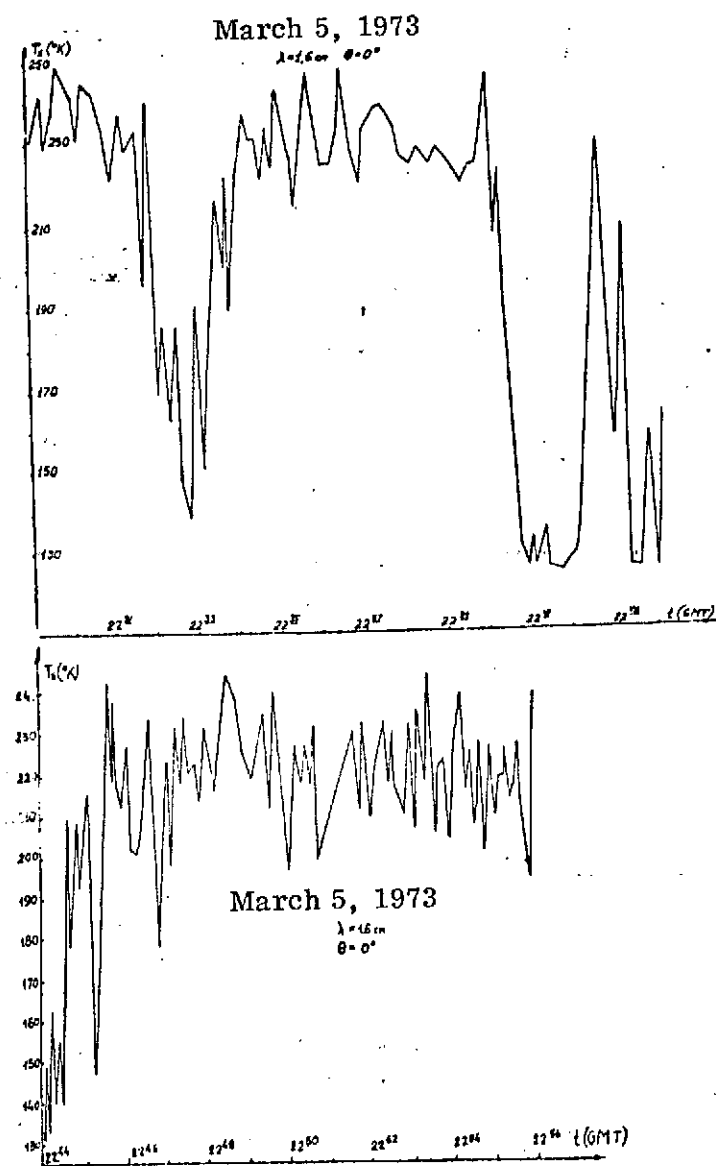
/172

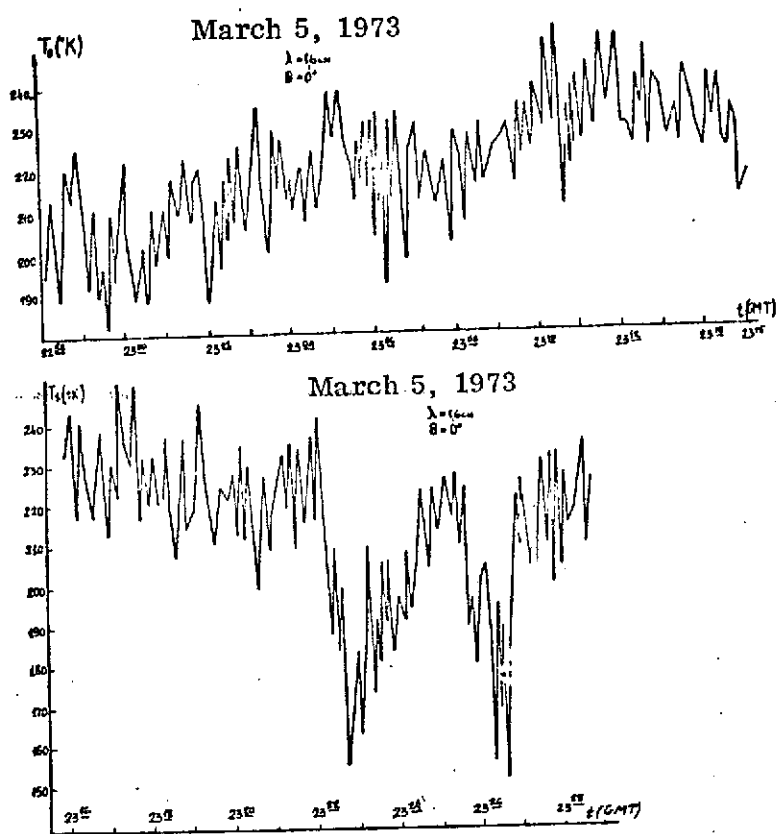




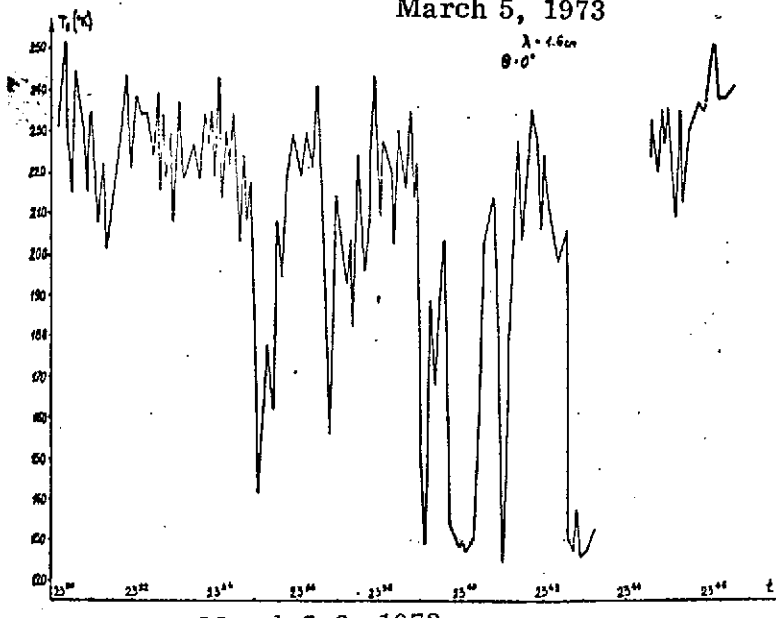
/174



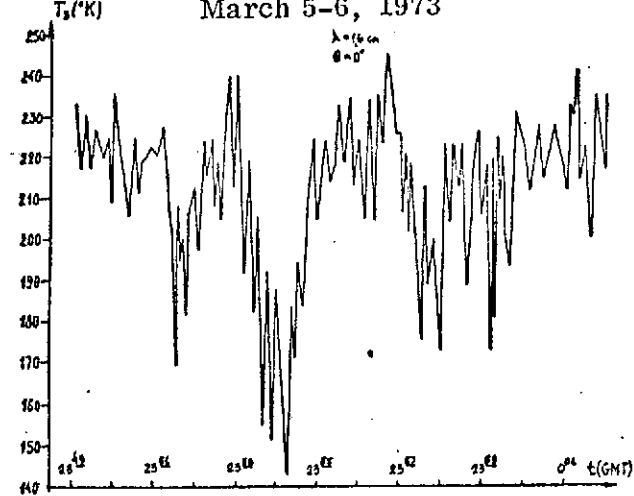


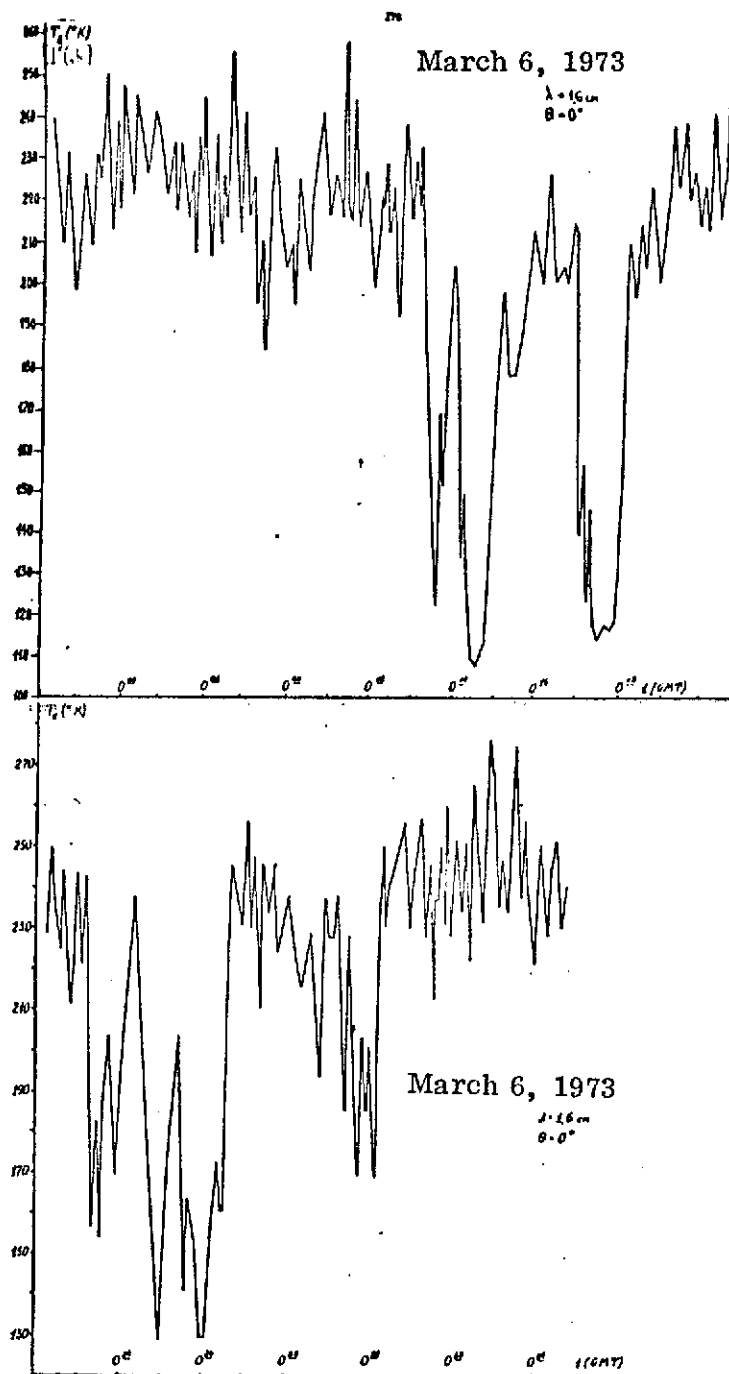


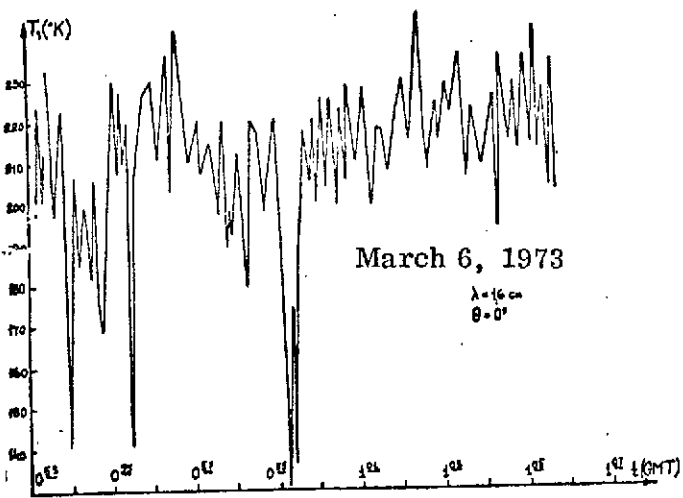
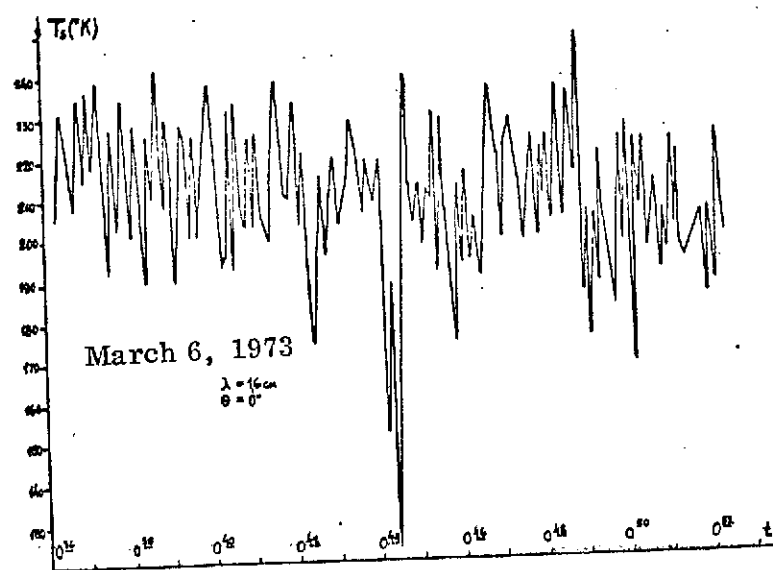
March 5, 1973

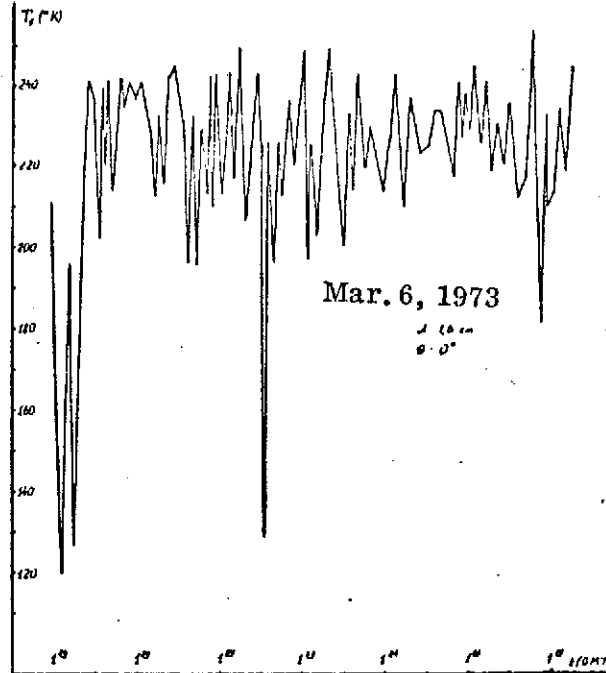
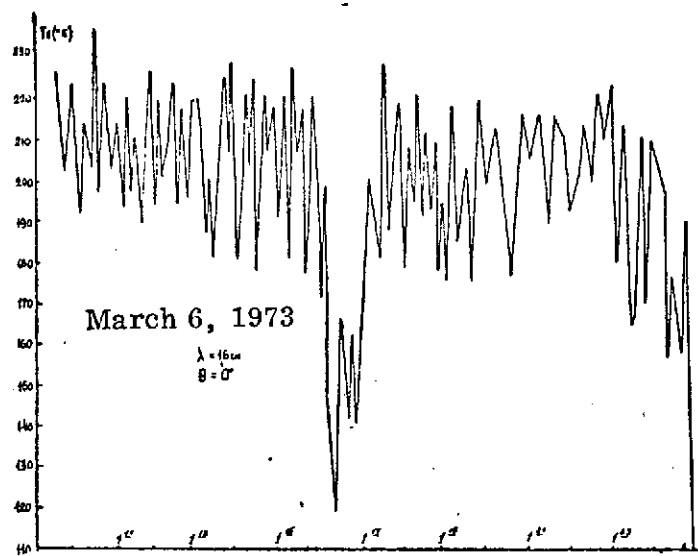
 $\lambda = 1.6\text{cm}$
 $\theta = 0^\circ$ 

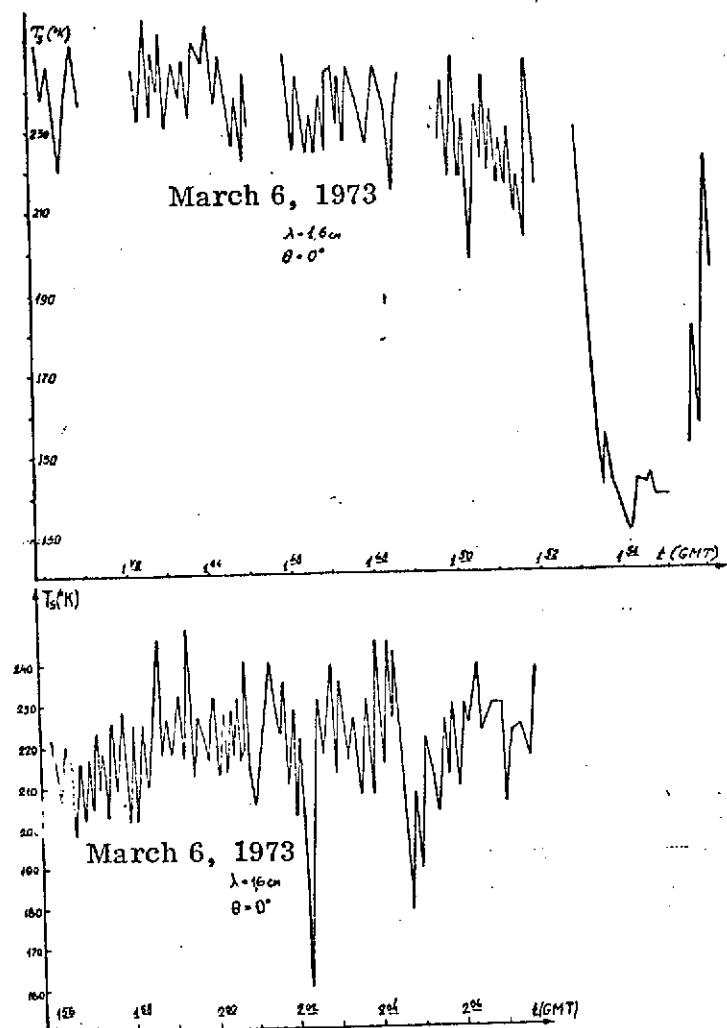
March 5-6, 1973

 $\lambda = 1.6\text{cm}$
 $\theta = 0^\circ$ 

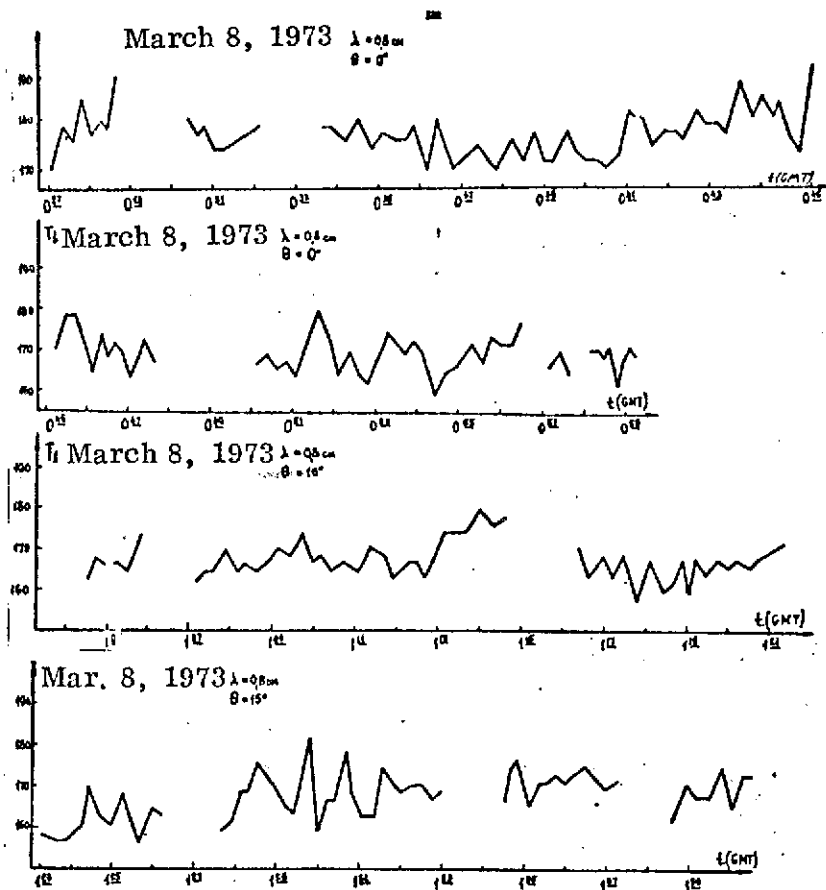


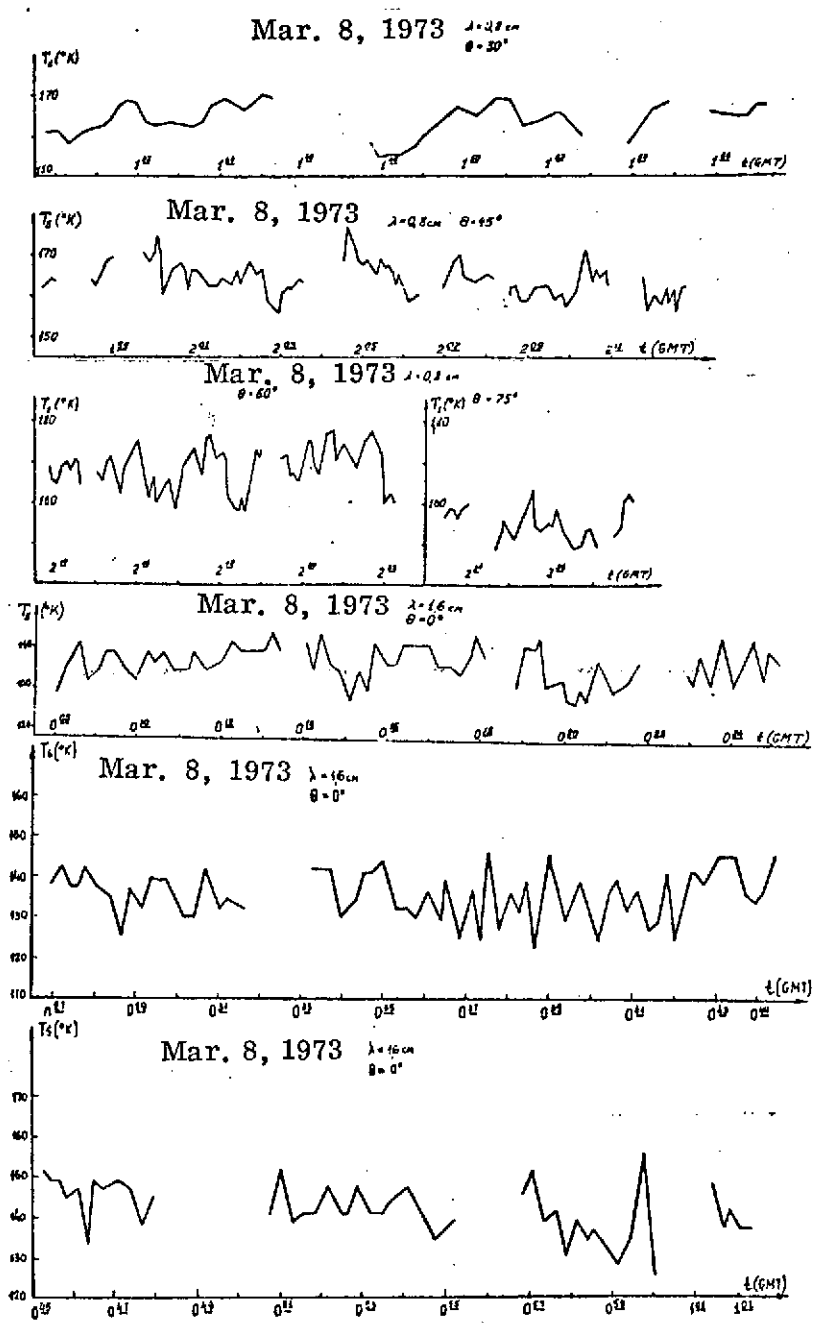




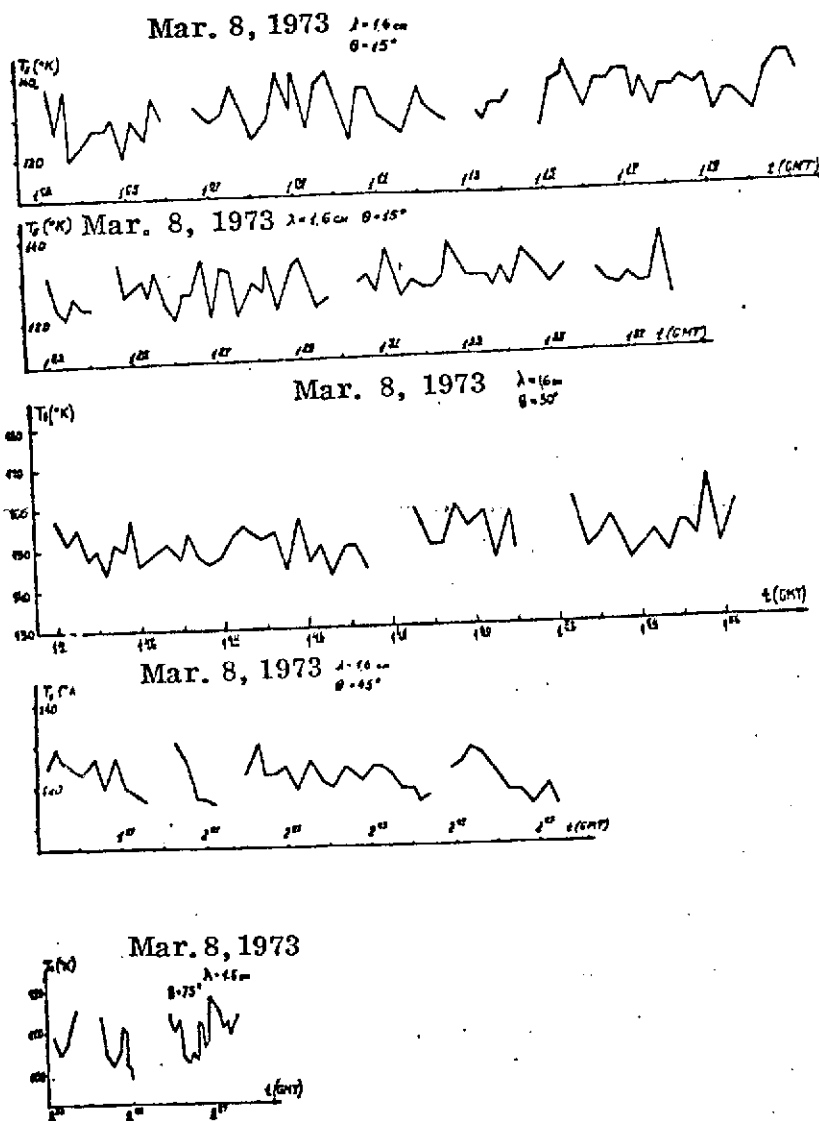


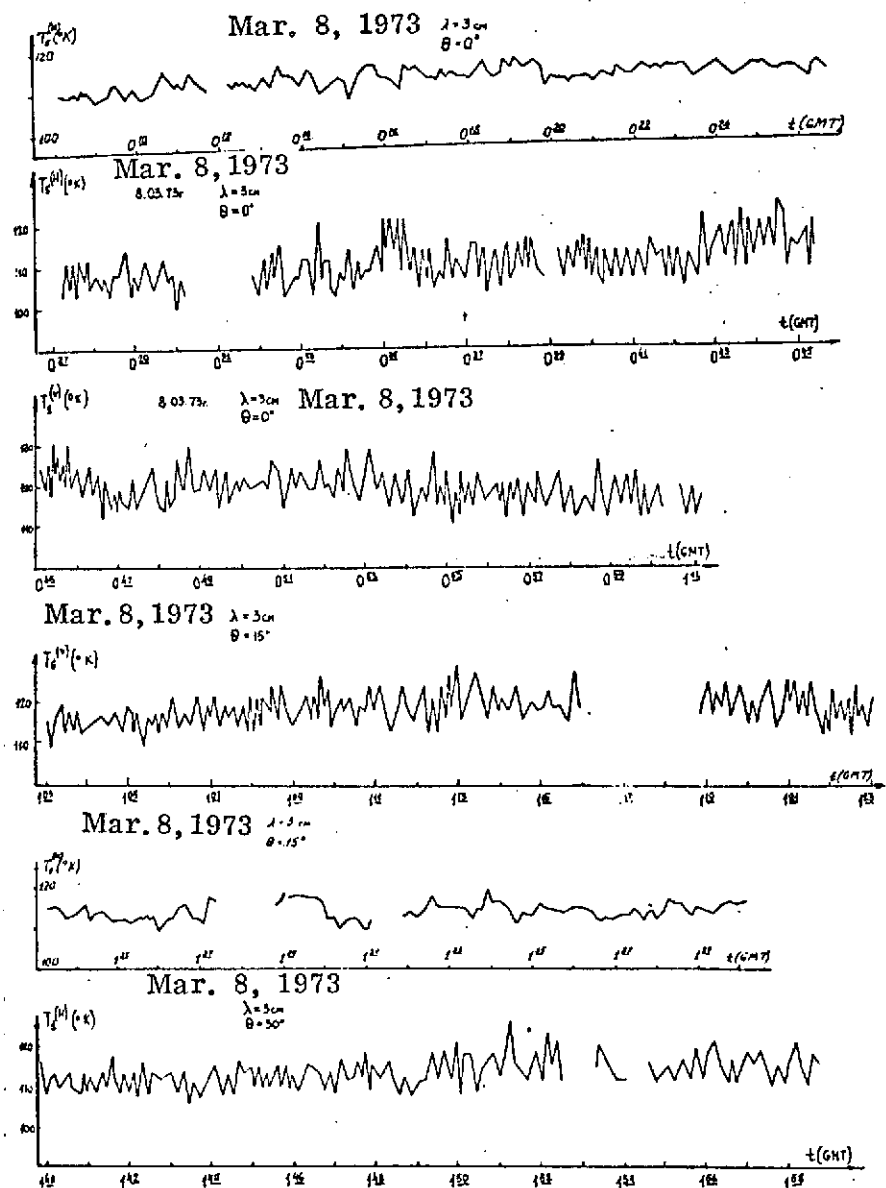
/182

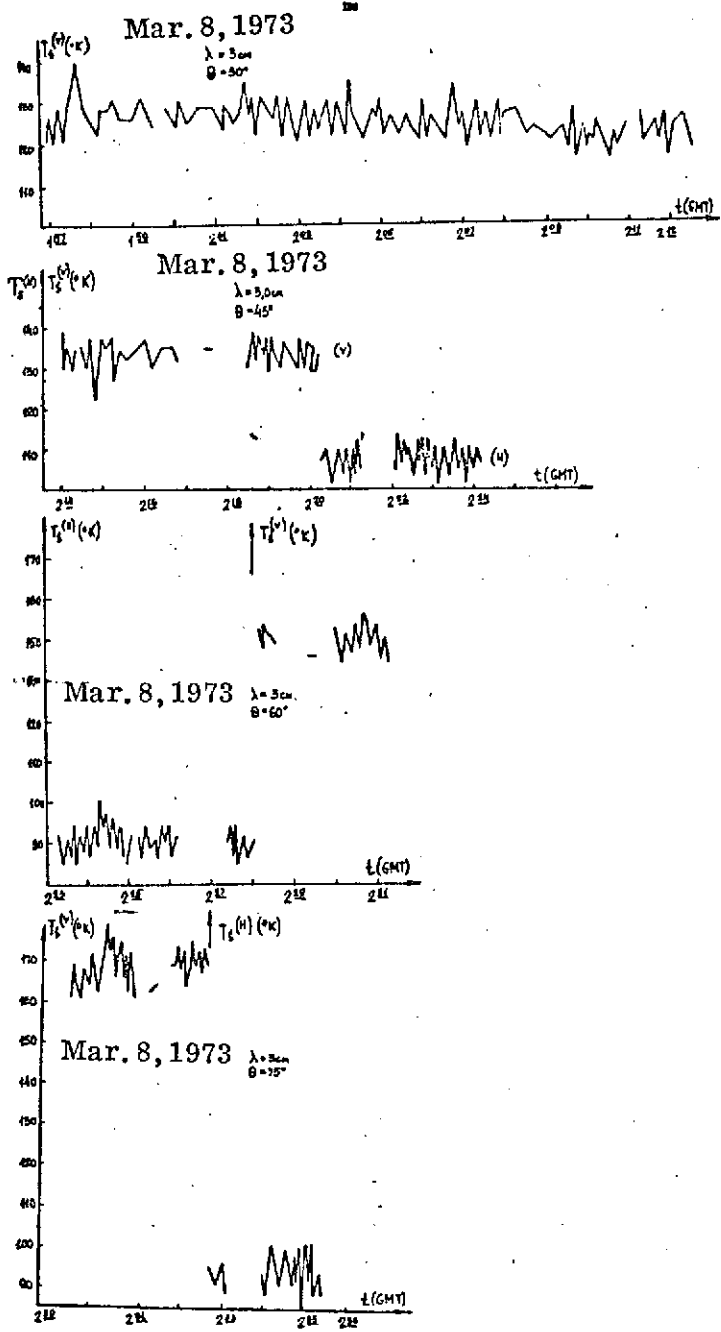




184







Translated for the National Aeronautics and Space Administration by Scripta Technica, Inc. NASw-2484.